

# **Self-Organized Radio Resource Management in OFDM Based Cellular Systems**

Vom Promotionsausschuss der  
Technischen Universität Hamburg-Harburg

zur Erlangung des akademischen Grades

Doktor-Ingenieur (Dr.-Ing.)

genehmigte Dissertation

von  
Ting Chen

aus  
Fuzhou, China

2010

1. Gutachter: Prof. Dr. rer. nat. Hermann Rohling
2. Gutachter: Prof. Dr. rer. nat. Volker Turau

Tag der mündlichen Prüfung: 28. September 2010

## Acknowledgement

The research work described in this thesis has been carried out during my stay at the Institute of Telecommunications at the Technische Universität Hamburg-Harburg.

I would like to thank especially Prof. Dr. Hermann Rohling for the supervision of my research and helpful support at all times during the years of my research. My thanks would be also given to Prof. Dr. Turau for being the external examiner and Prof. Dr. Brinkmeyer for chairing the examination procedures. Furthermore I am very thankful for all the colleagues with whom I have cooperated and enjoyed together the time at the institute. In particular, Dr. Rainer Grünheid, Dr. Niclas Meier, and Dr. Christian Stimming are appreciated for their great support and fruitful discussions.

Finally I would like to thank my mother and all my friends for their continuous support and encouragement during these years and finishing my thesis.

Fuzhou, China, November 2010



# Contents

<b>1</b>	<b>Introduction</b>	<b>1</b>
<b>2</b>	<b>Mobile Radio Channel</b>	<b>5</b>
2.1	Path Loss and Shadowing . . . . .	6
2.2	Multi-path Propagation . . . . .	6
2.3	Doppler Frequency Shift . . . . .	8
2.4	WSSUS Channel Model . . . . .	9
<b>3</b>	<b>OFDM Transmission Technique</b>	<b>13</b>
3.1	Why do we choose OFDM? . . . . .	14
3.2	An OFDM Transmission System . . . . .	15
<b>4</b>	<b>Radio Resource Management in Cellular Systems</b>	<b>21</b>
4.1	Conventional Cellular Network with FRA . . . . .	22
4.2	OFDM Based Cellular Systems . . . . .	24
4.2.1	Single Frequency Cellular Network . . . . .	24
4.2.2	Self-Organized Radio Resource Management . . . . .	26
<b>5</b>	<b>SO-RRM in OFDM Based Cellular Systems</b>	<b>27</b>
5.1	MAC Layer Description . . . . .	28
5.1.1	TDD Scheme . . . . .	28
5.1.2	MAC Frame . . . . .	28
5.1.2.1	Frequency and Time Direction . . . . .	29
5.1.2.2	Signal Measurement Slot . . . . .	30
5.2	Physical Layer Specification . . . . .	30

5.2.1	Simplification of Channel Model in Simulation . . . . .	30
5.2.2	Adaptive Modulation and Coding . . . . .	31
5.2.3	Resource Quality Mapping Function . . . . .	34
5.3	Resource Allocation for a New User . . . . .	36
5.4	Anti-dropping Scheme Applied to SO-RRM . . . . .	39
5.4.1	Interference Margin . . . . .	39
5.4.2	Reallocation Procedure . . . . .	40
<b>6</b>	<b>Signal Measurement and Resource Selection Procedure</b>	<b>43</b>
6.1	Measurement of Signal and Co-channel Interference . . . . .	44
6.1.1	Uplink/Downlink Interference Measurement . . . . .	44
6.1.2	Interference-free Signal Measurement . . . . .	45
6.2	SINR Based Resource Allocation . . . . .	46
6.2.1	Feedback of Downlink Candidate Resources . . . . .	46
6.2.2	SINR Calculation . . . . .	47
6.2.3	Resource Selection Algorithm . . . . .	47
<b>7</b>	<b>SO-RRM with Uniform User Distribution</b>	<b>51</b>
7.1	Cellular Network in Simulation . . . . .	52
7.1.1	Wraparound Cellular Network Structure . . . . .	52
7.1.2	Interference Calculation in a Wraparound Structure . . . . .	53
7.1.3	Simulation Scenario . . . . .	53
7.2	Performance Analysis . . . . .	55
7.2.1	Measurement of Test Signal . . . . .	55
7.2.2	System Capacity . . . . .	58
7.2.3	Anti-Dropping Schemes . . . . .	60
7.2.3.1	Interference Margin . . . . .	61
7.2.3.2	Reallocation . . . . .	62
7.2.3.3	Reallocation with Interference Margin . . . . .	66

---

<b>8</b>	<b>SO-RRM with Non-Uniform User Distribution</b>	<b>69</b>
8.1	Cellular Networks with Non-uniform User Distribution . . . .	70
8.1.1	Cellular Networks with Fixed Resource Allocation . .	70
8.1.2	Self-organized Cellular Network . . . . .	72
8.2	System Level Performance . . . . .	72
8.2.1	Hotspot and Fixed Resource Allocation . . . . .	72
8.2.2	Hotspot and Self-organized Resource Management . .	74
<b>9</b>	<b>Adaptive Resource Rearrangement</b>	<b>81</b>
9.1	Mathematical Description and Algorithms of ARR . . . . .	82
9.1.1	Mathematical Description . . . . .	82
9.1.2	ARR Algorithms . . . . .	84
9.1.2.1	Rotational Rearrangement . . . . .	84
9.1.2.2	Maximum Value Rearrangement . . . . .	85
9.1.2.3	Hungarian Algorithm Based Rearrangement	85
9.2	ARR in a Cellular Network with SO-RRM . . . . .	87
9.2.1	Performance in a Single Cell . . . . .	87
9.2.2	Performance in a Cellular Network . . . . .	90
<b>10</b>	<b>Conclusions</b>	<b>95</b>
	<b>Glossary</b>	<b>99</b>
	<b>Symbol</b>	<b>103</b>
	<b>Bibliography</b>	<b>107</b>





# Chapter 1

## Introduction

**F**UTURE mobile communication systems are going to connect various intelligent terminals in the wireless world with fast and reliable radio networks [Ibr02]. Providing a high-speed internet access and some other rich content services, a target peak rate of transmission will be as high as 100 Mbit/s for high mobility such as mobile access and 1 Gbit/s for low mobility such as nomadic or local wireless access [ITUR03]. Nevertheless, such a wireless system should have high flexibility and adaptivity to serve various applications with different transmission requirements. Comparing with the current second- and third-generations of mobile communications, the next system generation requires much more bandwidth and needs therefore a high computation power.

A transmission technique with high data rate applied in a multi-path radio channel environment shows a transfer function with large frequency selectivity. The resulting Inter-Symbol Interference (ISI) would require a complex equalizer technique at the receiver side, if a single-carrier transmission technique is applied. A multi-carrier transmission technique is proposed in this thesis, which is robust in multi-path propagation situations and leads to a simpler receiver structure by considering several narrow band subchannels processed in parallel. The Orthogonal Frequency Division Multiplexing (OFDM) transmission technique provides not only high spectrum efficiency, but also system flexibility and adaptivity. Different transmission parameters such as modulation and coding rate can be selected individually for each subcarrier. On the hardware side, the development of Digital Signal Processing (DSP) chips also promotes a practical large-scale application of the OFDM transmission technique.

With its above-mentioned characteristics, the OFDM digital transmission technique has been implemented already in several wireless applications today. It is integrated as the transmission technique in the IEEE Wireless

Local Area Network (WLAN) standard. It is used in digitized radio broadcasting services, e. g. Digital Audio Broadcasting (DAB) and Digital Radio Mondiale (DRM), as well as for digital television such as Digital Video Broadcasting (DVB). It has been also adopted as the underlying technique for the next generation mobile cellular communication system Long Term Evolution (LTE).

Radio resource management is one of the most basic and important topics in the design of a wireless system. Given a minimum Quality of Service (QoS) and a limited available radio spectrum, the goal is to serve simultaneously many users inside a large coverage size. A scheme of radio resource management can be defined as a manager of resources, which can be frequency band, time slot, spreading code, or even beam of intelligent antennas in space. For example, a combination of Frequency/Time Division Multiple Access (FDMA/TDMA) is used in the second-generation (2G) mobile communication system like Global System for Mobile communications (GSM), and Code Division Multiple Access (CDMA) technique is used in third-generation (3G) networks such as Universal Mobile Telecommunications System (UMTS). The Spatial Division Multiple Access (SDMA) has been introduced as Multi-Input Multi-Output (MIMO) technique in High Speed Downlink Packet Access (HSDPA). All those schemes can be applied conveniently with the OFDM transmission technique.

By introducing the concept of resource reuse in a cellular structure, the network can have a theoretically unlimited coverage. In a cellular network, the dominant restriction element is the so-called Co-Channel Interference (CCI). A resource used exclusively by a single transmission can be reused by another transmission at the same time, as long as the communicator pairs, Base Station (BS) and Mobile Terminal (MT), are sufficiently far away from each other. Based on the flexibility of resource allocation in a cellular network, two different methods can be categorized: Fixed Resource Allocation (FRA) and Dynamic Resource Allocation (DRA). Those two terms are extended respectively from Fixed Channel Allocation (FCA) and Dynamic Channel Allocation (DCA) for conventional FDMA based systems like GSM. The concept of frequency channel is replaced by radio resource in OFDM based systems.

In FRA, all resources are grouped and preassigned to each cell. The assignment operation is done periodically and globally, based on a long-term prediction of service situation in future. Between two planning stages, a resource has a “fixed” relationship with cells, which is selected to ensure any communication inside those cells being robust against CCI. To keep up with new situations, the GSM networks in Europe were redesigned nearly every month during its high-growth phases. A detailed description of the network planning stages in the nowadays 3G mobile system UMTS is presented in [Hol02].

When the resource usage is more serious than predicted, for example during a two-hour sport match in a stadium, it is unworthy of reconfiguring the complete network. Several alternative strategies have been proposed to improve the short-term performance in such cases. Two often-used methods are resource borrowing and directed retry. The former enables a cell to borrow idle resources from the neighbors. In the latter, a request blocked by one cell will be forwarded to an adjacent cell, which is equivalent to a directed handoff.

In contrast when the DRA is applied, all available resources are pooled together and shared by all cells in a network. Radio resources are chosen by a predefined criterion and are allocated during the establishment of each new connection. When the call is terminated, its allocated radio resources will be released and can be used again by another connection.

Independent of the resulting overhead, the DRA scheme has the potential to increase significantly bandwidth efficiency. DRA algorithms can be further classified into three categories: centralized, distributed, and self-organized. In a centralized DRA, the allocation is processed at a Central Controller (CC), based on all information about the resource allocations collected from all nearby cells. By contrast in a distributed DRA, a CC is not needed for allocation. Each BS broadcasts its allocation results to the others. Based on that information, a BS makes its own decision independently on new allocations.

Self-Organized Radio Resource Management (SO-RRM) is a measurement based DRA scheme. Any BS does not send to or receive information about allocation status from other BSs. The BS and the MT makes decision of resource allocation based on their own knowledge from the measurement about the surrounding environment and the status of resource usage. In comparison with the centralized resource allocation scheme, such a scheme has several advantages. Delays due to the information exchange between BSs and CCs are eliminated. Moreover, the computation complexity due to seeking a global allocation solution at CCs can be greatly reduced. The construction and operation costs of those CCs are saved as well. Comparing with other distributed DRA algorithms based on channel usage in nearby cells, a self-organized algorithm saves the cost in information exchange between BSs, especially in situation of heavy traffic.

An OFDM based cellular mobile communication system is investigated and will be presented in detail in this thesis, applied with a self-organized resource allocation procedure. In this case, each BS allocates independently radio resources to its MT based on the current network condition. Resources with low interference will be selected for each connection. The necessary interference information is obtained from network sensing, which is done continuously in advance at both BS and MT sides. The orthogonal-

ity between subcarriers in the OFDM transmission technique enables also adaptive transmission in individual channels. Providing an identical quality of service, more data packets can be transmitted in a radio channel with a high Signal-to-Interference-and-Noise Ratio (SINR). The efficiency of radio resources is thus improved. The power of signals in transmission is estimated by a dedicated test signal, as ensures an interference free measurement environment.

In SO-RRM, a new allocation implies unexpected additional CCIs to all transmissions, which exist already in any related resources. This may cause in some cases a dropping of connection due to the insufficient transmission rate. Two solutions against that phenomenon are proposed in this thesis, one active and the other passive. The active policy reserves an additional margin to the estimated SINR in the resource allocation procedure. It works as the tolerance room for new interferences after allocation. The passive one triggers a channel reallocation process when a degradation of transmission quality is observed. Resources will be reselected according to the updated network condition.

One typical advantage of the self-organized allocation procedure comparing with static allocation is shown in the situation with non-uniform user distributions. SO-RRM supports natively free shift of radio resources on demand among the whole network. Therefore, it is self-adaptive to any distribution of mobile users or traffic demands, and is able to react seamlessly to any change of them.

When FDMA is applied, the independent channel fluctuation in subcarriers between different users brings the multi-user diversity. A proper rearrangement of resources between users can in this case improve the system performance, when the channel estimation is valid for relatively long time duration.

All above topics are discussed in this thesis.

## Chapter 2

# Mobile Radio Channel

**I**N an ideal situation, a receiver can obtain exactly a copy of the original signal, which is sent from the transmitter. Unfortunately, this is never true in reality, especially in wireless communications. Besides various noise influences at the receiver, signals in transmission are attenuated due to the propagation of radio waves. Furthermore, signals are reflected, refracted, and diffracted by those obstacles spreading around the space between the transmitter and the receiver. All those phenomena belong to the large-scale fading, since their effects are noticeable only over a long distance.

The small-scale fading describes the fact that the amplitude of a radio signal fluctuates significantly in a short distance in the order of the signal wave length. In that case, the influence of large-scale fading is relatively negligible. At the receiver, signals are received from various propagation paths with very small differences in time delay. Constructive or destructive results can be observed consequently with signals in different frequencies, as is called frequency selectivity. Doppler frequency shift is another typical characteristic of mobile communication systems. The relative movement between the transmitter and the receiver results in frequency offsets between transmitted and corresponding received signals, and thus a time-variant radio channel behavior.

Performance of mobile communication systems depends strongly on radio channels. Because of its randomness, the radio channel is always presented with statistical models during researches. This chapter is going to describe the main characteristics of a common radio channel in mobile communications, and gives a model, which will be used for quantitative simulation.

## 2.1 Path Loss and Shadowing

For Line-Of-Sight (LOS) radio propagation in a homogeneous medium, the attenuation of signals can be precisely calculated. Based on the physical laws of wave propagation, the wave front of an omnidirectional signal is a sphere. A radio signal is attenuated along with the propagation, which is called path loss. Considering a receiver at a distance  $d$  to a transmitter, the power  $P(d)$  of the received signal can be derived by equation (2.1). The transmission power, antenna gains, and other constants have been included in  $P(d_0)$ , which is the power of the received signal at a reference distance  $d_0$ . The propagation coefficient  $\alpha$  implies how fast the signal is attenuated over the path. In a free space condition, it equals to 2 based on the natural expansion of electric-magnetic waves. In the air, the attenuation is stronger because of extra losses e. g. by absorption. The value of  $\alpha$  is selected as 2.6 in this thesis for a typical urban environment [Rap02].

$$P(d) = P(d_0) \cdot \left(\frac{d}{d_0}\right)^{-\alpha} \quad (2.1)$$

In realistic wireless transmissions, signals are reflected, diffracted, and scattered by the obstacles between the transmitter and the receiver. Several indoor and outdoor investigations based on the combination of theoretical analyses and practical measurements are explained in [Rap02]. The statistical results show that in various environments the shadowing effect has approximately a lognormal distribution. Considering both path loss and shadowing, a received signal power can be expressed (in dB) as

$$P(d) [\text{dB}] = P(d_0) [\text{dB}] - 10\alpha \log_{10} \left(\frac{d}{d_0}\right) + X_\sigma [\text{dB}] \quad (2.2)$$

The random variable  $X_\sigma$  has a Gaussian distribution with a zero mean and a standard deviation  $\sigma$ . A  $\sigma$  value of 4 dB is selected for the considered urban environment in this thesis [Gud91].

Figure 2.1 shows example values calculated with the above-described large-scale fading model. The logarithmic scale is used for a friendly plotting of distances between a transmitter and a receiver.

## 2.2 Multi-path Propagation

In a wireless environment, radio signals may arrive at a receiver via several propagation paths from all directions. A simple example is illustrated in figure 2.2. The LOS is not considered here, because a typical urban cellular

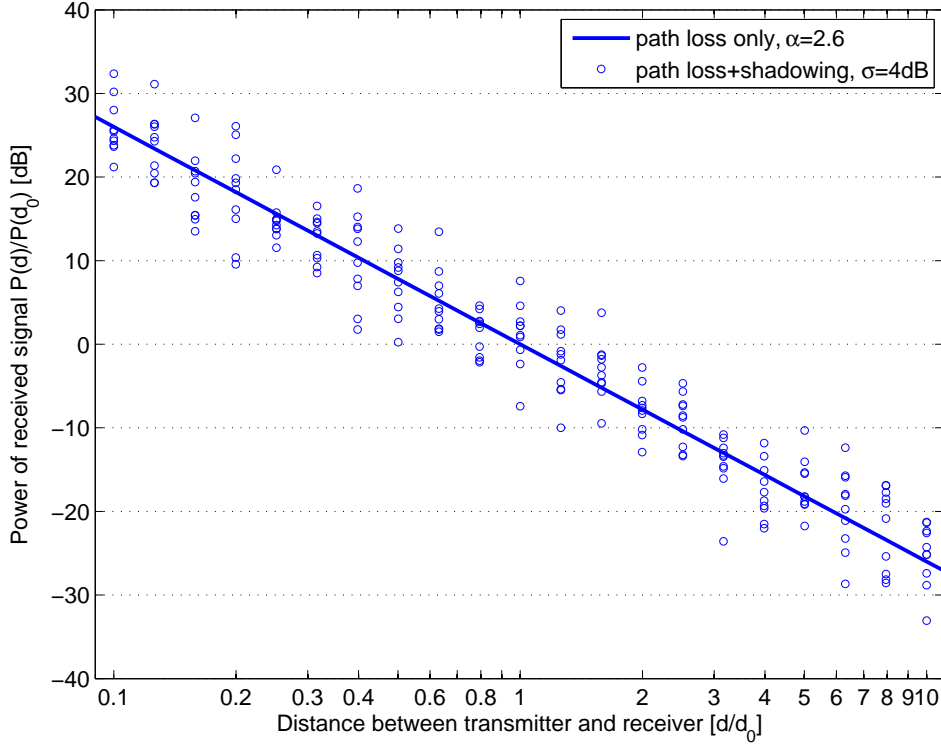


**Figure 2.1:** Received power with large-scale fading

environment is considered.

The received signal is the summation of copies of the sent signal from various paths with different attenuation factors  $a_l$  and propagation delays  $\tau_l$ . The impulse response  $h(\tau)$  can be thus expressed as

$$h(\tau) = \sum_l a_l \cdot \delta(\tau - \tau_l) \quad (2.3)$$

It is more convenient to write the response in baseband as:

$$h_b(\tau) = \sum_l a_l \cdot e^{j\theta_l} \cdot \delta(\tau - \tau_l) \quad (2.4)$$

The variable  $\theta_l$  is the phase shift between the received signal and the transmitted one in the carrier frequency  $f_0$ . Their relationship can be expressed by

$$\theta_l = -2\pi f_0 \tau_l \quad (2.5)$$

The corresponding baseband channel transfer function  $H_b(f)$  is then obtained by the Fourier transformation.

$$H_b(f) = \sum_l a_l \cdot e^{j\theta_l} \cdot e^{-j2\pi f \tau_l} \quad (2.6)$$

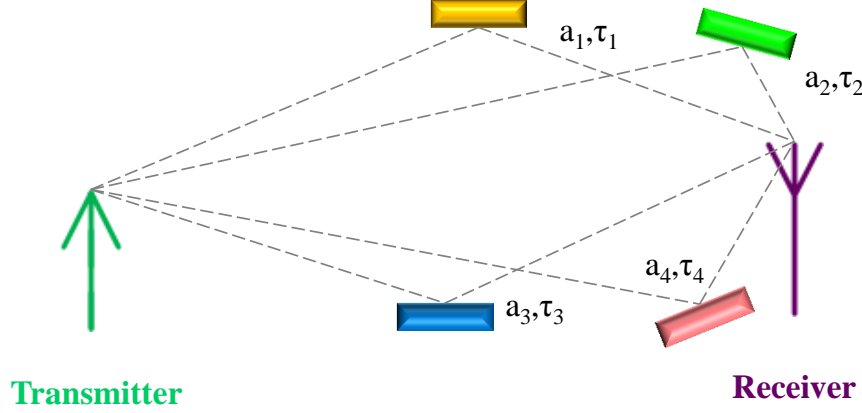


**Figure 2.2:** Multi-path Propagation

It is derivable that the amplitude of this function is not constant on the frequency axis. Signals on some frequencies are enhanced with the copies from those paths, whereas destructive effects can be also observed on some other frequencies. This phenomenon is termed frequency selectivity. The coherent bandwidth  $B_c$  is defined as the range, over which the signals are affected with similar channel gain. If a correlation of  $H_b(f)$  above 0.5 is restricted, the coherent bandwidth is approximately inversely proportional to the maximum delay spread  $\tau_{\max}$  between those propagation paths.

$$B_c \approx \frac{1}{\tau_{\max}} \quad (2.7)$$

### 2.3 Doppler Frequency Shift

The previous section discusses a Linear Time Invariant (LTI) channel, which considers the multi-path dispersion of the channel. It is suitable to describe a stationary propagation environment. Besides, time variance is another unavoidable and important nature in mobile communications, because of the relative movement between a transmitter and a receiver, or even a movement of any object in the propagation path.

Those movements result in a time-variant propagation channel between the transmitter and the receiver. It is assumed in figure 2.2 that the receiver is approaching the receiver at a constant equivalent velocity  $v_l$  (negative if departing) in path  $l$  from the time  $t=0$ . Thus the delay is calculated as a function of time by equation (2.8), in which  $c$  is the speed of light.

$$\tau_l(t) = \tau_l(0) - \frac{v_l}{c}t \quad (2.8)$$



The time-variant impulse response in this situation can be rewritten from equation (2.4) as

$$h_b(\tau, t) = \sum_l a_l \cdot e^{j\theta_l} \cdot e^{j2\pi f_0 \frac{v_l}{c} t} \cdot \delta(\tau - \tau_l) \quad (2.9)$$

Defining the Doppler frequency shift  $f_{D,l}$  in the  $l$ -th path as

$$f_{D,l} = f_0 \cdot \frac{v_l}{c} \quad (2.10)$$

the time-variant channel transfer function can be derived from equation (2.6) as

$$H_b(f, t) = \sum_l a_l \cdot e^{j\theta_l} \cdot e^{j2\pi f_{D,l} t} \cdot e^{-j2\pi f \tau_l} \quad (2.11)$$

The frequency shift reflects how rapidly the channel changes over time. A high value implies the channel will be nearly uncorrelated even after a short time period. To describe this property in a mathematical way, a coherence time  $T_c$  is defined as the time duration, in which a high correlation of  $H(f, t)$  is observed. If 0.5 is used as the threshold to the time correlation function, the coherence time is approximated to equation (2.12). The variable  $f_{D,\max}$  denotes the maximum Doppler frequency shift.

$$T_c \approx \frac{1}{f_{D,\max}} \quad (2.12)$$

## 2.4 WSSUS Channel Model

As the real mobile radio channel has strong randomness in different situations, a stochastic model will help in the researches on relevant systems. The Wide-Sense Stationary Uncorrelated Scattering (WSSUS) channel model is commonly used for mobile wideband channels.

Shown in figure 2.3, a finite number of  $L$  paths (without LOS) are considered in the model and constructs a time-variant channel impulse response as

$$h_b(\tau, t) = \frac{1}{\sqrt{L}} \sum_{l=1}^L e^{j2\pi f_{D,l} t + j\theta_l} \cdot \delta(\tau - \tau_l) \quad (2.13)$$

All  $L$  paths are assumed to have an identical normalized attenuation factor  $1/\sqrt{L}$ . Those associated delays  $\tau_l$ , Doppler frequency shifts  $f_{D,l}$ , and initial phases  $\theta_l$  will be generated from random number generators. The delays are exponentially distributed with a mean delay  $\tau_0$ , and the initial phases

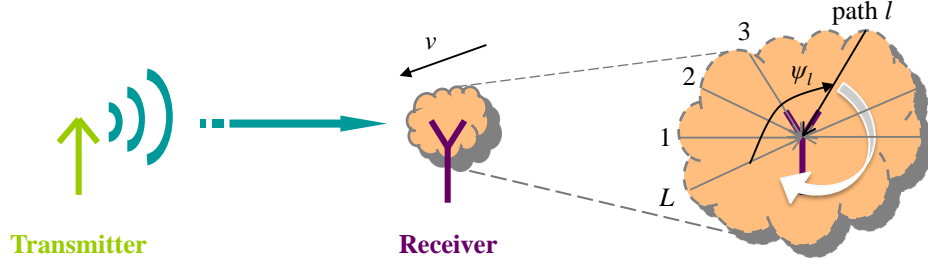


**Figure 2.3:** Multi-path model in generation of WSSUS channel

are uniformly distributed between 0 and  $2\pi$ . Their Probability Density Functions (PDF) can be described as follows.

$$p(\tau_l) = \frac{1}{\tau_0 \cdot (1 - e^{-\tau_{\max}/\tau_0})} e^{-\tau_l/\tau_0}, \quad \tau_l \in [0, \tau_{\max}] \quad (2.14)$$

$$p(\theta_l) = \frac{1}{2\pi}, \quad \theta_l \in [0, 2\pi) \quad (2.15)$$

Furthermore, the arriving azimuthal angle  $\psi_l$  of those paths are assumed also uniformly distributed between 0 and  $2\pi$ , and the caused Doppler frequency shift is calculated as

$$f_{D,l} = f_0 \cdot \frac{v}{c} \cdot \cos \psi_l = f_{D,\max} \cdot \cos \psi_l \quad (2.16)$$

$$p(\psi_l) = \frac{1}{2\pi}, \quad \psi_l \in [0, 2\pi) \quad (2.17)$$

This leads to consequently a Jakes' spectrum for the PDF of  $f_{D,l}$ .

$$p(f_{D,l}) = \frac{1}{\pi f_{D,\max} \sqrt{1 - (f_{D,l}/f_{D,\max})^2}} \quad (2.18)$$

With the WSSUS model, a radio channel is more frequency selective when a long mean delay is assumed. A fast movement, i. e. a great Doppler frequency shift, results in strong fluctuation in the time direction. The magnitude of an example channel transfer function generated by the WSSUS model is shown in figure 2.4,

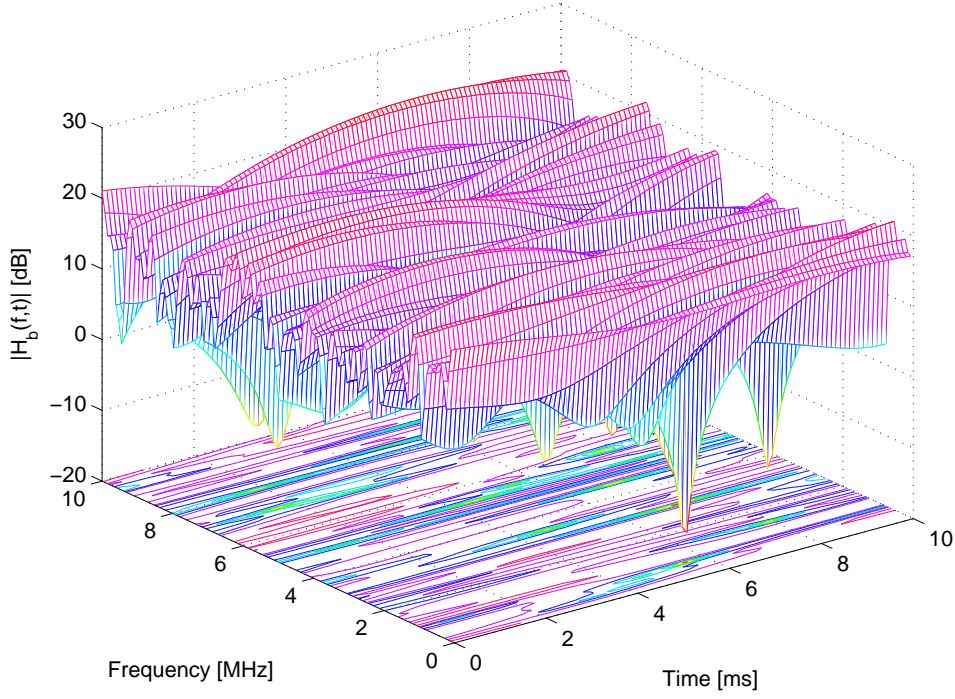


**Figure 2.4:** Magnitude of channel transfer function in a WSSUS channel

with  $\tau_{\max}=3.2\mu\text{s}$  and  $f_{D,\max}=50\text{ Hz}$ . A high correlation of radio channel attenuation can be observed within the corresponding coherent bandwidth  $B_c=312.5\text{ kHz}$  and the coherence time  $T_c=20\text{ ms}$ .

Derived from the wide sense stationary property of this model, the amplitude of channel transfer function has the same stochastic distribution in the direction of time and frequency. This characteristic will be used in the later discussion.



## Chapter 3

# OFDM Transmission Technique

A transmitted signal arrives at the receiver via a large number of echo paths. This results in interference between adjacent transmitted symbols. Future wireless communication systems require very high data rates, which imply that the symbol duration is much shorter than the typical delay spread. In this situation, ISI becomes critical in the design of communication systems.

Splitting the data stream into a number of low rate substreams and transmitting each on different carriers can increase the symbol duration and thus decrease the ISI. However, in conventional multi-carrier transmission systems a guard band in frequency is necessary between adjacent subchannels, in order to avoid Inter-Carrier Interference (ICI) completely. That causes an inefficient usage of frequency spectrum.

Orthogonal frequency division multiplexing, as an advanced multi-carrier transmission technique, introduces orthogonality between transmitted signals in different subcarriers by a specially designed mask spectrum. The transmission of signals in those subbands is interference free to each other, so that a guard band is not needed any more. Each subband can be further treated as a narrow band channel, which requires only a simple receiver. The ISI can be also avoided completely by appending a guard interval to each symbol.

This chapter gives a short motivation of using the OFDM technique in wide-band radio transmissions, and describes the basic structure of an OFDM transmission system and relevant signal processing procedures.

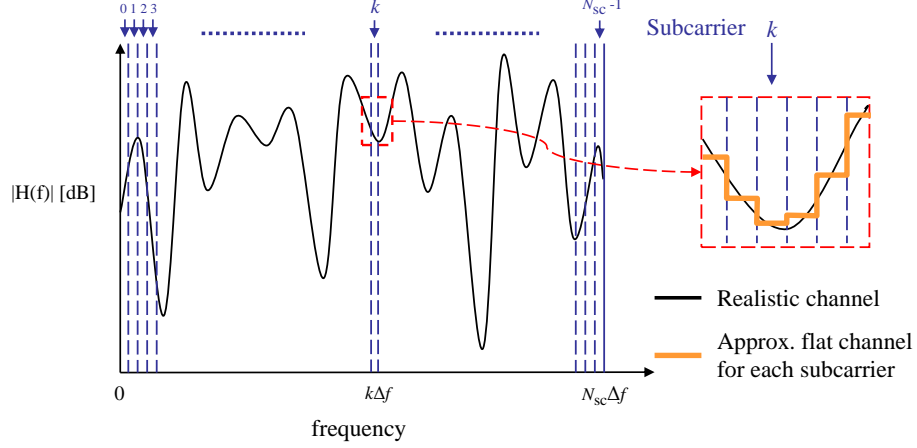


**Figure 3.1:** OFDM subcarriers

### 3.1 Why do we choose OFDM?

Due to the delay spread of multi-path propagation in wireless communications, a symbol from long-delay echo paths may be received together with one or several successive symbols from short-delay paths, as is called ISI. The number of influenced adjacent symbols  $N_{\text{isi}}$  is decided with the maximum delay spread  $\tau_{\text{max}}$  and the symbol duration  $T_s$  by

$$N_{\text{isi}} = \left\lceil \frac{\tau_{\text{max}}}{T_s} \right\rceil \quad (3.1)$$

At a receiver, an equalizer is usually applied to compensate the effect of ISI. Several adaptive equalization algorithms are presented in [Pro91, Pro01], including their performance characteristics and limitations. Their computation complexities are approximately proportional to  $N_{\text{isi}}$  and in some cases even have an order of  $N_{\text{isi}}^2$ . In a high data rate and wideband wireless communication system where  $\tau_{\text{max}} \gg T_s$ , this factor becomes critical and the needed equalizer becomes more impracticable.

Considering the fact that a channel is unchangeable, the only way to reduce ISI according to equation (3.1) is to increase the symbol duration. This can be achieved by applying a multi-carrier transmission, as shown in figure 3.1. A subband centralized with a subcarrier can be further thought as a flat channel. The narrow signal frequency band leads to longer symbol duration than the delay spread. However, without an ideal isolation the signals in those subcarriers interfere with each other. By convention, those ICIs are controlled by a filter with small side lobes and guard frequency bands between adjacent subbands.

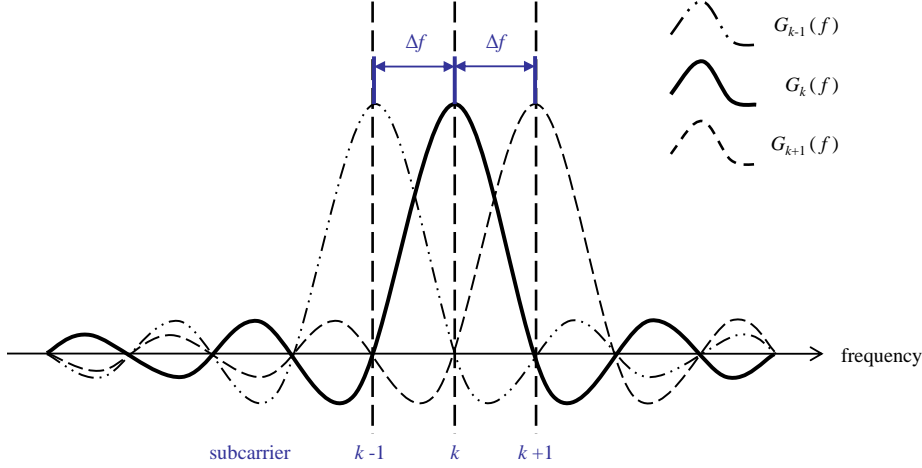


**Figure 3.2:** A part of OFDM spectrum

The OFDM transmission technique, with a specific but simple signal spectrum for all subcarriers, eliminates the interference from one subcarrier to another. Those in-between frequency guard bands can be removed and the bandwidth can be utilized to the most content.

### 3.2 An OFDM Transmission System

As mentioned above, the OFDM technique realizes a seamless connection of neighboring subbands by designing a spectrum for signals in each subcarrier. In figure 3.2, the signal in subcarrier  $k$  has always a zero power at the frequencies of all other subcarriers. To construct such a format, the following mask spectrum is generated with the sinc function

$$G_k(f) = T_s \cdot \text{sinc}(\pi T_s (f - k\Delta f)) \quad (3.2)$$

The symbol duration  $T_s$  is calculated as the inverse of frequency spacing  $\Delta f$  between two adjacent subcarriers. The width of each subband fulfills the condition  $\Delta f \ll B_c$ , so that each subcarrier can be regarded as a “flat” narrow-band channel.

$$T_s = \frac{1}{\Delta f} \quad (3.3)$$

In the time domain, the adopted sinc mask is equivalent to the rectangular function  $\text{rect}(\cdot)$  with a time-variant phase shift for each subcarrier.

$$g_k(t) = e^{j2\pi k\Delta f t} \cdot \text{rect}\left(\frac{t}{T_s}\right) \quad (3.4)$$

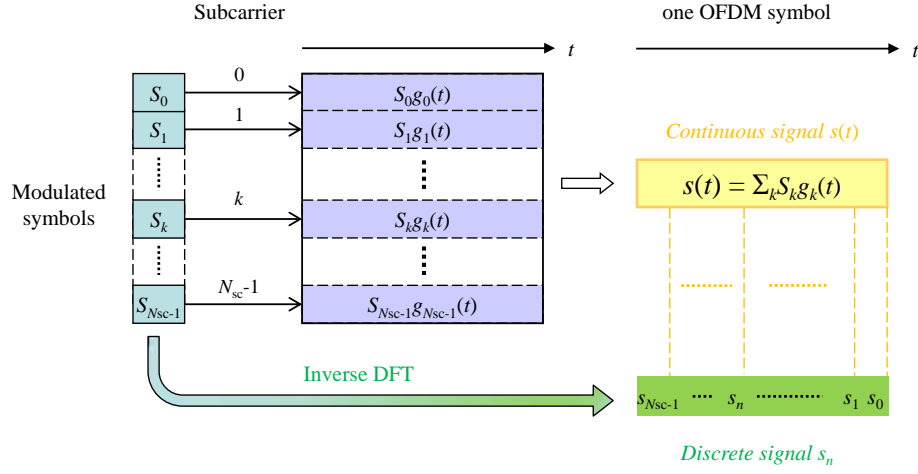


**Figure 3.3:** Modulation symbols are mapped to a single OFDM signal

With the OFDM transmission technique, the complete bandwidth is divided into  $N_{sc}$  subcarriers. A group of successive modulated symbols is mapped to a single OFDM symbol, with one symbol  $S_k$  for each subcarrier  $k$ . The transmitted signal  $s(t)$  inside the OFDM symbol can be given as the below equation (3.5). The processing procedure is shown in figure 3.3.

$$s(t) = \sum_{k=0}^{N_{sc}-1} S_k \cdot g_k(t) = \sum_{k=0}^{N_{sc}-1} S_k \cdot e^{j2\pi k \Delta f t} \cdot \text{rect}\left(\frac{t}{T_s}\right) \quad (3.5)$$

Although the symbols in different subcarriers are transmitted simultaneously in a mixed manner inside an OFDM symbol, the orthogonality is still preserved between any subcarriers  $m$  and  $k$  if  $m \neq k$  with the selected mask.

$$\frac{1}{T_s} \int_0^{T_s} g_k(t) g_m^*(t) dt = \frac{1}{T_s} \int_0^{T_s} e^{j2\pi(k-m)\Delta f t} \cdot dt = \begin{cases} 1, & \text{if } m = k \\ 0, & \text{if } m \neq k \end{cases} \quad (3.6)$$

Therefore, the symbol  $S_m$  transmitted in subcarrier  $m$  can be easily recovered by the following calculation.

$$S_m = \frac{1}{T_s} \int_0^{T_s} s(t) g_m^*(t) dt \quad (3.7)$$

The orthogonality property in the OFDM transmission technique is shown in figure 3.4.

In digital communications, the transmitted time discrete symbols can be calculated with an Inverse Discrete Fourier Transformation (IDFT) operation,



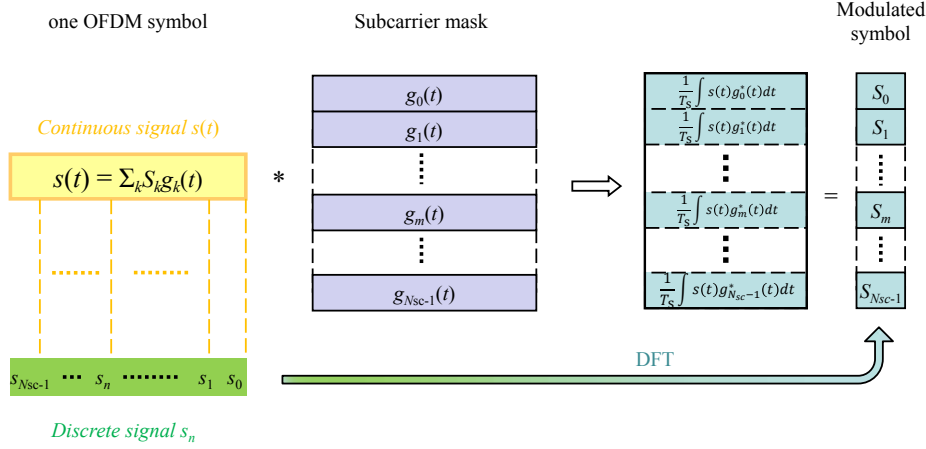


**Figure 3.4:** Orthogonality in the OFDM transmission technique

$N_{sc}$  modulated symbols are mapped to a same number of complex values  $s_n$ , which are transmitted sequentially over time. The sampling period  $\Delta t$  is calculated from the total signal bandwidth.

$$\Delta t = \frac{1}{N_{sc} \cdot \Delta f} \quad (3.8)$$

A factor  $1/\sqrt{N_{sc}}$  is added for the purpose of normalization.

$$s_n = \frac{1}{\sqrt{N_{sc}}} \sum_{k=0}^{N_{sc}-1} S_k \cdot e^{j2\pi nk/N_{sc}}, \quad n = 0 \dots N_{sc} - 1 \quad (3.9)$$

To remove the ISI completely, a guard interval is appended in front of each OFDM symbol. The length of guard interval should be not shorter than the maximum delay spread, i. e.  $T_g \geq \tau_{\max}$ . This guard interval is also named Cyclic Prefix (CP), because it is a copy of last part of a OFDM symbol. In the discrete time domain, a number of  $N_g$  samples are duplicated into a prefix.

$$s_n = s_{n+N_{sc}}, \quad n = -1 \dots -N_g \quad (3.10)$$

The appending of CP does not cause any change in the frequency of transmitted signal. Furthermore, the CP can act as a buffer region, where the delayed information from the previous symbol can get stored.

In figure 3.5, three symbols received from paths with different delays are presented. The enclosed area shows an ISI free time range, where the information from the other symbols has been excluded.

The usage of CP also ensures that the orthogonality between subcarriers in OFDM is not affected by the multi-path propagation. As a cost, the total

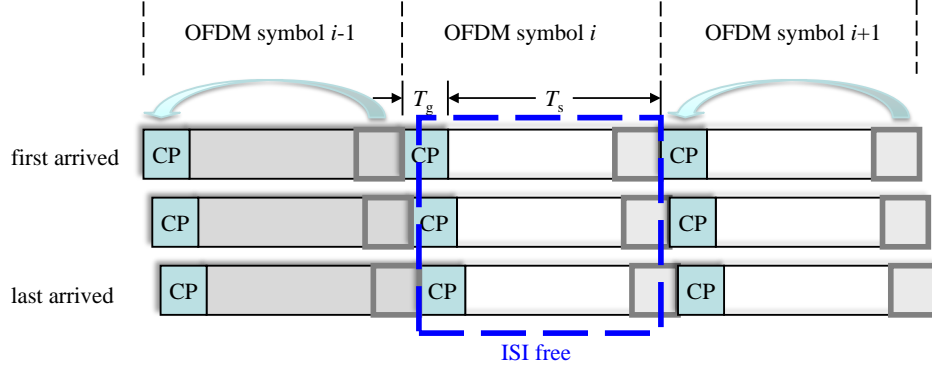


**Figure 3.5:** ISI free range in an OFDM symbol with cyclic prefix

symbol duration is consequently increased, and the data rate is reduced.

$$T = T_s + T_g \quad (3.11)$$

The above described signal processing are done at the transmitter in an OFDM transmission system shown in figure 3.6. At the receiver, the CPs are removed. The modulated signals  $S'_k$  are calculated from the received discrete signal  $s'_n$  in the time domain with a Discrete Fourier Transformation (DFT) operation.

$$S'_k = \frac{1}{\sqrt{N_{sc}}} \sum_{n=0}^{N_{sc}-1} s'_n \cdot e^{-j2\pi kn/N_{sc}}, \quad k = 0..N_{sc} - 1 \quad (3.12)$$

Because there is no ICI between subcarriers, and each subband is approximately a flat channel, a simple relation between a received signal and the

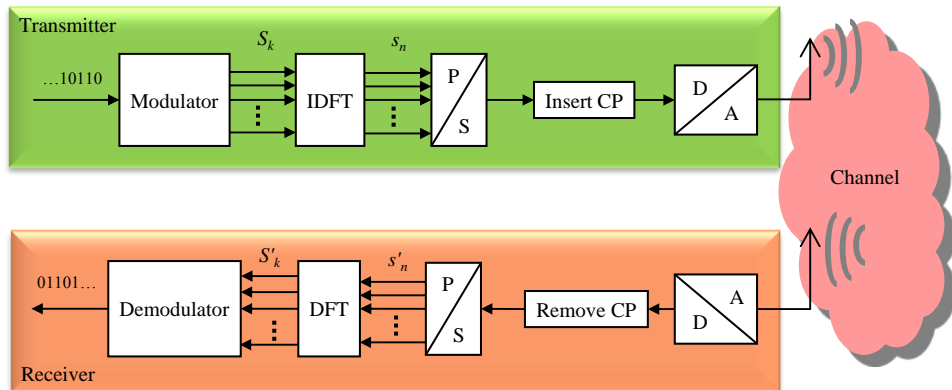


**Figure 3.6:** An OFDM transmission system

transmitted signal can be obtained.

$$S'_k = H_k \cdot S_k + N_k \quad (3.13)$$

Here  $H_k$  is the channel transfer factor in subcarrier  $k$ , and  $N_k$  is the noise at the receiver in the same subcarrier. With an also simple equalizer, the transmitted symbol can be recovered.

Due to the eigenfunction property of LTI systems, the subcarrier signals are even orthogonal at the output of a frequency selective radio channel. This is an important feature in the OFDM transmission technique.



## Chapter 4

# Radio Resource Management in Cellular Systems

CAPACITY and coverage are two main objectives in the design of a mobile communication system. The cellular concept serves and satisfies multiple users in a larger service area. Each user is allocated a number of radio resources, which can be reused at a certain spatial distance. Each BS is responsible for only a part of the network, named as a cell. The same radio resources can be used simultaneously in several adjacent cells as long as they are far away from each other, in order to avoid any potential CCI.

In conventional FDMA based cellular systems like GSM, the full bandwidth is divided into several frequency subchannels, each of which can be regarded as an independent radio resource. In a detailed network planning procedure, each individual cell allocates one or several of these resources in a way that almost all CCIs can be avoided. As the allocation is unchanged between two planning operations, it is named fixed resource (channel) allocation.

The OFDM based cellular system facilitates the usage of Single Frequency Network (SFN), where each BS transmits signals in the same central carrier frequency but with different resources. With the self-organized radio resource management, the network planning process is not required. The radio resources in such a cellular network can be utilized in a more flexible and more efficient way.

The concept of resource reuse and the FRA scheme in conventional cellular networks will be firstly presented in this chapter. After the introduction of an OFDM based cellular SFN, the SO-RRM scheme will be described briefly.

## 4.1 Conventional Cellular Network with FRA

The CCI is a major limitation to the performance of cellular networks. The same radio resource can be used simultaneously by two or more BSs, if they are spatially separated by a long distance, or more precisely, their CCIs to each other are weak enough. This is called resource reuse. An efficient cellular wireless system relies on an intelligent reuse of radio resources throughout the coverage region.

In a basic reuse picture, cells are organized in clusters. A cluster size is defined as the number of cells that use all resources exclusively and completely. All resources are allocated to a cluster of neighboring cells. The number of radio resources assigned for each cell depends on the amount of predicted traffic load. Assuming a uniform distribution of users inside the observation area, each cell will be allocated an identical number of resources. The similar allocation pattern is expanded to other portions within the service area.

A part of a cellular network with a cluster size of 7 is illustrated in figure 4.1 as an example. The adjacent cells labeled with number 1 to 7 compose a single cluster. In the GSM system, a single radio resource is defined as one subchannel in frequency. For example with a predicted uniform traffic load, all resources will be grouped into 7 subsets with an identical number of subchannels. The same subset of frequency resources is available in cells with a same label in the figure. Adjacent cells with different labels are assigned different subsets.

In conventional cellular systems, the cluster size is determined with the worst case as shown in the figure. An MT is assumed locating at a vertex of a cell. Only interference from those six first-tier co-channel cells is taken into account. The interference from the second and higher tiers of co-channel cells (out of the display range of the figure) is neglected because of their relatively small contribution to the CCI.

In the network planning procedure, only the path loss is included for the reason of statistical averaging. All BSs are assumed to transmit with an identical power in any frequency channel. The SINR at the target MT in the Downlink (DL) can be expressed by

$$SINR_{DL} = \frac{S}{\sum_{i=1}^6 I_{i,DL} + N_0} \quad (4.1)$$

where  $S$  denotes the power of the signal received from the transmitter, and  $I_{i,DL}$  denotes the interference from the  $i$ -th co-channel cell in the DL. Considering that  $I_{i,DL} \gg N_0$  in most cases, the SINR can be rewritten as

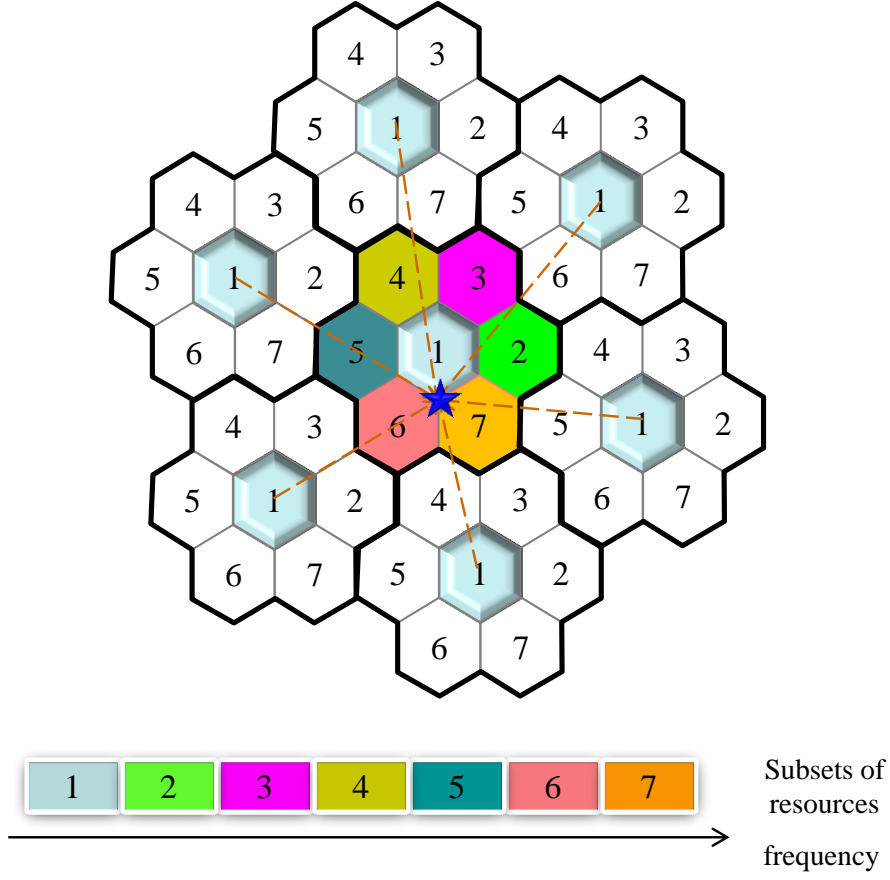


**Figure 4.1:** A part of cellular network with cluster size 7, showing the worst case in downlink

$$SINR_{DL} = \sum_{i=1}^6 \left( \frac{D_{i,DL}}{R_c} \right)^{-\alpha} \quad (4.2)$$

In the above equation,  $\alpha$  is the propagation coefficient,  $R_c$  is the radius of a cell, and  $D_{i,DL}$  is the distance between the MT and the interferer BS at the  $i$ -th co-channel cell. A similar calculation can be figured out for the Uplink (UL). Assuming  $\alpha=4$ , the SINR in downlink is approximately 17.8 dB, which is already sufficient to support a common communication. Further results with various cluster sizes and path loss exponents are presented in [Rap02].

A similar planning process can be done in the situation of a predicted non-uniform traffic load distribution among the network [Zha91]. That assignment of subchannels for each cell is valid until the next planning procedure. However, with an FRA scheme, a network reconfiguration must be always

performed when a new BS is connected to or disconnected from the cellular system. Nevertheless, because the planning is based on an ideal analytical model, the further radio network optimization must be processed according to the actual situation and be kept updated throughout the whole operation of the GSM system.

The basic FRA scheme is based on the prediction of long-term network traffic load. Such a scheme has a low flexibility and no adaptivity to changing environment condition and user distributions. For example, an unexpected increase of call requests occurring in a hotspot and lasting for a few hours will result in a radio traffic jam. Obviously, such a short-term behavior does not deserve a planning update in the whole network. Orienting to that situation, additional free resources may be temporarily “borrowed” from adjacent cells. This is called resource borrowing, which can work as a complementary to the basic FRA. Because a shift of any resources will induce the change on interference structure in the network, the borrowed resources and its owner must be carefully selected. Several different borrowing algorithms have been compared in [Kat96].

## 4.2 OFDM Based Cellular Systems

In an OFDM based cellular system, the classical FRA procedure can be still applied. However, in this section a specific cellular network with high flexibility in the resource allocation scheme and high adaptivity in time-variant and frequency selective radio channels will be designed. Based on the OFDM transmission technique with orthogonal subcarriers, a single frequency network technique with time and carrier synchronized BSs and MTs can be adopted. In this case, each cell can claim radio resources very flexibly in a self-organized way.

### 4.2.1 Single Frequency Cellular Network

A concept of SFN was firstly introduced by OFDM based radio and television broadcasting systems. All broadcast stations transmit identical signals on the same carrier frequency, in order to enhance the transmission quality, as well as to enlarge the network coverage and spectral efficiency. Electronic devices will receive signals simultaneously from several adjacent stations. The synchronization in time (clock) and frequency with high accuracy is required in this case [Zir01]. Today’s OFDM based broadcasting systems, such as DAB, DVB, and DRM, are all designed as SFN.

This SFN concept can also be applied inside a cellular communication system. Figure 4.2 shows the basic concept of resource usage in an OFDM based SFN cellular system.



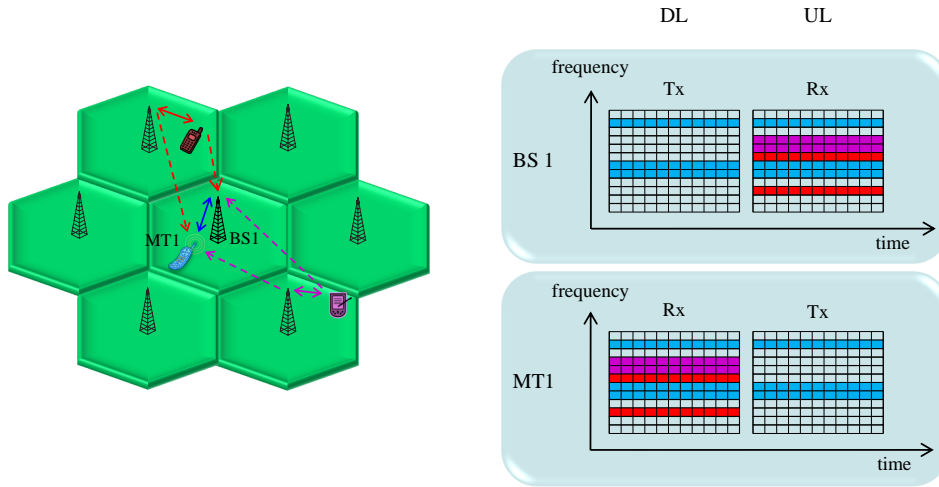


**Figure 4.2:** OFDM based single frequency cellular network

All BSs and MTs can operate in the same frequency band simultaneously. BSs and MTs in adjacent cells transmit signals with different resources, in order to avoid the CCI. In the example, the Transmitter (Tx) BS1 transmits signals to the Receiver (Rx) MT1 in the allocated subcarriers in downlink. However, the MT1 receives not only the signals from the BS1, but also signals from the adjacent BSs. Due to the orthogonality between subcarriers in the OFDM transmission technique, those signals from different BSs do not interfere with each other. Similarly, the BS1 receives signals from both its own MTs and those in other cells in the uplink.

It is worthy being mentioned, that a single radio resource in an OFDM based SFN system can be defined not only as a number of subcarriers or as a number of timeslots, but also more flexibly as a time-frequency block, i. e. a combination of OFDM symbols and subcarriers.

A first system concept of OFDM based SFN has been proposed in [Gal03], with a self-organized radio resource management scheme. The same basic concept is considered in this thesis.

As all BSs transmit their individual signals on the same central carrier frequency, a synchronization of all BSs in time and frequency is required to avoid any cross talks between adjacent OFDM symbols or subcarriers. A synchronization scheme has been proposed in [Roh04], with which a fast and precise synchronization can be realized in a self-organized way by continuous measurement and adjustment at both BSs and MTs.

### 4.2.2 Self-Organized Radio Resource Management

To use the spectrum efficiently, a self-organized radio resource management scheme is proposed for OFDM based SFN cellular mobile communication systems. Resources are not fixed to any cell, but instead concentrated in a common pool. Each BS has a full access to those resources all the time, and allocates some of them to a transmission only upon a user's request. The reuse distance is thus time-variant and adaptive to the current traffic load situation in the cellular network. A flexible and efficient resource reuse can be realized, especially in the case of non-uniform user distribution.

The decision of resource allocation is made independently at each BS in the proposed SO-RRM scheme, based on the measurement of signal and interference strengths. Although there is no information exchange with any other BS, the status of resource occupation in adjacent cells can be obtained from the measured CCI. A strong interference received in a radio resource implies that the considered resource is already used in the nearby cells. From those resources with sufficient SINR, the ones with highest values will be allocated.

The Adaptive Modulation and Coding (AMC) technique can be applied additionally to the resource allocation procedure, so as to increase the spectrum efficiency. A high rate data stream is transmitted with a less interfered resource, while another strongly interfered resource will be assigned only for a low rate transmission, or even be set idle. Link adaptation is also applied against the channel fluctuation over time during a transmission.

The central controllers in conventional cellular systems are not needed in the proposed RRM scheme. As an important advantage, that self-organized policy enables a seamless expansion of cellular network and a fast change in the cellular structure. The startup or shutdown of a BS anywhere in the network does not require a global channel reconfiguration.

The detailed structure of such an OFDM based cellular system and the self-organized resource allocation algorithm will be described in the next chapter.

## Chapter 5

# SO-RRM in OFDM Based Cellular Systems

THE radio resource management works in the Medium Access Control (MAC) sublayer, which is an interface between the Physical (PHY) layer and the Logic Link Control (LLC) sublayer in the Open System Interconnection (OSI) reference model. It defines the segmentation and organization of radio resources, and the multiplexing scheme that enables simultaneous transmissions by multiple users. Therefore, the design of this sublayer is one basis for any RRM scheme. The system parameter should be selected carefully, taking into account both the user requirements and the radio channel behaviors.

The selection of radio resource in the SO-RRM is done independently and individually at each BS in a self-organized way, based on measurement of both signal and CCI. The spectrum efficiency can be further increased by introducing the AMC technique and the link adaptation technique in the PHY layer. To have an easy quality estimation of possible data transmission, a quality mapping function is introduced. Such a function maps the measured statistical characteristics of the radio channel of a resource directly to system level QoS indicators.

Because a decision is made according to the network situation at the time of allocation, a connection may be interrupted during the transmission because of the accumulating CCI, which is caused by new co-channel transmissions. Anti-dropping solutions would be applied to mitigate this issue.

This chapter describes firstly the MAC and PHY layer specifications of the proposed OFDM based cellular system. Afterwards the protocol of resource allocation for a new call request in the SO-RRM scheme is presented in detail. Two anti-dropping schemes will be proposed and compared as well.

## 5.1 MAC Layer Description

This section describes two main parts in the MAC layer: duplex and multiplexing, and frame structure.

### 5.1.1 TDD Scheme

The proposed OFDM based cellular network uses Time Division Duplex (TDD) to separate the downlink and uplink transmissions. The TDD mode has been included in systems such as Digital Enhanced Cordless Telecommunications (DECT), Time Division Synchronous CDMA (TD-SCDMA), Worldwide interoperability for Microwave Access (WiMAX), and UMTS-TDD.

Comparing with the alternative Frequency Division Duplex (FDD) scheme, TDD has a strong advantage when uplink and downlink transmissions show an asymmetry. The amount of resources can be easily shifted when the uplink/downlink demand ratio changes. Another advantage is that the radio channels in two link directions are quite similar in the case of low mobility. A channel estimated in one direction is also valid for the other, so that the related overhead can be reduced.

FDMA is selected as the multiple access protocol for the proposed system. Users are transmitting in this case on different subcarriers. Future mobile communication systems are expected to support a large number of applications like transferring a file with a big size, or stream data applications such as video on demand. Comparing to TDMA and CDMA, FDMA is quite suitable for such kind of time-continuous high rate applications, because predetermined subcarriers can be used during the entire period of communication.

Moreover, FDMA brings another advantage in a wideband system with strong frequency selectivity. The spectrum efficiency will increase remarkably, when the AMC technique is applied in transmission. Each user can transmit data with different rates in subcarriers according to their channel conditions. On contrast, with TDMA or CDMA a compromised transmission rate must be chosen to find balance between light and deep faded subcarriers.

### 5.1.2 MAC Frame

The MAC frame in the proposed system has a structure in figure 5.1.

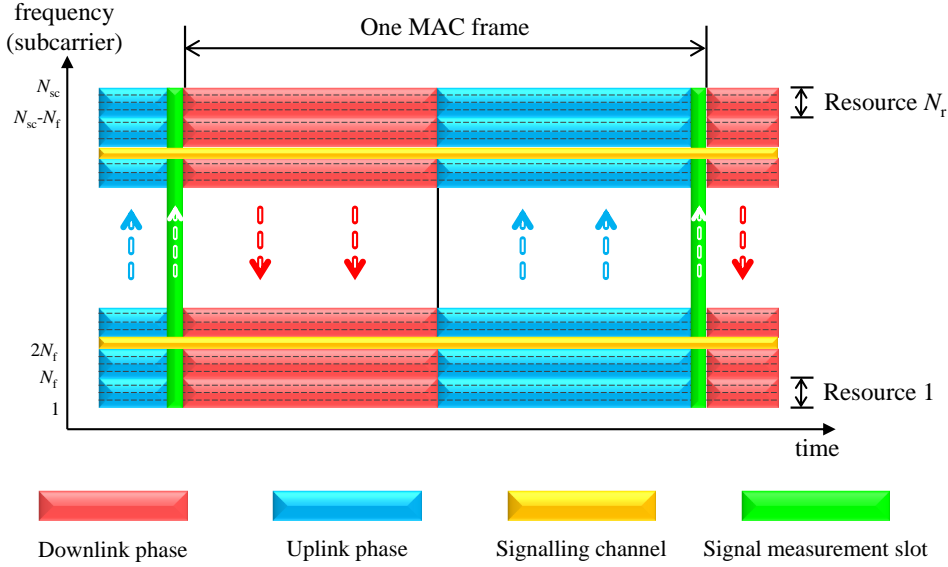


Figure 5.1: MAC frame structure

#### 5.1.2.1 Frequency and Time Direction

In the frequency dimension, the entire OFDM bandwidth is divided into  $N_{sc}$  subcarriers with an equal frequency spacing  $\Delta f$ . Besides traffic channels that are used for data transmission, some subcarriers are reserved as the signaling channel. It is used for all BSs to broadcast paging messages. During the call setup phase, that channel is also used for exchange of controlling information between a BS and an MT. Those subcarriers used for signaling are uniformly located in the spectrum, in order to minimize the influence of frequency selectivity.

One single subcarrier can supply only a very low data rate, which is insufficient to fulfill the minimum requirement of future applications. Therefore, a single resource is defined as a cluster of  $N_f$  adjacent subcarriers. Each user will be allocated one or several resources, depending on the radio channel condition and its requirement on data rate.

Assuming  $N_{sig}$  signaling subcarriers, the total number  $N_r$  of available payload resources can be calculated by

$$N_r = \frac{N_{sc} - N_{sig}}{N_f} \quad (5.1)$$

A single frame covers one downlink phase plus one uplink phase in the time direction. The DL phase is designed for the data transmission from the BS to MTs, while the UL phase is for the inverse purpose. Although

TDD facilitates asymmetric traffic loads, transmission in both directions are assumed to occupy an identical portion in the considered system. Either of them contains  $N_s$  successive OFDM symbols. The time gap for the hardware transitions between UL and DL are neglected here. The time duration  $T_f$  of one MAC frame can be calculated from the duration  $T$  of one OFDM symbol by

$$T_f = 2 \cdot N_s \cdot T \quad (5.2)$$

### 5.1.2.2 Signal Measurement Slot

To have a precise measurement of power, the user signal should be transmitted when all interferers are silent. A dedicated signal measurement slot (shortened as SM-slot) is introduced for this purpose. This slot covers the last OFDM symbol in the uplink phase of each frame. It is reserved exclusively for transmissions of test signals from any new MT inside the cell. In the frequency direction, all subcarriers except the signaling channel are included.

The detail of signal measurement will be introduced in the next chapter.

## 5.2 Physical Layer Specification

Those parameters related to the OFDM based transmission in the simulation are listed in table 5.1.

### 5.2.1 Simplification of Channel Model in Simulation

The system level simulation focuses mainly on the long-term behavior of mobile communication systems. Some rational simplification can be applied to the WSSUS channel model, which is described in section 2.4.

It can be carried out from those parameters that the MAC frame duration is less than the coherence time, which implies that the radio channel has no significant change inside single frame duration. In the frequency direction, the total bandwidth of a resource is narrower than the coherent bandwidth. In other words any  $N_f$  adjacent subcarriers have an approximately identical channel transfer factor and can be used together as one flat channel. Those two conditions can be mathematically described as

$$\begin{aligned} T_f &< \frac{1}{f_{D, \max}} \\ N_f \cdot \Delta f &< \frac{1}{\tau_{\max}} \end{aligned} \quad (5.3)$$

**Table 5.1:** OFDM related parameters

Parameter	Value
Central carrier frequency	$f_0 = 5 \text{ GHz}$
System bandwidth	$B = 20 \text{ MHz}$
Subcarrier spacing	$\Delta f = 39.0625 \text{ kHz}$
Maximum delay spread	$\tau_{\max} = 3.2 \text{ }\mu\text{s}$
Maximum Doppler frequency shift	$f_{D, \max} = 50 \text{ Hz}$
Number of subcarriers	$N_{\text{sc}} = 512$
Number of signaling subcarriers	$N_{\text{sig}} = 8$
Number of subcarriers per resource	$N_{\text{f}} = 4$
Number of resources	$N_{\text{r}} = 126$
Duration of OFDM block	$T_{\text{s}} = 25.6 \text{ }\mu\text{s}$
Duration of guard interval	$T_{\text{g}} = 3.2 \text{ }\mu\text{s}$
Duration of OFDM symbol	$T = 28.8 \text{ }\mu\text{s}$
Number of symbols per UL/DL phase	$N_{\text{s}} = 60 \text{ symbols}$
Frame duration	$T_{\text{f}} = 3.456 \text{ ms}$

Therefore, a time-invariant flat channel within each  $T_{\text{s}} \times N_{\text{f}} \Delta f$  time-frequency block is assumed in the simulation. That is, an AWGN channel is assumed for the radio channel inside such a block. It is further assumed that those channel transfer factors in different blocks are uncorrelated.

From the adopted channel model, it can be carried out that the random channel transfer factors  $|H|$  in different time-frequency blocks are Rayleigh distributed.

$$p(|H|) = \frac{|H|}{\sigma_{\text{H}}^2} e^{-\frac{|H|^2}{2\sigma_{\text{H}}^2}} \quad (5.4)$$

The corresponding magnitude  $|H|^2$  has thus an exponential distribution as

$$p(|H|^2) = \frac{1}{2\sigma_{\text{H}}^2} e^{-\frac{|H|^2}{2\sigma_{\text{H}}^2}} \quad (5.5)$$

The channel is normalized when  $\sigma_{\text{H}} = 1/\sqrt{2}$ . Probability density functions of both  $|H|$  and  $|H|^2$  in this case are shown in figure 5.2.

### 5.2.2 Adaptive Modulation and Coding

In digital signal transmissions, the information bits are modulated and coded, in order to increase transmission efficiency and minimize error probability. The combination of those two parameters is commonly termed as

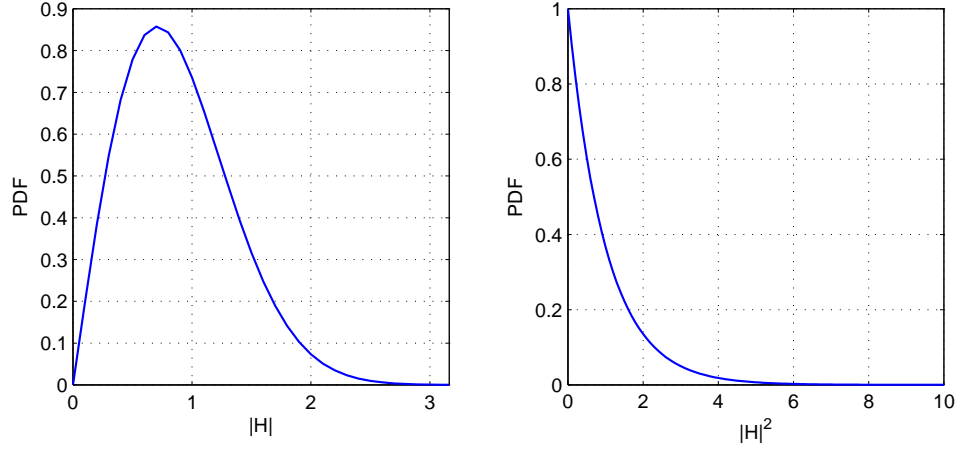


**Figure 5.2:** Rayleigh distributed channel transfer factor  $|H|$  and exponentially distributed  $|H|^2$

physical layer mode (PHY mode). A high rate mode supports fast transmission, which is robust however only with a high Signal-to-Noise Ratio (SNR). While a low rate mode is robust with strong noise, but can transfer only fewer data. The AMC technique matches the PHY mode parameters automatically to the channel condition. A high rate transmission is chosen for a cleaner channel, while a low rate mode is used for a noisy channel. This technique has been used in cellular systems such as General Packet Radio Service (GPRS), Enhanced Data rates for GSM Evolution (EDGE), and HSDPA.

The AMC technique is also used and is facilitated by the adopted FDMA scheme in the proposed OFDM based system. Five Quadrature Amplitude Modulation (QAM) modes are used in the simulated systems. The number of points in their constellation diagram is a power of 2. The 2-QAM and 4-QAM is also called as Binary Phase Shift Keying (BPSK) and Quadrature Phase Shift Keying (QPSK). In addition, a truncated convolutional coding scheme with a code rate  $1/2$  is adopted for all QAM modes.

In total  $L_f$  modulated symbols are transmitted with one resource in either the downlink or the uplink phase.

$$L_f = N_s \cdot N_r \quad (5.6)$$

The data are grouped and transmitted in packets. The number of bits  $L_p$  inside a packet is defined equal to the amount of info bits that can be transmitted in one DL/UL phase over a resource when the slowest transmission mode BPSK is selected with coding rate  $1/2$ .

$$L_p = \frac{L_f}{2} \quad (5.7)$$



**Table 5.2:** Available PHY modes

Parameter	Value				
Information bits per packet	$L_p = 120$ bits				
Convolutional coding rate	$1/2$				
Modulation scheme	BPSK	QPSK	16-QAM	64-QAM	256-QAM
Number of transmitted packets per resource per frame (UL/DL)	1	2	4	6	8

It can be carried out that the highest PHY mode with 256-QAM can transmit 8 packets in a single resource per frame. The supplied rates in all five PHY modes are listed in table 5.2.

The selection of a proper PHY mode is based on the estimated SNR value in a radio channel and the QoS requirement of a transmission, as shown in figure 5.3. A delay-oriented AMC algorithm is applied. Comparing with the alternative throughput-oriented AMC, it minimizes the average packet delay, which is important in real-time communication [Lam04].

Those Packet Error Rate (PER) curves are obtained from the physical layer simulation in Additive White Gaussian Noise (AWGN) channels with the selected five modulations and a constant coding rate  $1/2$ . Given a maximum PER of 1%, the threshold SNR values are listed in table 5.3.

An AMC mapping function is constructed accordingly as follows.

$$[N_{tp}, PER] = M_f(SNR) \quad (5.8)$$

The variable  $N_{tp}$  denotes the decided number of transmitted packets in each UL/DL phase of one frame.  $N_{tp} = x$  when  $2^x$ -QAM modulation is selected, while  $N_{tp} = 0$  means that the SNR of a channel is too less to supply a reliable transmission, and no data will be transmitted. The corresponding PER value is another output of this mapping function.

Those signals in the signaling subcarriers use only the BPSK modulation for a maximum possible robustness.

**Table 5.3:** PHY mode selection in AMC

Modulation	Unused	BPSK	QPSK	16QAM	64QAM	256QAM
SNR Range [dB]	$(-\infty, 0)$	$[0, 3)$	$[3, 8.6)$	$[8.6, 13.3)$	$[13.3, 17.3)$	$[17.3, +\infty)$

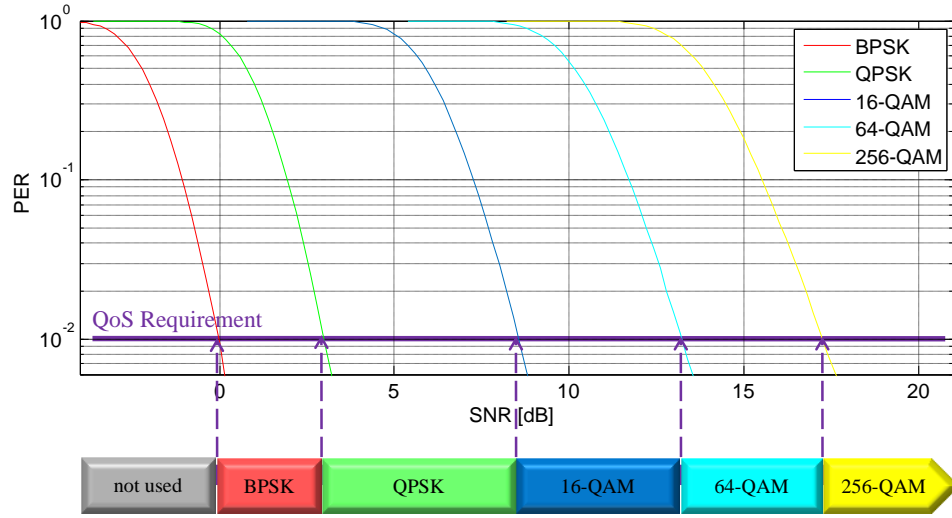


**Figure 5.3:** Selection of modulation and coding in AMC

### 5.2.3 Resource Quality Mapping Function

To evaluate the quality of a transmission in the system level simulation, a proper resource quality mapping function should be introduced to avoid the bit level simulation efforts. [Mei09] considers a time invariant channel and thus the quality of a resource can be easily represented by the corresponding transmission rate derived from a single channel SINR, calculated with the above-described AMC mapping function.

However, in the investigated system here a radio channel is time-variant from frame to frame in the whole transmission duration, although it is assumed invariant within each MAC frame. To describe completely the channel in such a long duration, a new mapping function is proposed to transfer the statistical characteristic of the channel of a resource to the supplied data rate.

The error rates of received packets are very sensitive to the fluctuation of channel attenuation. The transmission with a high rate PHY mode in a radio channel with frequent deep fading may cause unexpected great performance degradation [Gib99]. In order to have a robust communication and a simple structure, the early applications use commonly a low rate PHY mode. It is easy to realize and is reliable against the channel fluctuation, but the spectrum efficiency is very low.

Link adaptation adjusts dynamically the transmission parameters according to the change of a channel. A high-rate PHY mode is selected when the channel is inside the time windows with a high SNR value, while a low-rate one is used in case of deep fading. This technique has been successfully

implemented in the HSDPA system today.

The adaptation process relies on the available channel information at the transmitter. Such kind of information can be either a certain channel quality measured in physical layer [Fal04, Ste03, Ye02, For02, Lam02], or the acknowledgement message which is fed back to the transmitter in data link layer [Hal04]. In [Cat02] a combination of these variables is utilized together with the hot MIMO-OFDM technique, in order to reach both accuracy and robustness. In a TDD system, it can be directly acquired by assuming the channels are similar in downlink and uplink.

The link adaptation technique is also applied in the proposed OFDM based cellular system. The performance of imperfect link adaption is out of the range of this thesis, and a perfect adaptation is assumed in the further discussions. The selection of PHY mode is based on the AMC scheme described in the previous section.

Assuming there are in total  $N$  frames during the completed transmission, the supplied data rate in either the DL or the UL of a resource can be calculated as

$$R = \frac{L_p}{2 \cdot N \cdot T_f} \sum_{n=1}^N N_{tp,n} (1 - PER_n) \quad (5.9)$$

In the equation the variable  $L_p$  denotes the number of data bits transmitted in one packet,  $T_f$  is the time length of one frame. An extra factor of  $1/2$  is applied due to the division of every frame into two time-equal UL and DL phases in the TDD scheme.

The variable  $N_{tp,n}$  and  $PER_n$  is respectively the number of transmitted packets and the PER in the  $n$ -th frame. Both of them are derived from the AMC mapping function  $M_f(\cdot)$ , provided the SNR value of the channel in the frame.

$$[N_{tp,n}, PER_n] = M_f(SNR_n) = M_f(\overline{SNR} \cdot |H_n|^2) \quad (5.10)$$

According to the assumption that the channel transfer factor  $|H|$  in different frames in one resource has a Rayleigh distribution, the resource quality mapping function  $M_c$  of the considered time-variant channel can be constructed as the following equation.

$$R = M_c(\overline{SNR}) \quad (5.11)$$

Only one input parameter, the mean SNR value over time, is now needed in the function. The output is the data rate  $R$  in the considered resource.

The result of estimated data rates in one resource with different mean SNR values is plotted in figure 5.4. It is compared with the performance without

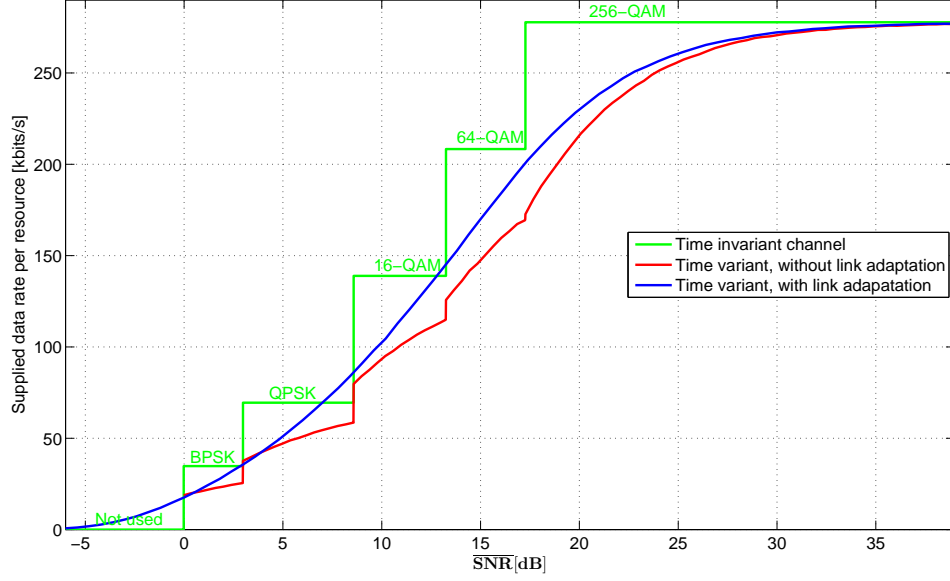


**Figure 5.4:** Resource quality mapping function

link adaptation, where a fixed PHY mode is selected based on the AMC mapping function with the same mean SNR value. It can be observed that link adaptation brings higher rates in a time-variant channel, especially when the average SINR is between 7 dB and 20 dB. The link adaptation also overcomes the quantization effect, i.e. the staircase-like transition of transmission rate at those threshold points for the PHY mode selection. The resource quality mapping function in a time invariant channel is also given as a reference.

### 5.3 Resource Allocation for a New User

In the proposed measurement-based and self-organized resource allocation, the best possible resources are chosen in the term of SINR values for each conversation request from a new active MT. Those values are calculated from the measured strengths of the user signal and the CCIs.

The user signal is measured at the BS by transmitting a test signal from the MT in the uplink. The uplink interferences are measured by the BS during the uplink transmission phase. Those CCIs received at the BS reflect indirectly the usage of resources in its surrounding cells. On the other side, the downlink interferences are measured by the MT before it sends a request to the BS.

Resource qualities are then estimated for all available resources in both downlink and uplink. The detailed procedure of resource assignment for a

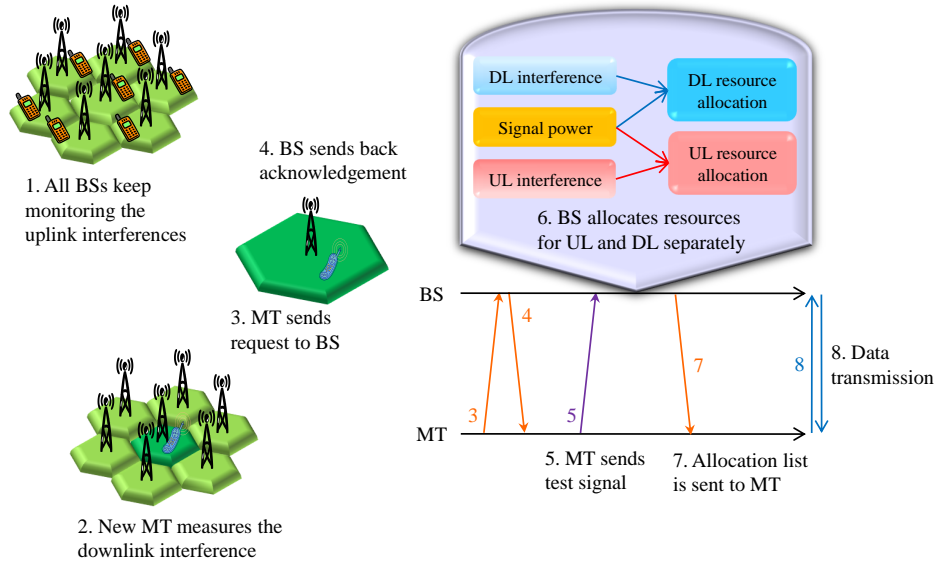


**Figure 5.5:** Procedure of self-organized resource allocation

new user is described in steps shown in figure 5.5.

#### 1. Uplink interference power tracked at each BS

Each BS receives simultaneously signals from its own MTs and from the MTs in adjacent cells. The latter signals are regarded as interference in the uplink. In order to keep watching, each BS records the received CCI strength in every frame. As the collected information is used only for the resource allocation, that tracking operation is performed only in those idle resources, i. e. the ones which is not used by the BS itself.

The strength of the uplink interference is estimated by averaging the measured values in a certain number of recent frames, in order to cancel out the influence of channel fluctuation and to keep the value up to date.

#### 2. Downlink interference measurement at the new MT

When an MT is going to make a call, it listens to the network at first. During the downlink phase, it receives signals from all surrounding BSs. Such a measurement lasts for a sufficient number of frames, and the values are averaged over time for each resource. Thus, the MT has a clear understanding about the allocated resources in downlink, which also works as a basis for the resource selection. The list of resources with least interferences will be afterwards reported to the BS.

#### 3. Locking BS and sending call request with identification

All BSs broadcast their identification codes and other necessary information on the reserved broadcast channel. The terminal then is able to choose one

BS as its server, normally from which the strongest signal is received in a dedicated Broadcast Control Channel (BCCH). Afterwards the terminal sends to the selected BS its request message and the other related data on the Common Control Channel (CCCH).

#### 4. Acknowledgement and timeslot assignment for test signal

Confirming the request from an MT, the BS sends back an acknowledgement. At the same time it reserves one timeslot, which will be used exclusively for the test signal. This timeslot occupies the last OFDM symbol at the end of the uplink phase of one frame and the whole band in frequency. The information of this timeslot is then sent back to the MT.

#### 5. Radio channel estimation with test signal

In the reserved timeslot, the MT sends a test signal to the BS. The power of the received signal is measured at the BS for further channel quality estimation. Due to the reciprocity of uplink and downlink channel attenuation in signal transmissions, those values obtained from uplink are also used for the downlink calculation.

The list of candidate downlink resources and their measured CCI values are sent to the BS. Both of them are embedded into the test signal mentioned above. The number of info bits is limited, so that the embedded information does not cover all resources, but only those with least interferences.

#### 6. Resource allocation

With the power information on both the user signal and the CCIs in uplink/downlink, the mean SINRs in different resources can be calculated. With the predefined criterion, the resources with greatest mean SINR values are allocated for data transmission. The uplink and downlink transmissions are dealt separately. Each of them will be assigned an initial PHY mode as BPSK to achieve a highest possible robustness in the beginning of the transmission. The BS will block the call if there is no sufficient resource to fulfill the required data rate.

#### 7. Feedback of allocation information

With a successful allocation, the Identifier (ID) list of those selected resources is fed back to the user via the controlling channel. A rejection message will be sent alternatively in the case of call blocking.

#### 8. Conversation

The BS starts data transmissions on the allocated resources with selected transmission parameters, as soon as a final acknowledgement is received from the MT.

The general principle of the SO-RRM scheme is to select for each communication those resources with best possible channel conditions. The details

of the signal and interference measurement and the resource selection algorithm follow in the next chapter.

## 5.4 Anti-dropping Scheme Applied to SO-RRM

Comparing to a network with FRA, each transmission in a single frequency network has more free freedoms in the choice of radio resources. With self-organized resource allocation, every BS and its MT cooperate in estimation of signals and interferences, and perform accordingly and independently resource selection.

However, the resource is selected based always on the network condition measured at that moment of allocation. The interference situation for one connection may get worse if a new co-channel interferer appears in the network. When a BS allocates resources to a new MT, it causes more interference in the selected resources to all co-channel users in the other cells. In some cases, the CCI of an existing connection becomes too strong to support the data transmission with the same rate and quality. The call will be interrupted if no further action is adopted.

The dropping cannot be fully avoided. To reduce its chance of occurrence, two anti-dropping solutions are proposed. According to the different policies, they are respectively an active scheme and a passive scheme.

### 5.4.1 Interference Margin

“Interference margin” tries to fight with the potential increase of interference in an active way. The key policy is to reserve some space from the estimated SINR in order to increase the tolerance for interference caused by new co-channel users. Correspondingly, in the calculation a certain value  $SINR_{im}$  is subtracted from estimated mean SINR. The equation (5.11) is thus replaced by

$$R_k = M_c \left( \overline{SINR}_k - SINR_{im} \right) \quad (5.12)$$

It is expected that in most cases the accumulated increase of interference is less than the preset margin and thus does not bring destructive impact to the communication. When a user transmits in several resources, a margin pool is automatically established. Even if the interference in one resource exceeds the margin, the margins in the other resources can still compensate the loss in data rate. That is, the transmission of a part of data is shifted to another less interfered resource.

The decision on the value of an interference margin depends on several aspects. A large margin has obviously high robustness against potential

interference. However, it loses in efficiency and may require more resources for the same data rate. Consequently the network can serve fewer users at the same time. On the other side a low margin does not bring too much improvement on performances, i. e. the connection still often drops.

#### 5.4.2 Reallocation Procedure

“Reallocation” works in a passive way. That procedure will be triggered if long-term channel degradation is detected. Moreover, when one user is transmitting in several resources, another resource may take over the loss of transmission rate in the strong interfered resource. Therefore, a reallocation occurs only when the required data rate cannot be supplied by all allocation resources together. A reallocation process is similar to the normal resource allocation procedure, including a new signal and interference measurements.

Because the BS keeps receiving signals from the surrounding transmissions on all unused resources, there is no extra effort on uplink interference measurements. During a reallocation, the MT measures firstly the downlink interference for a number of frames and generates a new candidate resource list. The BS will arrange a new timeslot for a test signal. The MT sends the updated list and the corresponding interference information in that test signal. The SINR is then calculated and a new set of resources are allocated.

With a successful reallocation, new resources will be fed back to the terminal so that the data transmission continues. Before the reallocation, the previously allocated resources have been already released and can be included in the pool of resources. A dropping occurs eventually when a reallocation fails without sufficient resources.

A side effect may come with reallocation is dead lock. Although it seldom happens, two or more connections in different cells may trigger in turn the individual reallocation and allocates always the same resource. The reason of that phenomenon is the asymmetry of interference in a cellular network and no exchange of allocation information between BSs. To avoid such an endless loop, the amount of reallocation trials within certain time duration is restricted. If an extremely frequent reallocation happens, the call will be stopped and the connection is terminated.

Because a separate allocation for downlink and uplink is adopted in the proposed algorithm, the reallocation is also performed separately and independently in DL and UL.



**Table 5.4:** Comparison of anti-dropping schemes

	Interference margin	Reallocation
Style	Active	Passive
When?	During allocation	Triggered by channel degradation
What to do?	Reserve a margin in SINR	Reallocate resources
Flexibility	Low	High
Cost	Less transmission rate in each resource	New resource allocation

A comparison between those two methods is listed in table 5.4.



## Chapter 6

# Signal Measurement and Resource Selection Procedure

**Q**UALITY prediction of radio channels works as the basis for the selection of a proper resource. In the self-organized resource allocation procedure, the resource evaluation is based on measurement.

In the proposed algorithm, strengths of the user signal and the CCIs are measured separately. A BS keeps watching on all its unallocated resources in the uplink. Before sending a new call request, an MT will firstly measure the interferences in all resources in downlink. A candidate list of least interfered resources will be fed back to the BS.

The strength of a user signal is measured by a test signal sent from the MT to the BS. To have an interference free measurement environment, those signals are sent in a dedicated timeslot in uplink. To reduce the overhead, the information about the candidate resources is carried by the test signal.

With that information, the SINR is calculated for available resources. The BS selects then the best possible resources for the MT, separately for downlink and uplink. The number of necessary resources is decided by comparing the supplied total transmission rate of those already selected resources with the required data rate.

This chapter presents mathematically in detail the above procedures.

## 6.1 Measurement of Signal and Co-channel Interference

For further SINR calculations, both the mean signal power and the mean CCI values in long time duration are required. Because a receiver cannot distinguish intuitively between signals received from the user and those interferers at the same time, they should be measured separately.

### 6.1.1 Uplink/Downlink Interference Measurement

Co-channel interferences are measured in downlink and uplink respectively. The BS keeps measuring the uplink interferences on its unallocated subcarriers in each frame. And the downlink interferences will be measured at the MT side.

At each BS, both signals from its own MT and those MTs in the surrounding cells arrive simultaneously. Only the signals from other cells are of interest, as they represent the situation of resource occupation as well as the corresponding interference strength. Assuming there are in total  $M_{k,UL}(t)$  co-channel interferers transmitting in subcarrier  $k$  in uplink at the time point  $t$ . The measured interference  $I_{k,UL}(t)$  at the BS can be expressed by

$$I_{k,UL}(t) = \sum_{m=1}^{M_{k,UL}(t)} P_{UL}(d_0) \cdot \left(\frac{d_m}{d_0}\right)^{-\alpha} \cdot 10^{\frac{X_{\sigma,m}}{10}} \cdot |H_m(k, t)|^2 \quad (6.1)$$

In the expression,  $P_{UL}(d_0)$  denotes the power of signal received from an MT at a distance  $d_0$ , assuming a free space transmission. It is also assumed that all MTs transmit with an identical power. The variable  $d_m$  denotes the distance between the BS and the  $m$ -th interferer,  $X_{\sigma,m}$  is the shadowing factor, and  $|H_m(k, t)|$  is the amplitude of uplink channel transfer factor in subcarrier  $k$  at this moment.

By averaging in a sufficient number of  $N$  frames, the small-scale fluctuation of channel in each subcarrier can be approximately discarded.

$$\frac{1}{N} \sum_{n=0}^{N-1} |H_m(k, t - nT_f)|^2 \simeq 1, \quad \forall k \quad (6.2)$$

Assuming no joining or removal of interferers during the last  $N$  frames, i. e.

$$M_{k,UL}(t - nT_f) \equiv M_{k,UL}(t), \quad n = 0 \dots N - 1 \quad (6.3)$$

the mean power of uplink interference  $\bar{I}_{k,UL}(t)$  can be actually calculated in simulations by the below equation.

$$\bar{I}_{k,\text{UL}}(t) = \sum_{m=1}^{M_{k,\text{UL}}(t)} P_{\text{UL}}(d_0) \cdot \left(\frac{d_m}{d_0}\right)^{-\alpha} \cdot 10^{\frac{x_{\sigma,m}}{10}} \quad (6.4)$$

The averaging operation is further done inside each resource, with its  $N_f$  subcarriers. This information is kept updated in each frame at the BS, so that it is always adaptive to the current network situation.

Before sending a call request, an MT starts firstly measuring the signals received from the existing transmissions inside the network over each subcarrier for a predefined number of frames. As an alternative, those measurements can be also performed after the request, which results in a longer waiting time for the call setup.

An MT is unable and does not make much sense to distinguish signals from its potential host BS and the other ones. When a strong signal is detected in a radio channel, the hidden word is that this resource is already occupied by a certain active communications nearby and is too noisy to be used simultaneously by the MT. Therefore, in the eyes of the MT the interference includes signals from both the located cell and the other ones.

Tracking also for  $N$  continuous MAC frames and provided the similar assumption as in the uplink, the mean strength of downlink CCI  $\bar{I}_{k,\text{DL}}(t)$  in subcarrier  $k$  at time  $t$  can be expressed as

$$\bar{I}_{k,\text{DL}}(t) = \sum_{m=1}^{M_{k,\text{DL}}(t)} P_{\text{DL}}(d_0) \cdot \left(\frac{d_m}{d_0}\right)^{-\alpha} \cdot 10^{\frac{x_{\sigma,m}}{10}} \quad (6.5)$$

Variables in the above equation have similar meanings to those in downlink. After a further averaging inside each resource, the results are sorted in ascending order. A candidate list will be generated and sent to the BS.

### 6.1.2 Interference-free Signal Measurement

To have a precise power measurement, the user signal should be transmitted when all potential interferers are silent. Therefore, an SM-slot is introduced, which covers a single OFDM symbol in the time direction and is located at the end of the uplink phase of each frame, as shown in figure 5.1. The SM-slots are reserved exclusively for transmissions of test signals from new terminals. In the frequency direction, the slot covers all subcarriers except the signaling ones.

The strength of the received signal at the BS in subcarrier  $k$  at time  $t$  can be written as

$$S_k(t) = P_{\text{UL}}(d_0) \cdot \left(\frac{d}{d_0}\right)^{-\alpha} \cdot 10^{\frac{x_{\sigma}}{10}} \cdot |H(k,t)|^2 \quad (6.6)$$

Defining  $S_0$  as the mean received power,

$$S_0 = P_{\text{UL}}(d_0) \cdot \left(\frac{d}{d_0}\right)^{-\alpha} \cdot 10^{\frac{x_\sigma}{10}} \quad (6.7)$$

an average received signal power over all subcarriers can be calculated as

$$\bar{S}(t) = S_0 \cdot \frac{1}{N_{\text{sc}} - N_{\text{sig}}} \sum_k |H(k, t)|^2 \quad (6.8)$$

As more subcarriers are used in the test signal, as more accurate the measurement will be.

With a realistic assumption that the transmission of signals have (i) constant path loss and shadowing in all subcarriers, and (ii) channel transfer factors  $|H|$  in time and frequency is a wide sense stationary stochastic process, it is reasonable in statistics to use the variable  $\bar{S}$  calculated by equation (6.8) as the mean received power  $\bar{S}_k$  in each subcarrier  $k$  in the time direction, and the value is identical in all subcarriers.

$$\bar{S}_k = S_0 \simeq \bar{S}(t), \quad \forall k, t \quad (6.9)$$

Due to the reciprocity of channel in the uplink/downlink transmissions, the signal power estimated from the uplink can be also used for the downlink.

## 6.2 SINR Based Resource Allocation

The resource allocation is done at the BS. The measured CCI information in the downlink at the MT must be firstly delivered to the BS.

### 6.2.1 Feedback of Downlink Candidate Resources

In order to control the overhead, not all resources are reported in the candidate list. Another reason is that normally only a small number of resources are needed for a successful data transmission.

The test signal in the self-organized resource allocation introduced above is also used to carry the information of selected candidates. The BPSK modulation with a coding rate of 1/2 is selected for all subcarriers, in order to have a relatively robust transmission. The total number of carried info bits can be derived as

$$N_i = \frac{N_{\text{sc}} - N_{\text{sig}}}{2} \quad (6.10)$$

For each selected resource, a resource ID and its measured downlink CCI value are to be transmitted. In case of  $N_r$  resources in total, each of them can be identified with a unique ID encoded with  $\lceil \log_2 N_r \rceil$  bits. In order to include more candidates, a quantization step is applied to reduce further the bits for each interference value. The rational interference range is subdivided into a certain number of  $2^q$  segments, each of which has an equal width in [dB]. The interference values within one segment are thus represented by an identical value. A number of  $q$  info bits are consequently required for each CCI value.

With above assumptions, the total number of candidate resources  $N_{\text{can}}$  included in a test signal can be derived as

$$N_{\text{can}} = \left\lfloor \frac{N_i}{\lceil \log_2 N_r \rceil + q} \right\rfloor \quad (6.11)$$

For example, when 504 payload subcarriers are organized as 126 resources and 32 segments are considered in quantization, 21 candidates at maximum can be carried with their interference information. This is already sufficient for further resource selection.

### 6.2.2 SINR Calculation

With several interferers, the summation of interferences behaves statistically similar to a Gaussian noise. The mean SINR in uplink and downlink can be calculated for a resource  $k$  at the BS as follows.

$$\overline{\text{SINR}}_{k,\text{DL/UL}} = \frac{\bar{S}}{\bar{I}_{k,\text{DL/UL}} + N_0} \quad (6.12)$$

Without misleading, the time variable  $t$  has been discarded from the expression.

For the uplink case, this is calculated for all unused resources. For the downlink case, it is calculated only for those resources in the submitted candidate list.

The calculated average SINR values are used as the basis of channel selection.

### 6.2.3 Resource Selection Algorithm

Before the allocation process starts, all available resources are sorted by their SINR values. This list is considered as the candidate pool. The selection process starts with the first available resource, which has the best possible

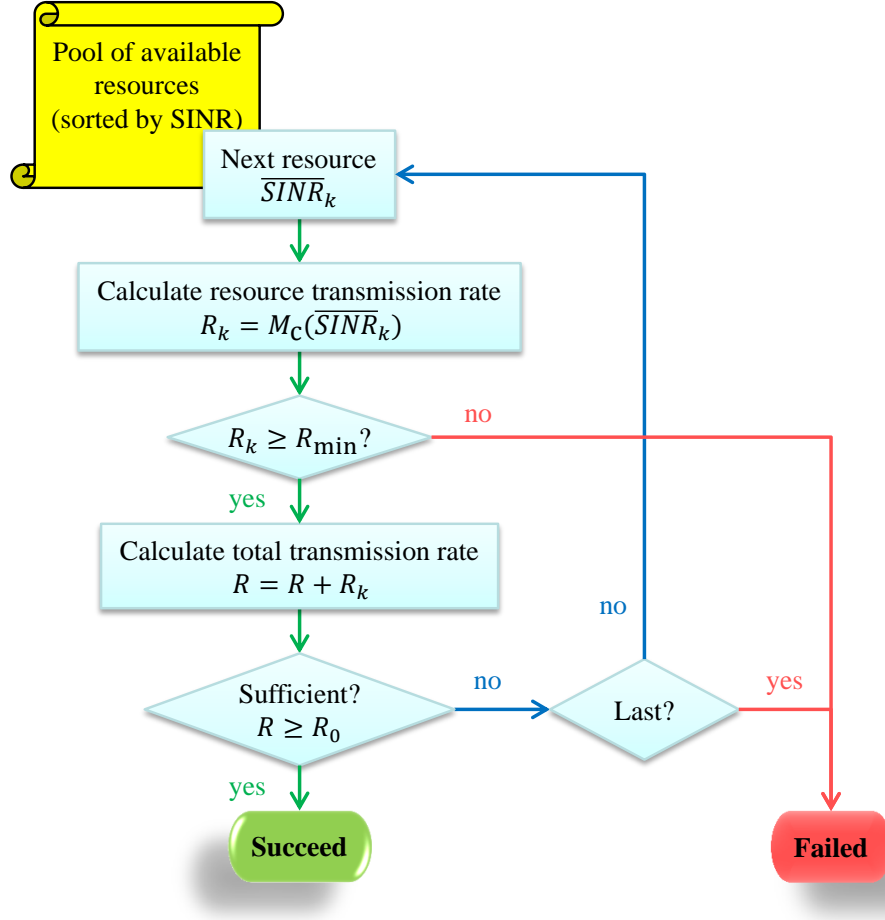


**Figure 6.1:** Resource allocation algorithm

channel quality. A recursive selection procedure is then applied, as shown in figure 6.1.

The supplied data transmission rate  $R_k$  in the checked resource  $k$  is derived, using the mapping function proposed in section 5.2.3.

$$R_k = M_c(\overline{\text{SINR}}_k) \quad (6.13)$$

The total transmission rate supplied by currently allocated resources is then calculated and compared to the required data rate  $R_0$ . Once the requirement is already fulfilled, i. e.

$$\sum_k R_k \geq R_0 \quad (6.14)$$

all necessary resources are prepared. Otherwise, the next best resource will be checked. This process continues until those selected resources are suffi-



cient for data transmission. The BS will then send a “Successful” message to the MT, together with the IDs of allocated resources.

In the realistic system, to avoid the case with a large number of allocated resources supplying only very low transmission rate, a minimum average SINR is introduced to keep efficiency. That minimum transmission rate  $R_{\min}$  for a resource is defined as 32 kbit/s in this thesis.

An allocation process fails in the case that the last resource in the list has been checked when the total transmission rate is not sufficient yet, or all unallocated resources cannot afford the minimum rate  $R_{\min}$ . A rejection message will be sent to the call originator. The MT will wait for some time and start a new link setup procedure.



## Chapter 7

# SO-RRM with Uniform User Distribution

SYSTEM level simulations are performed in this chapter to investigate the performance of SO-RRM in an OFDM based cellular network. As a first step, a uniform user distribution will be considered. A wraparound cellular structure is applied against the side effect in the calculation of CCI in simulations. The single frequency cellular network and self-organized resource allocation are expected to bring high efficiency in the considered system.

After a description of the network structure and the scenario in simulation, the performance study is separated to two parts: measurement of test signals and system capacity. The former discusses only the feasibility and effect of the proposed method for signal measurement. The latter evaluates the SO-RRM scheme on the system level.

Although test signals are transmitted in exclusive SM-slots, as ensures that they are not interfered by normal data traffics. However, as the usage of those slots is also independent in different cells with the self-organized concept, a collision of two or more test signal transmissions may occur. The influence of those collisions will be observed in simulation.

The main criterion, system capacity, is defined as the maximum number of satisfied users, provided a certain individual QoS parameters such as PER and some global ones like the blocking and dropping probability. Based on those criteria the performance of proposed anti-dropping methods to the SO-RRM scheme will be also investigated.

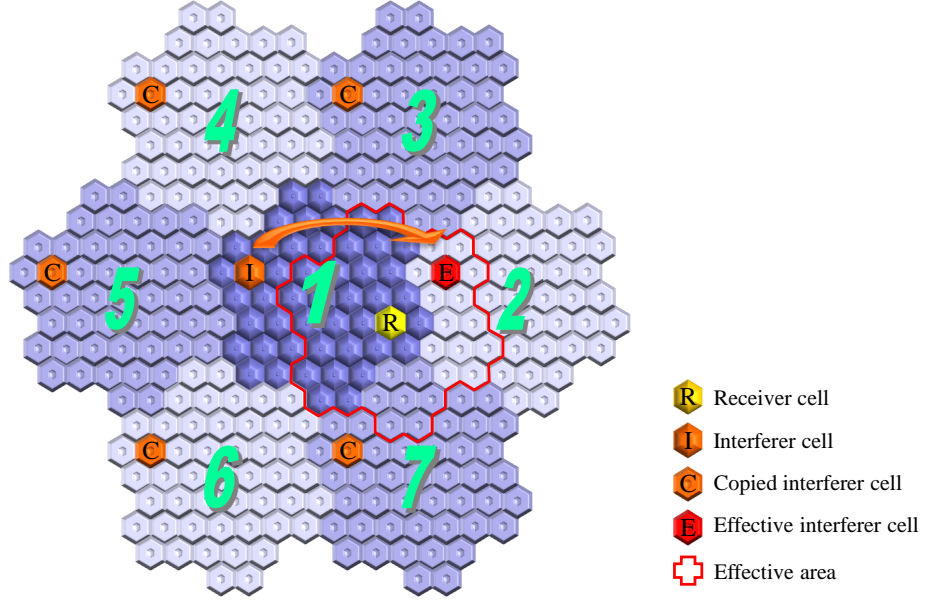


**Figure 7.1:** Simulated cellular network with wraparound structure

## 7.1 Cellular Network in Simulation

This section introduces at first a wraparound structure for generating a boundless cellular network in simulations. The calculation of CCI values in considered resources is given afterwards. The operation procedures of the simulated cellular system will be described at the end.

### 7.1.1 Wraparound Cellular Network Structure

All simulations are running at the platform of a cellular network consisting of 49 hexagonal cells with a same shape and an identical size, and one BS locates at the center of each cell. In order to eliminate the edge effect and to enable effective result collections in all cells, the wraparound technique is implemented [802-05]. As shown in figure 7.1, six copies of the 49-cell network are generated, surrounding the original one in a symmetrical manner. The real subnetwork is labeled 1, and its virtual copies are labeled 2 to 7 respectively.

All BSs and MTs in subnetwork 1 appear also at the same positions in the other subnetworks. For example, the BS and MTs at cell I are duplicated as its six copy BSs or MTs at the corresponding copy cells (marked with C and E in the figure), including all related properties such as the transmission power, the allocated radio resources, and the adopted PHY modes. Regarding to the radio channel between any pair of original/copy transmitter and

original/copy receiver, the effects of shadowing and multi-path fading are also duplicated, as well as the fluctuation over time. However, each path loss will be recalculated with its individual transmission distance.

In this wraparound structure, simulation results are collected only in the original subnetwork.

### 7.1.2 Interference Calculation in a Wraparound Structure

Assuming in the original cellular network, a co-channel transmitter at cell I interferes a transmission at cell R in resource  $k$ . In the network with a wraparound structure, this interferer has six copies at cells C (and E) in subnetworks 2 to 7. Out of those seven interferers, only the nearest one to the cell of the interfered receiver is included in the interference calculation. Such a cell (marked with E in the figure) is called an effective interferer cell in this case. All effective cells compose an interference effective area. It can be carried out easily, that the red-edge area in figure 7.1 has the same shape as the original network. The receiver cell R locates at the center of this area.

The distance  $\tilde{d}$  between an effective interferer and the interfered receiver is defined as the minimum one out of those distances  $d^{(i)}$ .

$$\tilde{d} = \min_i d^{(i)}, \quad i = 1 \dots 7 \quad (7.1)$$

The total received interference at a receiver in resource  $k$  can be rewritten from equation (6.1) as

$$I_k(t) = \sum_{m=1}^{M_k(t)} P(d_0) \cdot \left( \frac{\tilde{d}_m}{d_0} \right)^{-\alpha} \cdot 10^{\frac{X_{\sigma,m}}{10}} \cdot |H_m(k, t)|^2 \quad (7.2)$$

The mean CCI value in each resource can be also derived as follows.

$$\bar{I}_k(t) = \sum_{m=1}^{M_k(t)} P(d_0) \cdot \left( \frac{\tilde{d}_m}{d_0} \right)^{-\alpha} \cdot 10^{\frac{X_{\sigma,m}}{10}} \quad (7.3)$$

### 7.1.3 Simulation Scenario

Each simulation starts with no active communication. A BS is located at the center of each cell. MTs arrive sequentially and locate uniformly in the network. Their arrival is simulated as a Poisson process. After activated each MT requires a data transmission with a predefined data rate and PER, which are assumed identical for all users in both uplink and downlink. All BSs are assumed to have an identical transmission power. Similarly all MTs have an identical transmission power.

**Table 7.1:** Additional parameter in system level simulation

Parameter	Value
Number of resources	$N_r = 126$
Frame duration	$T_{\text{frame}} = 3.456 \text{ ms}$
Path loss attenuation coefficient	$\alpha = 2.6$
Standard deviation of shadowing	$\sigma = 4 \text{ dB}$
Number of subcarriers in a test signal	$N_{\text{ts}} = 504$
Call duration	$T_{\text{call}} = 1 \text{ minute}$
Target data rate (for both UL/DL)	$R_0 = 200 \text{ kbit/s}$
Minimum supplied data rate of one resource	$R_{\text{min}} = 32 \text{ kbit/s}$

The reference distance  $d_0$  in the path loss model (see equation (2.1)) is selected identical to the radius  $R_c$  of a cell, i. e. the distance from a BS to any vertex of the ideal hexagonal cell boundary. The corresponding reference power  $P(d_0)$  is selected to be 20 dB higher than the universal noise power  $N_0$ . This assumption is applied to both downlink and uplink. The absolute power value has thus no impact to further investigation.

$$d_0 = R_c \quad (7.4)$$

$$P_{\text{UL}}(d_0) = P_{\text{DL}}(d_0) = N_0 + 20 [\text{dB}] \quad (7.5)$$

Each newly activated MT follows the link setup protocol proposed in section 5.3. It firstly locks the strongest BS by comparing the received signal from the common broadcast channels. Once received the request from the terminal, the selected BS will send back the information about the dedicated signal measurement timeslot. The MT sends with the test signal the information on candidate resources for downlink and the previously measured CCI strengths. Together with the uplink interference information that is always kept updated with measurement, the BS tries to select a sufficient number of least interfered resources.

The data transmission starts after a successful allocation. In case of a failed allocation due to insufficient resource, the call request will be rejected. Each calls ends after a fixed duration and release its allocated resources. Afterwards the terminal leaves the network. A constant duration is further assumed for all calls, so that a high user density implies a short mean arrival interval in simulations.

Main parameters used in this simulation are listed in table 7.1. Some other OFDM related parameters can be found in table 5.1 and 5.2.

## 7.2 Performance Analysis

Above all a separate simulation is run to investigate the performance on power estimation of test signal. After showing its feasibility and efficiency, the system level behaviors of a self-organized cellular network will be investigated.

### 7.2.1 Measurement of Test Signal

Upon each call request, a timeslot for signal measurement will be assigned by the BS at the end of the uplink of a MAC frame, in which a test signal will be sent from the MT. It contains one OFDM symbol in the time direction and all  $N_{ts}$  payload subcarriers in the frequency direction.

Such an SM-slot will be used exclusively for transmission of one test signal. That will not be impacted by other normal data transmissions. However, a collision may occur when several MTs in nearby cells are transmitting their test signals at the same timeslot. In a self-organized network, this is unavoidable because there is neither information exchange nor coordination between BSs in this aspect. Moreover, the averaging between measured signal powers in different subcarriers results in only an approximation of the theoretical mean power.

The performance investigation on the measurement of test signal includes two parts: inter-cell collision and the averaging performance. At first, they are analyzed separately, assuming no cross affect from the other phenomenon. Their synthesized effect on signal measurement is discussed afterwards.

Because this part concerns on only test signals, resource allocation and other following call activities are omitted in simulation.

#### *Collision in Signal Measurement*

In the case of collision, the measurement results are influenced by test signals transmitted in other co-channel cells. Because the BS is unable to filter out those interferences from the received test signal, both user signal and interferences will be included in calculation. Assuming a perfect averaging, the Signal-to-Interference Ratio (SIR) can be calculated consequently by

$$SIR = \frac{S_0}{\sum_j S_j} = \frac{d_{sig}^{-\alpha} \cdot 10^{\frac{X_{\sigma, sig}}{10}}}{\sum_j d_j^{-\alpha} \cdot 10^{\frac{X_{\sigma, j}}{10}}} \quad (7.6)$$

In the above equation,  $S_0$  is the theoretical mean power of the received test signal from the host MT, while  $S_j$  is the one from the  $j$ -th interferer. The

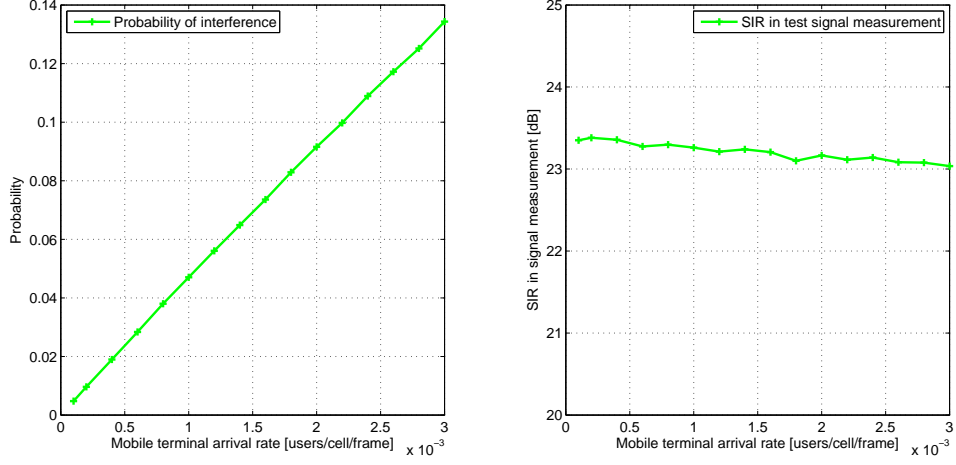


**Figure 7.2:** Probability of collision in signal measurement

variable  $d_{\text{sig}}$  and  $d_j$  denote the distances between the BS and the user or the  $j$ -th interferer. The shadowing factors  $X_{\sigma, \text{sig}}$  and  $X_{\sigma, j}$  are both random variables having a Gaussian distribution with a deviation  $\sigma$ .

The simulations run with different arrival rates of MTs. The corresponding probabilities of test signal collision are shown in the left of figure 7.2. It can be seen that the collision probability is linearly increasing with traffic load. A 14% collision probability is observed at the arrival rate of  $3 \times 10^{-3}$  users per cell per frame, which is equivalent to about one new user per second arriving at each cell (in the considered 49-cell network).

It is further shown in the right figure that the average SIR values in those collisions are greater than 23 dB in simulated situations, although all interferences have accumulated additive effect to the test signal. Even if that SIR decreases with shorter average arrival interval, the decreasing rate is quite small. Such a fact ensures that the host test signals are sufficiently robust against the interference in spite of collision.

#### *Accuracy of Averaging Operation*

The signal power is calculated by averaging the received power values in all subcarrier frequencies, which are used in the transmission of the test signal. To investigate the performance of an averaging operation, a collision-free environment for signal power measurements is assumed.

Not including the collision, the difference  $\Delta S_{\text{avg}}$  between the average power  $\bar{S}$  of received signals calculated with equation (6.8) and the theoretical value  $S_0$  can be expressed by

$$\Delta S_{\text{avg}} [\text{dB}] = 10 \cdot \lg \left( \frac{\bar{S}}{S_0} \right) = 10 \cdot \lg \left( \frac{1}{N_{\text{ts}}} \sum_{k=1}^{N_{\text{ts}}} |H(k)|^2 \right) \quad (7.7)$$



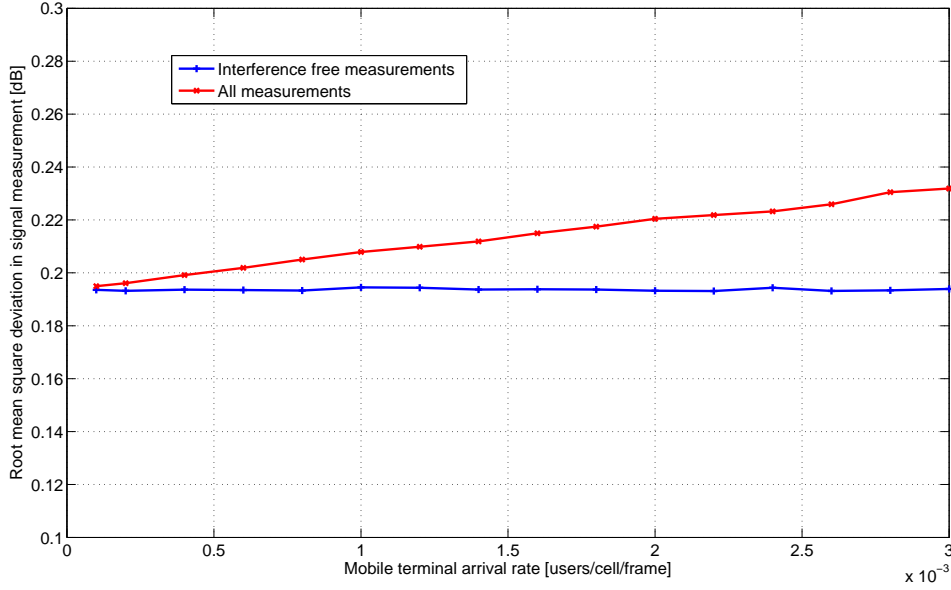


**Figure 7.3:** Average performance of signal measurement with/-out collision

Considering that the frequency band of a test signal is much wider than the coherent bandwidth, the magnitude of channel transfer factor  $|H(k)|^2$  in different subcarriers can be assumed exponentially distributed with a mean value of 1.

Taking both collision and averaging effects into account, the total error  $\Delta S$  will be written as

$$\begin{aligned} \Delta S [\text{dB}] &= 10 \cdot \lg \left( \frac{\bar{S} + \sum_j \bar{S}_j}{S_0} \right) \\ &= 10 \cdot \lg \left( \frac{1}{N_{\text{ts}}} \sum_{k=1}^{N_{\text{ts}}} \left( |H(k)|^2 + \sum_j \frac{d_j^{-\alpha} \cdot 10^{\frac{X_{\sigma,j}}{10}}}{d_{\text{sig}}^{-\alpha} \cdot 10^{\frac{X_{\sigma,\text{sig}}}{10}}} |H_j(k)|^2 \right) \right) \end{aligned} \quad (7.8)$$

The channel transfer factor  $|H_j(k)|$  in the above equation includes also the frequency selectivity of interfering signals.

The Root Mean Square Deviations (RMSD) of both measurement errors  $\Delta S_{\text{avg}}$  and  $\Delta S$  are plotted and compared in figure 7.3.

The lower curve shows the averaging error of the host test signal only. The deviations are constant about 0.193 dB, as expected in theory. A sufficient preciseness can be provided with the proposed scheme. When the interference is included, the deviation increases almost linearly with arrival rate. However as the starting value is quite low, and the difference introduced by collisions is also very small, the statistical root mean square deviation

of all measurement is still lower than 0.24 dB in the simulations. In most cases, such a value does not result in any effective impact to the further calculation.

Based on the above analyzes, the proposed signal measurement method is an efficient solution for the signal power estimation in the considered cellular network. In the system level simulations, that process will not be performed any more. Both perfect averaging and interference free measurement are assumed for simplicity.

### 7.2.2 System Capacity

A system level simulation is run to interpret the performance of a cellular network more from a macro point of view, e. g. by investigating how many users can be simultaneously served in the system. In statistics, a system capacity is defined as the maximum average number of satisfied users in parallel, providing each of them with a predefined QoS and a global satisfaction rate as well.

In principle, there are two main performance indicators: the blocking probability  $P_{\text{blk}}$  and the dropping probability  $P_{\text{drp}}$ . The former describes how often a call request is rejected by the system; while the latter reflects the case that a communication quality degrades greatly and the call cannot continue normally.

The simulation starts from a system without any active communication. The scenario described in section 7.1.3 is adopted. The arrival of MTs is simulated as a Poisson process. They are uniformly distributed inside the cellular network.

Each terminal selects the BS that sends the strongest signal on the broadcasting channel. Resources are allocated to the MT according to the proposed self-organized allocation scheme. Each user is assumed an identical data rate in both downlink and uplink. When a call is finished, the allocated resources are released. All calls have an identical duration of one minute. A blocking occurs when a call request is rejected, in case of insufficient radio resources to supply the required communication.

A dropping occurs when a call is disturbed by too much interference, which degrades the channel quality so that the required data rate cannot be afforded any more. The resources allocated previously to a dropped terminal are released immediately. The MT deactivates and leaves the network.

The simulation runs with different user densities. The obtained blocking and dropping probabilities are shown in figure 7.4.

It can be observed that nearly no blocking occurs in the network in simulation, even with very high user density, e.g. more than 800 users. By

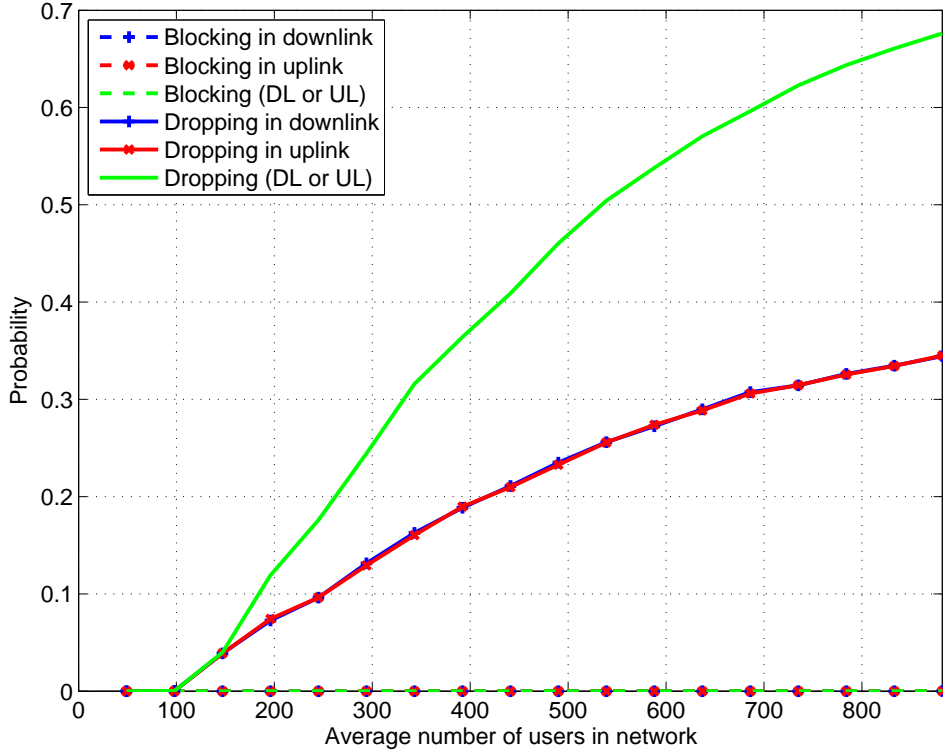


**Figure 7.4:** Blocking and dropping probabilities in a cellular network with SO-RRM

contrast, the dropping happens more frequently in simulation. With a low user density, MTs in adjacent cells are most likely to use resource exclusively. Co-channel transmitters are separated by long reuse distances. In this case, dropping is under an acceptable level, or even no dropping was recorded with less than 100 users. However, with a large number of users, a shorter reuse distance starts appearing. This increases dramatically the chance of a dropping. In particular, with more than 200 users, more than one-tenth of them will be interrupted during their calls.

In conventional systems with FRA, blocking is the major limitation to the system capacity. However in a self-organized cellular network, the dropping has become the dominant factor.

A variable, the user satisfaction rate  $P_{\text{sat}}$ , can be defined based on the blocking probability  $P_{\text{blk}}$  and the dropping probability  $P_{\text{drp}}$  as follows.

$$P_{\text{sat}} = (1 - P_{\text{blk}}) \cdot (1 - P_{\text{drp}}) \quad (7.9)$$

The results with various user densities are plotted in figure 7.5.

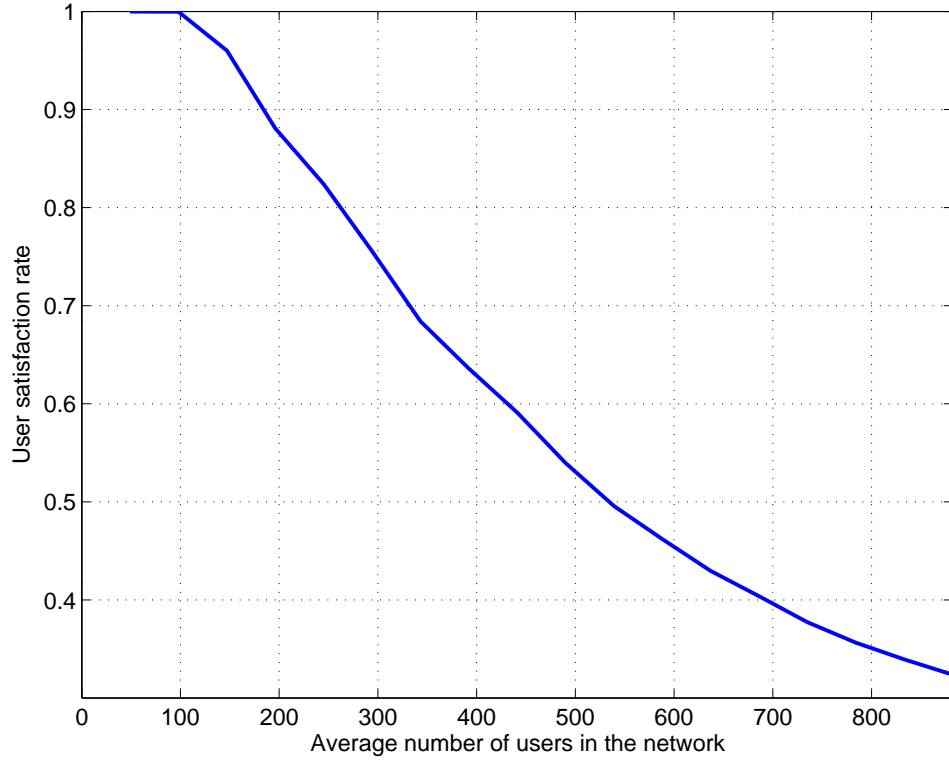


**Figure 7.5:** User satisfaction rate in a cellular network with SO-RRM

The user satisfaction rate decreases almost linearly with more user traffics. The system capacity is defined as the number of average users in the network, provided 95% of them are satisfied. The simulation results show that a 49-cell cellular network can support simultaneously 150 users with the assumed conditions.

In conclusion, the SO-RRM offers an extremely low blocking rate to call requests. However, the high dropping probability results in a large number of unstable connections and has a strong impact in system capacity. To solve this problem, different anti-dropping schemes should be implemented.

### 7.2.3 Anti-Dropping Schemes

Dropping instead of blocking becomes the dominant restriction factor in a self-organized resource allocation, because those new co-channel interferers after an allocation are not predictable and not included in the SINR calculation for resource selection. Two anti-dropping schemes have been proposed to deal with high dropping probability for the considered system with SO-RRM.

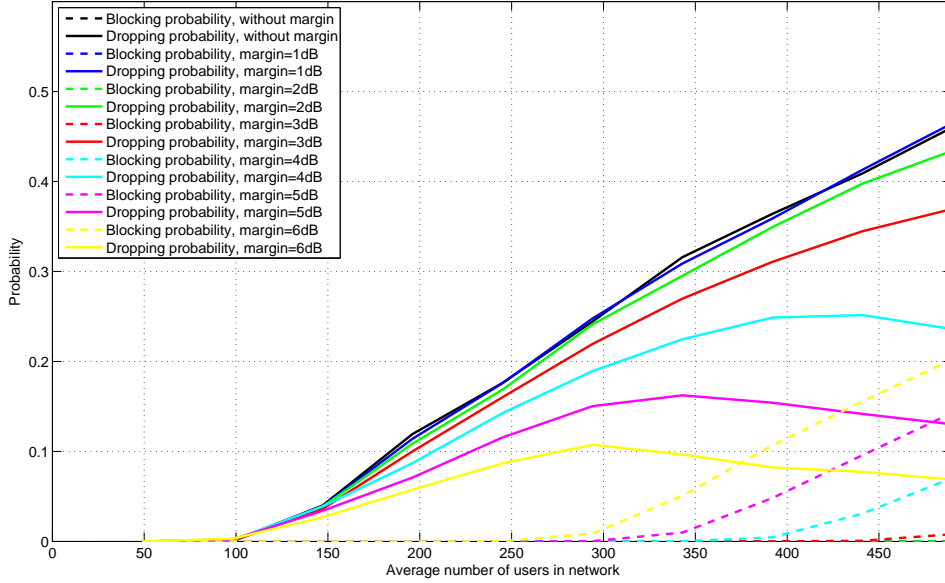


**Figure 7.6:** Blocking and dropping probabilities in systems with interference margin

System level simulation runs to evaluate the effects of proposed schemes. The parameters are same as in the previous simulations.

### 7.2.3.1 Interference Margin

In this simulation, various margins are adopted in the system, from 1 dB to 6 dB. The resulted blocking and dropping probabilities with different margin sizes are plotted in figure 7.6.

It can be seen that a margin of 1 dB does not bring an obvious change. Such a value is too less to have an effective influence. When the margin size increases, the dropping probability keeps decreasing. The value is reduced approximately 50% when a margin of 6 dB is applied.

On the other side, with a large margin each user is likely to get more resources and the blocking starts to appear. With a margin of 5 dB, the number of blockings has exceeded the number of droppings, when nearly 500 users are activated simultaneously in the network. With a 6 dB margin, this phenomenon is already observed with about 375 users. In those cases the blocking phenomenon has becomes again the dominant restriction to the cellular network, as same as in a system with FRA applied. With more users in the network, the dropping rate even decreases, because of the less number of co-channel transmitters.

The user satisfaction rate is calculated and compared in figure 7.7. Intro-

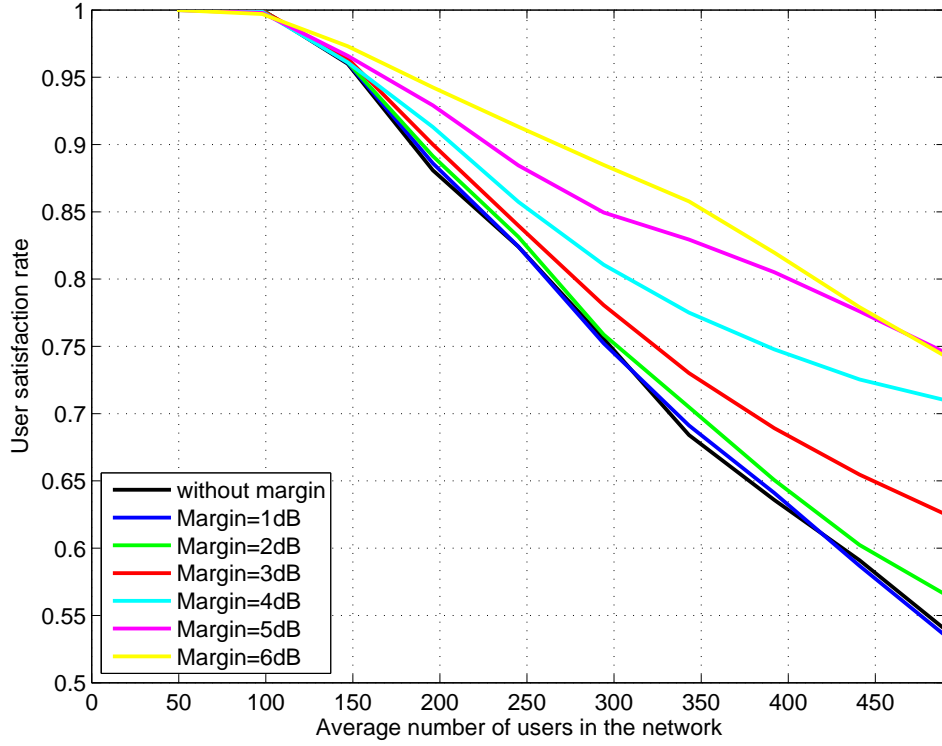


**Figure 7.7:** User satisfaction rate in system with different interference margins

ducing a margin enables the system to serve more users. However, when a margin larger than 5 dB is chosen, the satisfaction rate gets even worse with the enlarged margin size, when a high user density is considered. Thus, a margin of 5 dB may be a good choice. Also defining as the number of users at the working point with a satisfaction rate of 95%, the system capacity is increased from about 150 users to about 170 users.

### 7.2.3.2 Reallocation

Without reallocation, an MT drops directly when the communication suffers from its interference stronger than acceptable. With reallocation, the BS and the MT try to avoid dropping by an updated allocation in this case. Provided updated measurements on both the signal and the interference, new suitable resources will be selected to replace those in the out-of-date allocation.

Figure 7.8 shows the blocking and the dropping probabilities when reallocation is introduced into self-organized resource allocation.

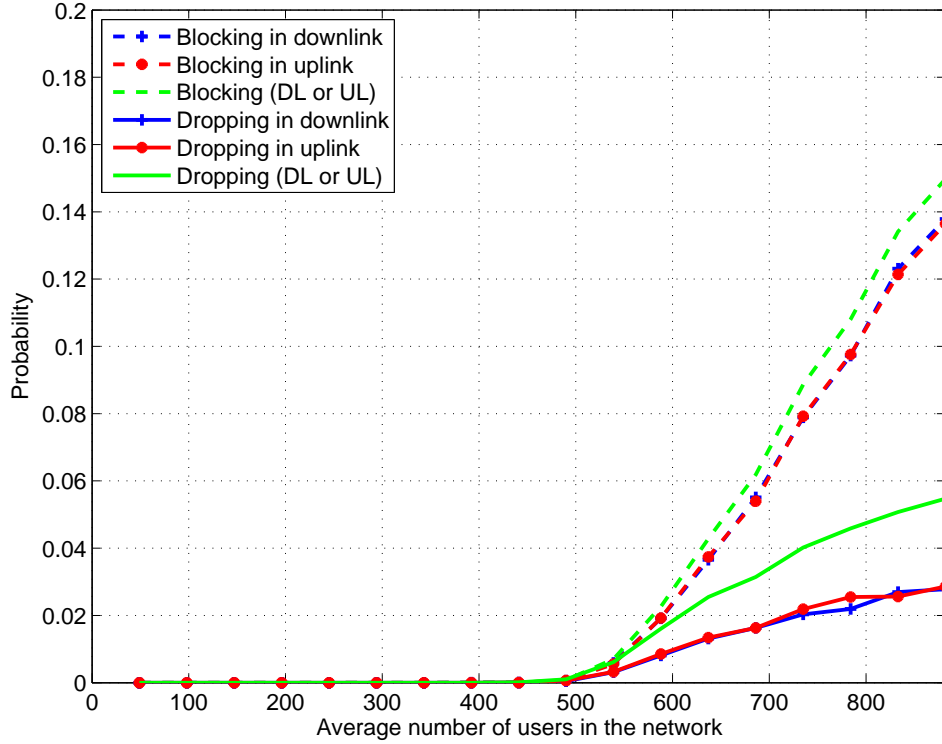


**Figure 7.8:** Blocking and dropping probability in a cellular network with SO-RRM, reallocation enabled

A significant improvement in performance is that the blocking and dropping phenomena appear only when more than about 400 MTs active in the network. As a reference, that number in a system without reallocation is about 100 users. Moreover as the direct result of reallocation, the dropping probability is reduced remarkably. With a high amount of 900 users, the dropping rate is still less than 6%.

Regarding to another key index, the blocking probabilities with reallocation enabled is higher than the system without reallocation. Its reason is that the reallocation keeps many users inside the network instead of the dropping. In another words, with a same user density, more users are served simultaneously in the system with reallocation. Therefore the number of idle resources inside each cell is reduced.

Of course, those gains are obtained at a certain cost, which is the effort on extra network sensing for reallocation. The average number of necessary reallocations during the call time of each user is shown in figure 7.9.

Reallocation is required when more than 100 MTs are in communication simultaneously. With about 420 users, each of them has one reallocation

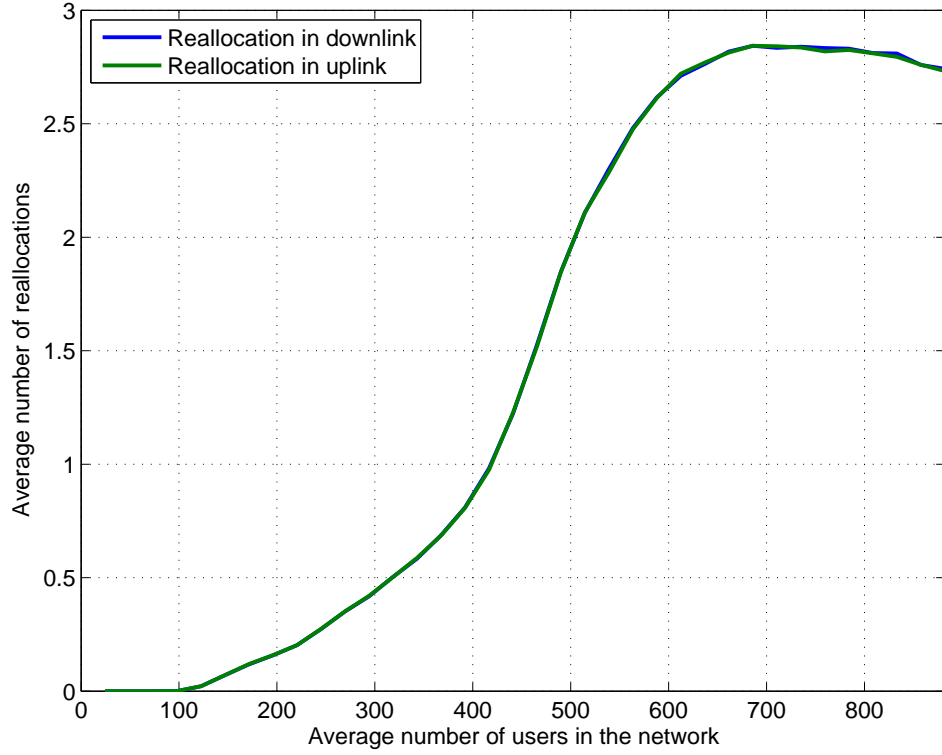


**Figure 7.9:** Average number of reallocation during a call

in uplink and one in downlink during the whole call time of 1 minute. This number increases to 2 with 500 users and reaches almost 3 at a situation with 700 users. With even more users, the required amount of reallocations decreases slightly. The high blocking rate in this case reduces the appearance of potential new interference. In all situations, the numbers of required reallocations are almost identical in downlink and uplink.

To check the effect of reallocations, a criterion named reallocation successful rate is defined as the ratio of number of avoided droppings in all reallocations. The results are shown in figure 7.10. It can be seen that the reallocation is quite useful to reduce the dropping rate, especially when less than 400 users are in the network. Almost all dropping can be avoided by an updated resource allocation. Even with about 900 users, only about 1.2% dropping is eventually unavoidable.

The user satisfaction rates can be then calculated based on equation (7.9). The results are compared with the system without reallocation, as shown in figure 7.11.

When there are only a small number of users in the network, e. g. less than 100 users, nearly all of them can be satisfied in either considered scheme.



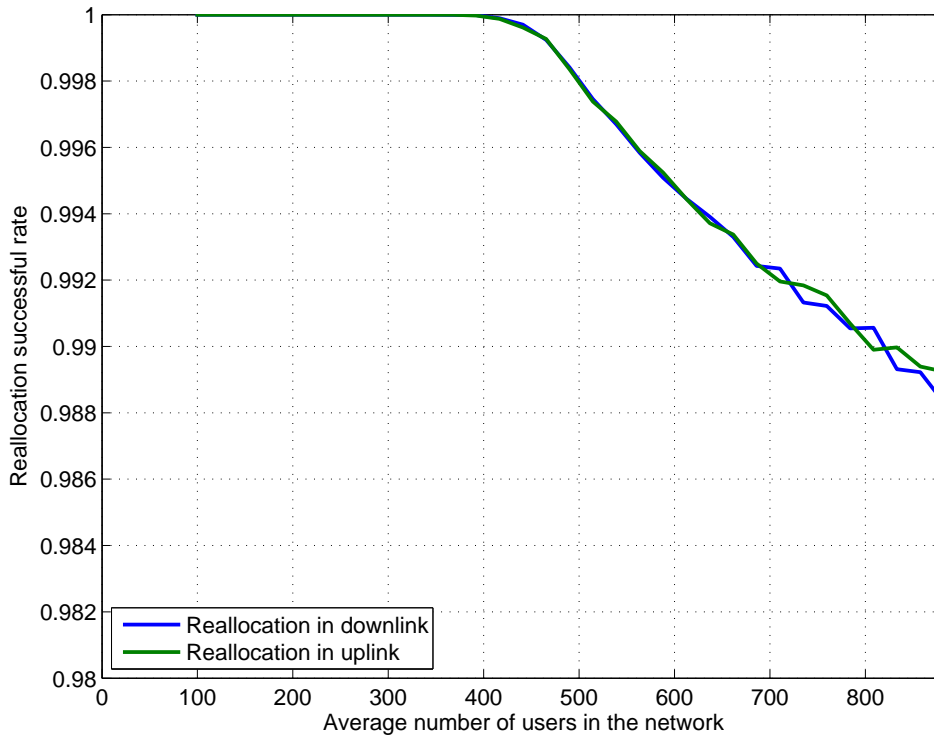


**Figure 7.10:** Reallocation successful rate

Reallocation seldom occurs in this situation. With an increasing number of users, the reallocation method shows its advanced performance in keeping user satisfied. A complete satisfactory is provided with up to nearly 500 users, while the system without reallocation can serve only a bit more than half of them. With reallocation there is still more than 700 users can complete their calls, even when a total number of 900 users are trying to communicate simultaneously. In comparison, a system without reallocation is able to satisfy only not more than 300 MTs.

The system capacity is defined as the average number of simultaneously active users in the network, when 95% of them can be satisfied. With a uniform distribution of MT locations, a capacity of 150 users can be supported by a system without reallocation. When reallocation is enabled, this capacity is increased remarkably to 600 users, which is almost 4 times more.

At the working point of the defined system capacity, 2.7 reallocations are in average needed for each call. For the transmission duration of one minute, the resource allocation process runs every 22 seconds. Such an overhead is negligible in communication systems.

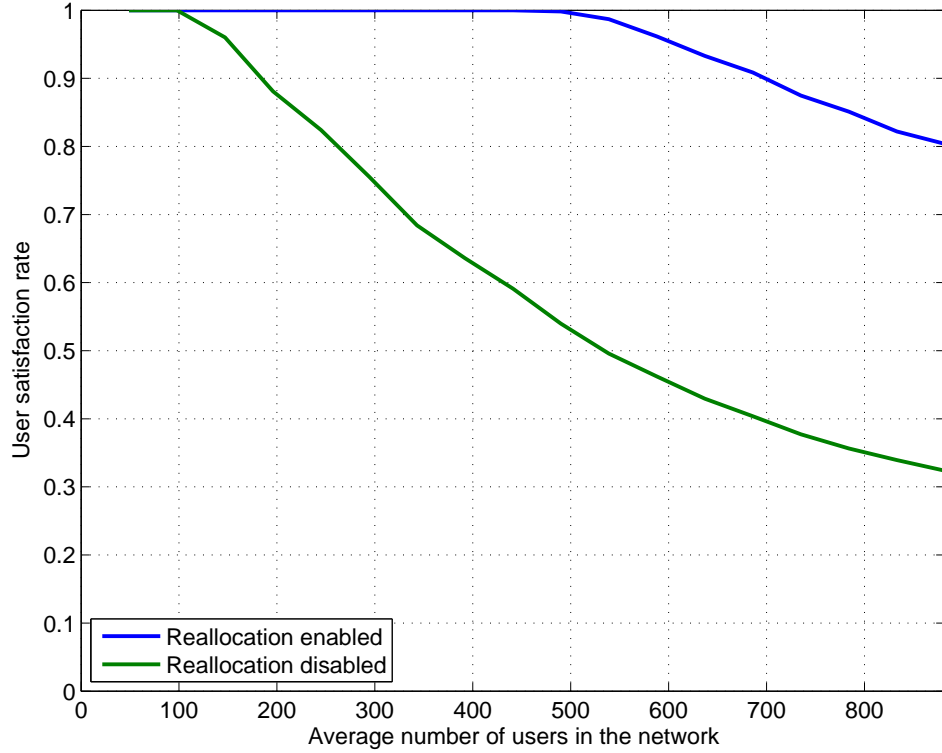


**Figure 7.11:** Comparison of user satisfaction rates in cellular networks with and without reallocation

### 7.2.3.3 Reallocation with Interference Margin

This part of simulation investigates the synthesized effect of above two anti-dropping methods. The results of blocking and droppings are shown in figure 7.12, while the user satisfaction rates are shown in figure 7.13.

Unfortunately, the integration of an interference margin degrades the performance of a system with already reallocation enabled. The blocking probability is increased because of more required resources for each user.

As a conclusion, reallocation is recommended as an efficient anti-dropping method.

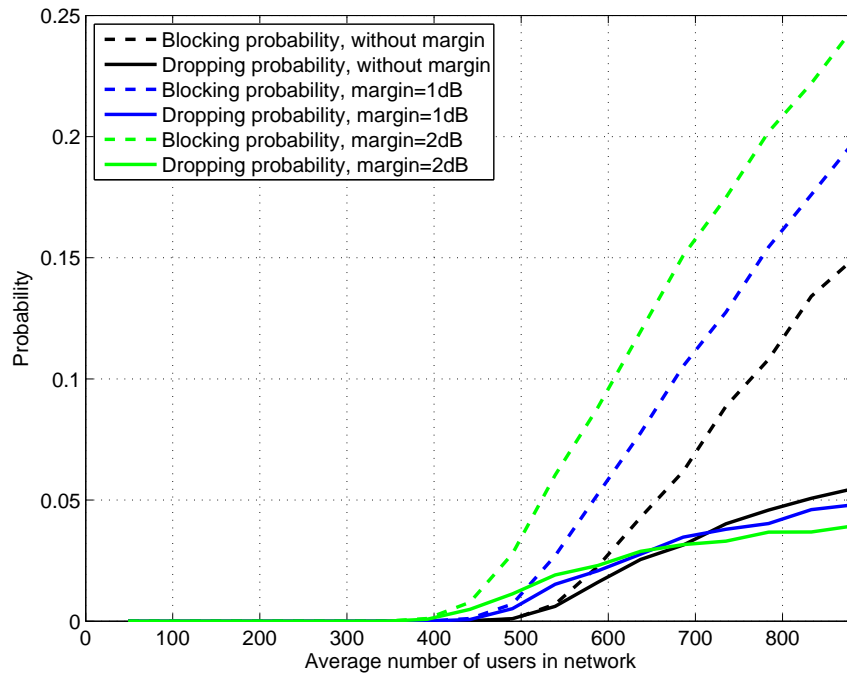


**Figure 7.12:** Blocking and dropping probability in a system with both reallocation and interference margin

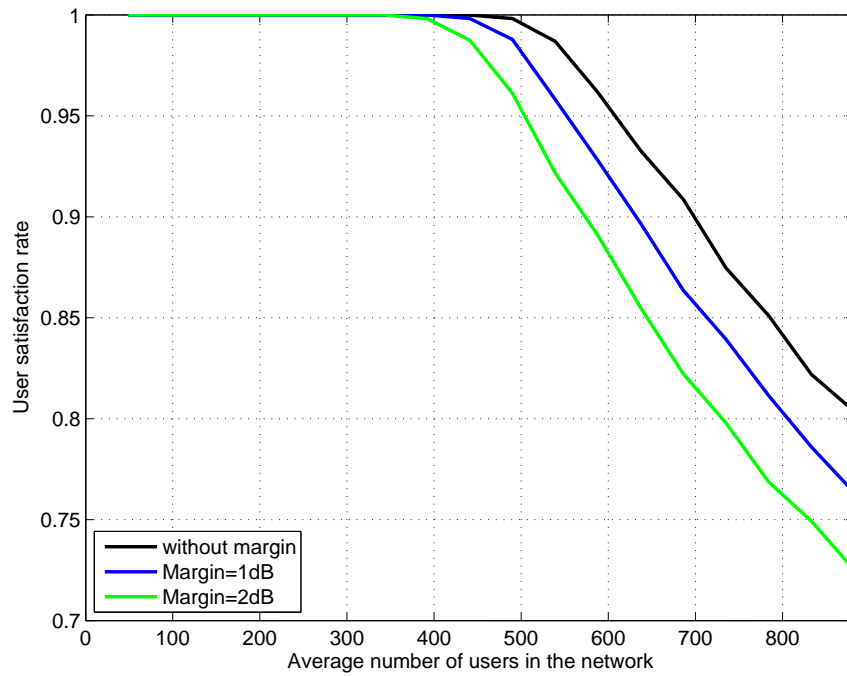


**Figure 7.13:** User satisfaction rate in a system with both reallocation and interference margin



## Chapter 8

# SO-RRM with Non-Uniform User Distribution

**N**ON-UNIFORM spatial distribution of mobile users and communication requirements become more popular today in cellular systems. The solution in a conventional system concept with fixed allocation applied is to assign more resource to the corresponding cell by a new network planning process. However, this method is effective only at a place with a long-term predictable high user density, for example an airport or a railway station.

If the user density at a spot varies frequently or unpredictably, the fixed assignment strategy is unable to have immediate reactions. Congestions will thus occur at that spot, while the resources in nearby cells with only sparse users may be wasted at the same time. A reconfiguration of frequency pattern among the network is also inefficient because the demand may last only for a short duration.

In this case, the self-organized scheme will show its native benefit with respect to the adaptivity to any user distribution. The resources in SO-RRM are shared universally and can be used anytime in a cell when the call demand increases. The ability of real-time reaction brings a full flexibility in all situations.

This chapter focuses on a cellular network with non-uniform user distribution. The system level performances with both fixed resource allocation and self-organized radio resource management will be investigated and compared in simulation.

## 8.1 Cellular Networks with Non-uniform User Distribution

A hotspot in a cellular network means a concentration of mobile users inside a certain area. A hotspot may appear somewhere for a short time period, for example in a stadium when a sport or a social event is held. Much more communications than usual will be required in this case.

According to the adopted resource management schemes, cellular networks will have different hotspot behaviors. This section will show the example behaviors of a cellular network including a hotspot cell, respectively when a fixed or a self-organized resource allocation is applied.

### 8.1.1 Cellular Networks with Fixed Resource Allocation

A cellular system with FRA pre-allocates resources to each cell, in accordance with the long-term prediction of traffic load distribution in the network. For a typical uniform distribution of mobile users, each cell will be assigned an identical number of resources. The cells are organized as clusters, inside which resources are assigned exclusively to cells. The resources are reused in co-channel cells when the interference between them is sufficiently weak.

An example of such a network has been given in figure 4.1. The cells labeled with a same number use the same subset of resources. With a cluster size of 7, one-seventh of all resources can be used in each single cell.

To give an intuitive image, a simulation is run to get a snapshot of the cellular system. The same network as in previous simulations is considered. Although the wraparound technique is applied, the snapshot only shows those 49 originated cells. A number of 100 MTs are generated in the network. The simulation starts without any user. Terminals arrive one after another and locate uniformly in the network. The resource allocation procedure is same to the one discussed previously. Not investigating the quality of transmission, each MT is assumed to keep communicating until the end of simulation. The dropping is not considered, and the simulation runs until all users are in the network.

The snapshots of those BSs and MTs in the considered cellular network and the power of received signals in all resources at the central BS are shown in figure 8.1. The MTs communicating with the central cell is denoted by blue dots. Those terminals belonging to six co-channel cells are marked cyan, and all others are presented in magenta. The signals received at the central station are illustrated with same colors as their transmitters. The

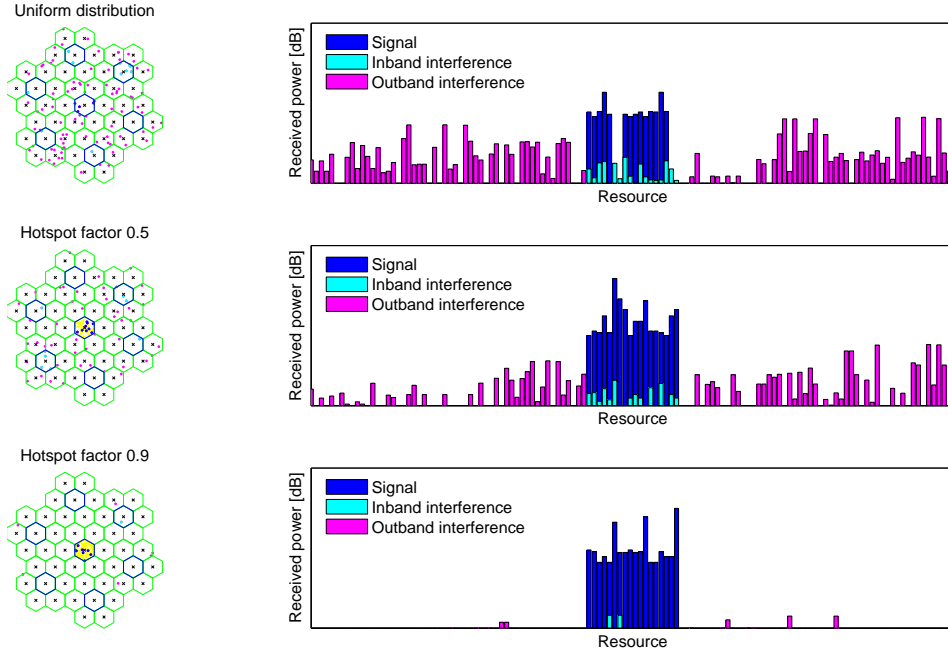


**Figure 8.1:** Snapshot of a cellular network with hotspot, fixed resource allocation

CCI to the central cell is also called in-band interference, while the others are named out-band interference.

With 100 uniformly distributed MTs shown in the top subfigure, there are still free resources in the central cell, although the CCI appears already in some resources. Interference in the other resources, which are not assigned to the central cell, can be also received. In this example, no blocking is observed.

Let us assume now an event happening in the central cell and MTs starting to concentrate. A “hotspot factor”  $\rho$  is defined to quantitatively describe the user concentration in hotspot by:

$$\rho = \frac{\text{Number of users in central hotspot cell}}{\text{Number of users in network}} \quad (8.1)$$

For example, in a 49-cell network  $\rho=0.2$  means that 20% of total users locates in the central cell, and the rest 80% are distributed in the other 48 cells. Inside either the hotspot cell or any other non-hotspot cell, MTs have always a uniform distribution. The uniform user distribution in the whole system can be also represented by a hotspot factor  $\rho=1/49$ .

The second and the third subfigures in figure 8.1 are respectively the network snapshot, in which 50% and 90% of users is locating in the central cell. When

half users are in the central cell, available resources in the hotspot are not sufficient for all users. Those blocked MTs are shown as yellow dots, which are only in the central cell in this case. At the same time, many free resources in other cells are not utilized. This situation is more serious in the case with a hotspot factor of 0.9. Nearly 80% of the resources are in an idle status in those adjacent cells with few users.

According to the above example, a network with FRA has obviously an insufficient resource usage, in the case with a user distribution different from the predicted one.

### 8.1.2 Self-organized Cellular Network

With the SO-RRM scheme, a flexible resource allocation can be realized based on real-time measurement of interference situation in the network. Because each BS can use any resource, the hotspot cell can declare more resources on its demand.

A simulation in the same environment is run to get snapshots for comparison. The results are shown in figure 8.2, from up to down respectively with a uniform user distribution, 50% users in the hotspot, and 90% users in the hotspot. Because of the full access of resources in each cell, any interference is regarded as CCI here.

In the case of a uniform user distribution, no CCI is observed in the uplink at the central cell. When the hotspot factor increases, more resources are allocated to those concentrating users. Even when 90% of users are in the central cell, no blocking is observed. The self-organized resource allocation shows here its high flexibility and adaptivity.

Of course when a larger number of users are considered, the blocking would still appear. Quantitative discussions will be presented in the next section.

## 8.2 System Level Performance

System level simulations are performed to evaluate the long-term performance in cellular networks with a hotspot cell, when fixed resource allocation or self-organized resource allocation is applied.

### 8.2.1 Hotspot and Fixed Resource Allocation

The same cellular network in figure 7.1 is considered in the simulation. The central cell is selected as a hotspot. Inside each cell, MTs are uniformly distributed.



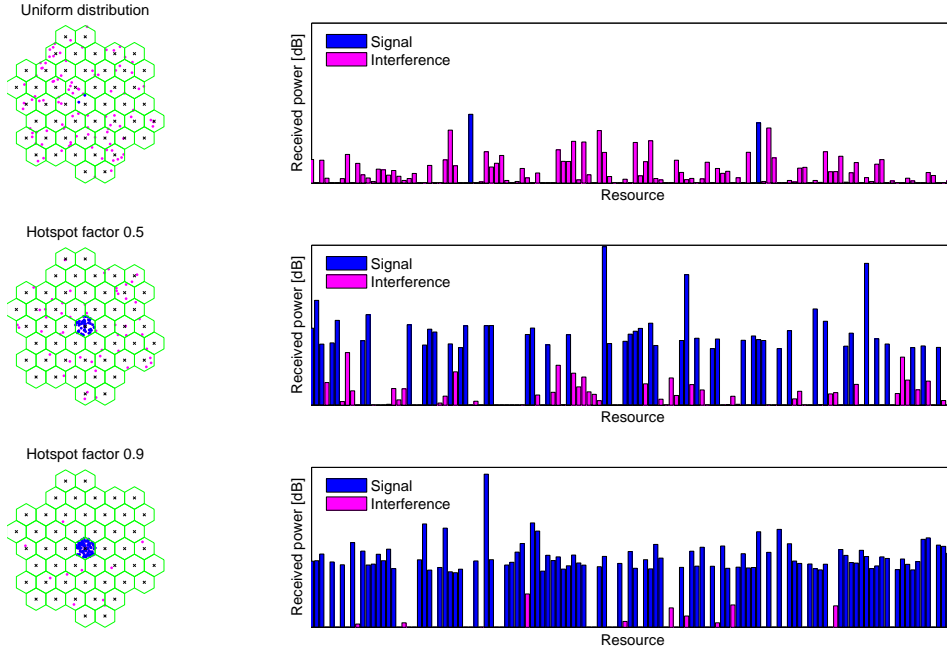


**Figure 8.2:** Snapshot of a cellular network with hotspot, self-organized resource allocation

The simulation starts from a system without any active communication. Users arrive at the network sequentially, which is simulated as a Poisson process. They are randomly allocated following the distribution based on the selected  $\rho$ .

As a reference system, the resources are preassigned to each cell. A reuse factor of 7 is selected. All available resources are divided into seven equal partitions and are assigned exclusively to cells in a cluster. Each BS selects resources to each users based on the worst-case interference calculation and the measured signal power.

The simulation runs with various hotspot factors, from 0.1 to 1 in a step of 0.1. The blocking and dropping probabilities in the whole network are plotted in figure 8.3. The performance in a cellular network with a uniform distribution of MTs is also plotted as the reference.

From the left subfigure it can be concluded that a new user is more likely to be blocked when more users are concentrated in the hotspot cell. The limited number of preassigned resources restricts the total amount of supported users in the cell. In the extreme case with  $\rho = 1$ , although those radio resources in the other cells are totally not used, a highest blocking probability is observed in the system.

Concerning on the dropping behavior, it shows different properties when the

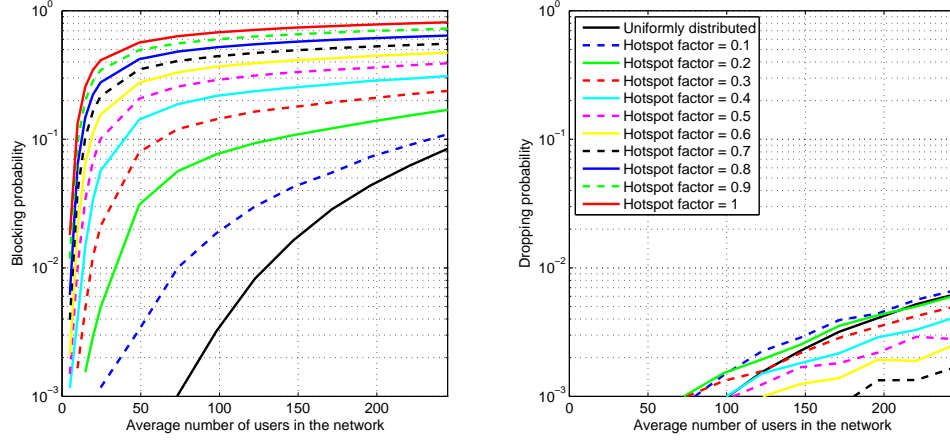


**Figure 8.3:** Blocking and dropping probabilities in a cellular network with hotspot, fixed resource allocation

number of users changes. With comparatively few users, not all cells reach the full capacity. The dropping occurs seldom and contributes little to the system performance. When no more users can be served in the hotspot, new-coming users will be blocked. On the other hand, fewer users in the other co-channel cells produce also less interference. The dropping probability is consequently decreased with higher hotspot factors in this case. When the hotspot factor is greater than 0.8, even no dropping is observed.

Figure 8.4 compares the satisfaction rates in different user distributions. It is obvious that the satisfaction rate decreases dramatically when more and more users locate at the hotspot cell. The capacity of the whole network depends gradually more on the capacity of the hotspot cell, where however only  $1/7$  of the resources is available.

As a conclusion, the inflexibility of fixed allocation strategy may cause great performance degradation with an unexpected change of user distribution in the cellular system.

### 8.2.2 Hotspot and Self-organized Resource Management

Similar simulations are run with self-organized radio resource management. The same network structure and user arrival model are applied, as well as the data rate and the QoS requirement.

Different from a system with preassigned resource sets, all resources can be used in any cell in the system with SO-RRM. The possible quality of data transmission in a resource is estimated, based on real-time signal and interference measurements. The central cell is simulated also as a hotspot. Simulations run in two scenarios: without reallocation and with reallocation.

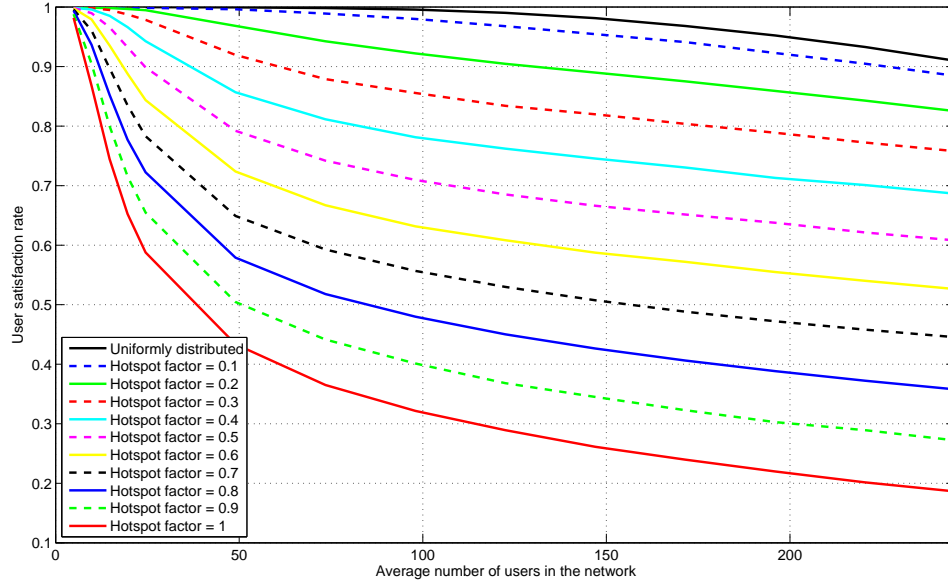


**Figure 8.4:** User satisfaction rate in a cellular network with hotspot, fixed resource allocation

#### *Without Reallocation*

Without reallocation, the corresponding blocking and dropping performances are compared respectively in figure 8.5.

With a small number of users, neither blocking nor dropping is observed in systems with all simulated hotspot factors. As the algorithm selects resources with least interference, the firstly served MTs are more likely to use resources in an exclusive way. In other word, no CCI is generated in any resource. Because all resources can be used in both hotspot and non-hotspot cells, there is no difference for resource allocation when a user changes its location from one cell to another, provided the total number of users is not greater than the possible number of served users in a single cell.

The dropping probability increases with more MTs activated and a higher hotspot factor  $\rho$ . The obvious blocking occurs only when 50% of the users are located in the hotspot, and the worst situation happens when all users are in the same cell.

Corresponding user satisfaction rates are calculated and presented in figure 8.6. It can be seen that the capacities are nearly unchanged in the simulated cases when the hotspot factor is less than 0.4, and not more than 200 users are in the network. With for example 120 users, this similarity extends to even  $\rho = 0.7$ . When the hotspot cell saturates in term of radio resource, the user satisfaction rate decreases very fast with increasing hotspot factors.

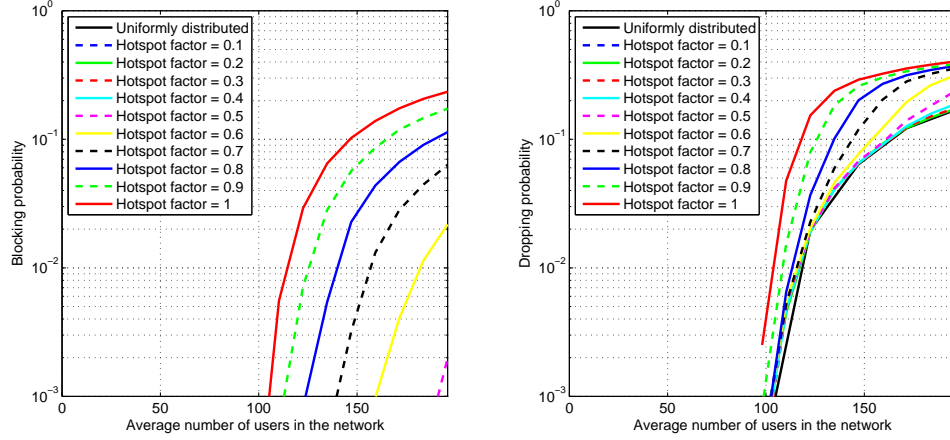


**Figure 8.5:** Blocking and dropping probabilities in a cellular with hotspot, self-organized resource allocation without reallocation

#### *With Reallocation*

The performances of a system with reallocation are shown in figure 8.7 and 8.8.

The reallocation scheme can eliminate most of droppings by a new resource selection, so that the dominant limitation turns from dropping to blocking. Both the blocking and the dropping probabilities increase with the hotspot factor. However when a large number of mobile users is considered, the dropping probability does not change significantly.

The dropping still exists even when all users locate at the central cell, because of the shadowing effect. A user locates in a cell does not always communicate with the BS in the same cell.

Comparing figure 8.8 with figure 8.6, a system with reallocation is able to satisfy much more users, although this enhancement shrinks when a high hotspot factor is considered. In the case where all users are located in the central hotspot cell, the satisfaction rates are approximately identical, no matter the reallocation is applied or not.

#### *Comparison of System Capacity*

The system capacity is defined as the maximum number of served users when a user satisfaction rate of 95% is achieved. The capacities of above simulated systems are compared in figure 8.9.

The capacity of a system with fixed allocation decreases very fast from 200 users to 17 users, when half users are located in the hotspot cell. The inflexibility in FRA induces such a remarkable loss of spectrum efficiency. Many users in the hotspot cell cannot be served whereas a large number

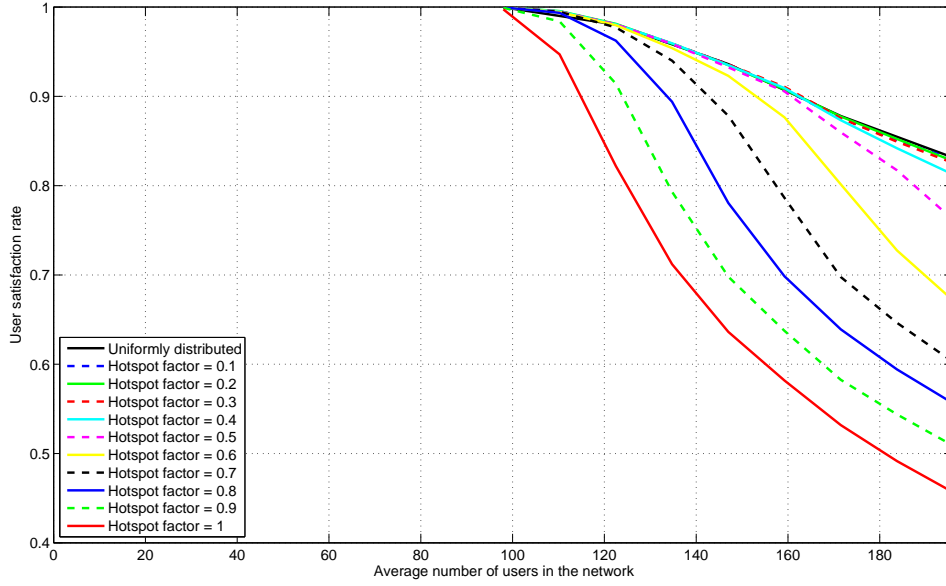


**Figure 8.6:** User satisfaction rate in a cellular network with hotspot, self-organized resource allocation without reallocation

of resources in other cells are idle. In an extreme situation that all users concentrate in one cell, only 6 users can be served.

Without an anti-dropping scheme like reallocation, the self-organized resource allocation performs even worse than the fixed allocation in case of a uniform or an approximately uniform user distribution. The capacity is 30% less in the situation with a uniform user distribution. The unpredicted new interferers cause more droppings in transmission. In FRA, the worst-case consideration of CCI in the resource allocation brings more tolerance

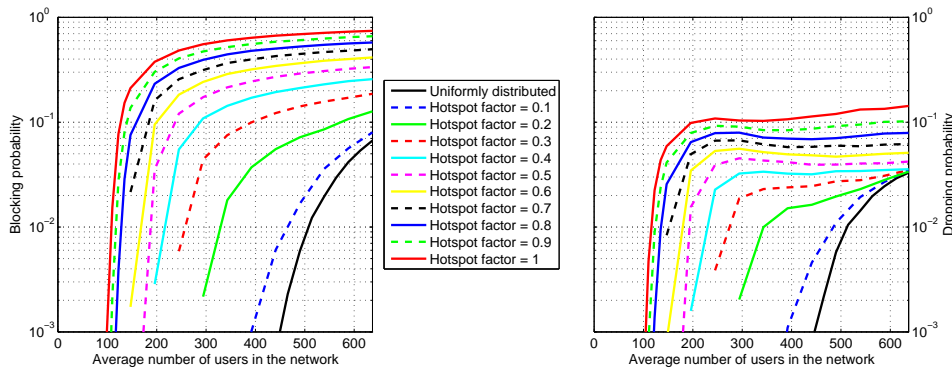


**Figure 8.7:** Blocking and dropping probabilities in a cellular network with hotspot, self-organized resource allocation with reallocation

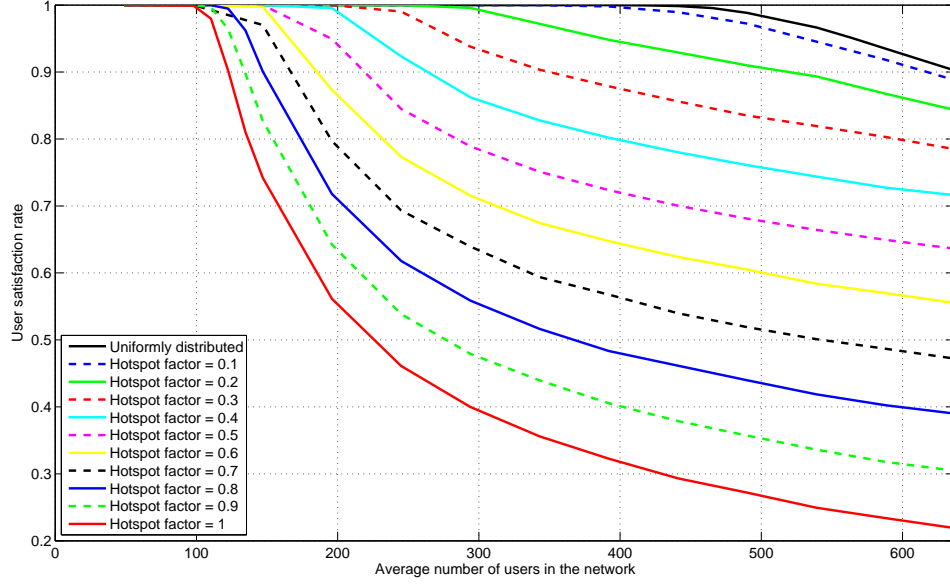


**Figure 8.8:** User satisfaction rate in a cellular network with hotspot, self-organized resource allocation with reallocation

against the potential new interference during a transmission.

However, the SO-RRM is robust to the variety of user locations. It outperforms FRA with a hotspot factor of 0.12 and above. Even when all users are in the hotspot, the system can still serve 110 users, which is almost 18 times more than the one with fixed allocation. The gains comes from two aspects: on one hand the accessibility of all resources in any cell brings 7 times more capacity; on the other hand the resource quality estimation based on network sensing reflects a real interference situation and thus a more efficient usage of resource can be ensured.

The reallocation scheme, as an additional method to overcome dropping caused by new interference, is proved quite effective in all cases. In a system with a uniform user distribution, it can reach a capacity of 600 users, which is 3 times more than the one with fixed allocation. The system reacts to the updated interference image in the network and keeps all resources in usage with high efficiency. Although the capacity decreases along with the increase of hotspot factor, it performs always the best out of the considered three systems. When a hotspot factor greater than 0.8 is considered, i. e. most of users are locating at a same cell, the new interference becomes seldom so that it is not likely to destruct an existing communication. The reallocation cannot bring further gains, and the system behaves approximately to the one without reallocation.

In conclusion, the flexibility and efficiency of the proposed self-organized ra-

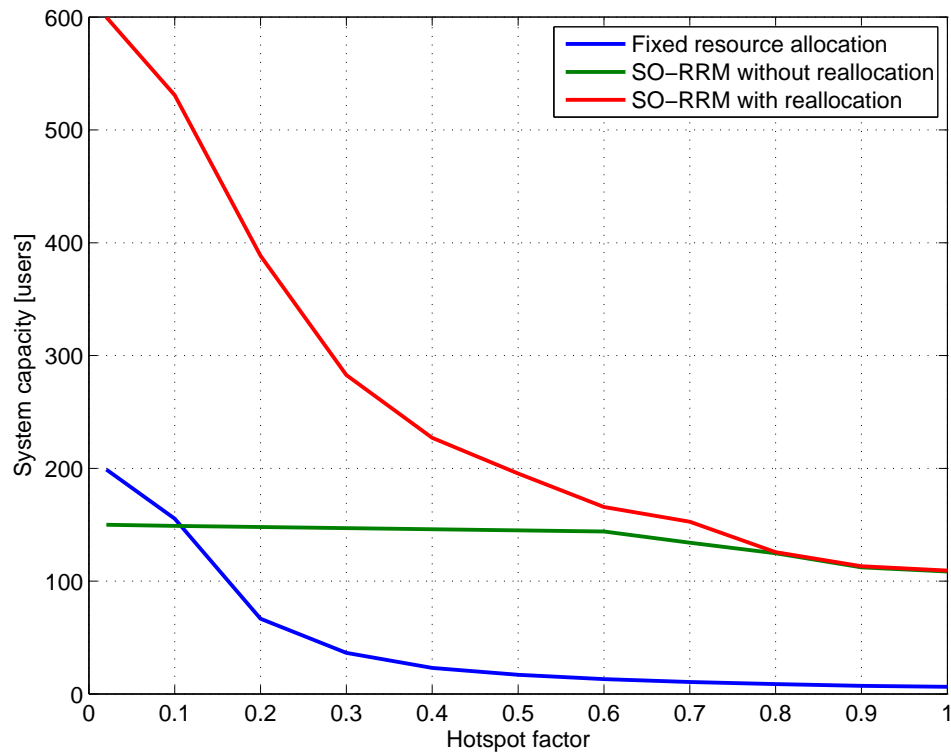


**Figure 8.9:** Comparison of system capacity in a cellular network with hotspot

dio resource management makes it obvious the winner for a cellular network with non-uniform user distribution. The gain is remarkable, and the cost, e. g. network sensing and reallocation, is feasible and worthy.





## Chapter 9

# Adaptive Resource Rearrangement

**B** EING a multi-carrier technique, the OFDM system subdivides the whole bandwidth into a certain number of subcarriers. The band of each is sufficiently narrow to be treated as a “flat” channel. In a multi-user system, each user is using a subset of subcarriers when the FDMA scheme is applied.

Multi-path propagation in wireless radio transmissions results in variant attenuation over the whole signal bandwidth, which is called frequency selectivity. The channel independence of all users carries out a useful consequence that a deep faded subcarrier to a user may be in a good condition in the eyes of another user. Such a multi-user diversity enables high spectrum efficiency by trying to serve different users with individually best possible subcarriers. When the necessary channel knowledge is available, an optimized redistribution of resources between MTs can be figured out. Such a process is called Adaptive Resource Rearrangement (ARR).

To support an ARR process, the channel information in all candidate resources should be known in advance for all users. Moreover, those channel conditions should keep unchanged for a long time. Therefore, this technique is considered for a system with static or quasi-stationary terminals.

In this chapter, some methods of ARR are introduced for the OFDM based cellular system, after given a common mathematical description. Those algorithms and their performances will be compared, respectively in a single cell and in a cellular network.

## 9.1 Mathematical Description and Algorithms of ARR

The goal of any resource management in mobile communication systems is always to maximize the spectrum efficiency and meanwhile to fulfill the QoS requirement. In OFDM-FDMA based systems, the multi-user diversity gives a chance to improve the system performance by an intelligent allocation of subcarriers to serve each user with individually best possible subcarriers. Nevertheless, OFDM as a multi-carrier technique, enables assigning different PHY modes adaptively for each subcarrier.

The proposed ARR algorithms include two concatenated steps: adaptive resource allocation and adaptive PHY mode selection. The first step attempts to allocate to each user its best possible resources. The second step selects a suitable modulation and coding for each allocated subcarrier.

The PHY mode is selected based on the estimated SINR value of each resource. The AMC algorithm has already been presented in section 5.2.2. The first step of ARR, i. e. adaptive resource allocation, will be the focus in following sections.

### 9.1.1 Mathematical Description

This section describes the ARR problem in a mathematical way and gives a criterion on performance evaluation.

As the start point,  $N_{\text{user}}$  users are assumed communicating simultaneously with the BS in a cell. Considering only one single cell is because of the fact that The ARR is supposed to be performed independently by each station in a cellular network.

There are in total  $N_r$  resources available in the cell. Users may have different numbers of resources depending on individual propagation attenuation. It is further assumed, that the redistribution of resources is performed only within those already allocated resource. Thus the following equation can be derived.

$$\sum_{u=1}^{N_{\text{user}}} L_u = N_r \quad (9.1)$$

To each user the large-scale fading is statistically identical for all resources, and the frequency selectivity is reflected with the channel transfer factor matrix  $|H|$ . This matrix contains  $N_{\text{user}}$  independent transfer factor arrays, each of which has  $N_r$  elements. The received signal at  $u$ -th MT has an SNR in subcarrier  $k$  of

$$SNR_{u,k} = \overline{SNR}_u \cdot |H_u(k)|^2 \quad (9.2)$$

The average SNR value  $\overline{SNR}_u$  is calculated with only the large-scale fading. The interference is also considered as noise, because the accumulated effect of several independent interferences behaves similarly to a Gaussian noise. The ARR tries to redistribute for each user the best possible resources.

First of all a quantitative criterion has to be defined for comparison. The normalized system capacity is a good rule, which gives an upper bound of the spectrum efficiency in a practical communication system. In an OFDM-FDMA based system, each resource of any user can be thought approximately as an AWGN channel within a short duration. Based on the Shannon theorem, the spectrum efficiency  $C_u(k)$  [bit/s/Hz] in resource  $k$  for user  $u$  can be expressed by

$$C_u(k) = \log_2 \left( 1 + \overline{SNR}_u \cdot |H_u(k)|^2 \right) \quad (9.3)$$

To summarize, the resource allocation problem for the considered case can be described mathematically as follows.

<i>Input:</i>	<ul style="list-style-type: none"> <li>• An <math>N_{\text{user}} \times N_r</math> matrix of transfer function. Each element <math> H_u(k) </math> represents the transfer function in resource <math>k</math> for user <math>u</math>. <math>u \in [1, N_{\text{user}}]</math>, <math>k \in [1, N_r]</math>.</li> <li>• An array <math>L(u) = L_u</math>, <math>u \in [1, N_{\text{user}}]</math>. Each element denotes the number of resources currently allocated to user <math>u</math>.</li> </ul>
<i>Output:</i>	<ul style="list-style-type: none"> <li>• An allocation vector <math>\mathcal{A}(k) = u_k</math> with <math>N_r</math> elements, each of which denotes that resource <math>k</math> is allocated to user <math>u_k</math>.</li> </ul>
<i>Restriction:</i>	<ul style="list-style-type: none"> <li>• <math>\frac{1}{N_r} \sum_{k=1}^{N_r}  H_u(k) ^2 = 1, \forall u</math>.</li> <li>• The number of element in the set <math>\{k : \mathcal{A}(k) = u\}</math> equals to <math>L_u</math>, <math>\forall u</math>.</li> </ul>

As a reference the average spectrum efficiency of user  $u$  is calculated by

$$\bar{C}_u = \log_2 \left( 1 + \overline{SNR}_u \right) \quad (9.4)$$

The difference  $\Delta C(u, k)$ , a variable to describe the capacity gain by using resource  $k$  comparing to the average SNR at user  $u$ , is thus defined by

$$\Delta C_u(k) = C_u(k) - \bar{C}_u = \log_2 \left( \frac{1 + \overline{SNR}_u \cdot |H_u(k)|^2}{1 + \overline{SNR}_u} \right) \quad (9.5)$$

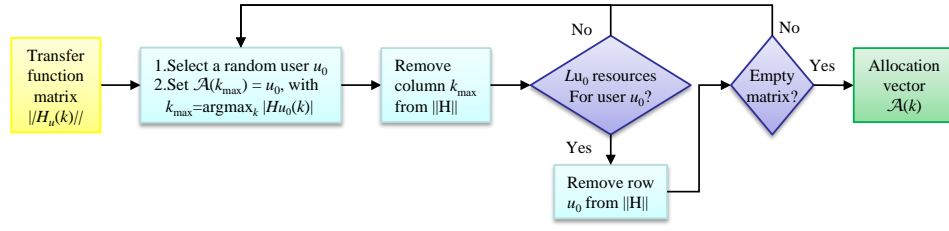


**Figure 9.1:** Rotational rearrangement algorithm

Considering that  $\overline{SNR}_u \gg 1$  in most cases, the equation 9.5 can be further simplified as

$$\Delta C_u(k) = \log_2 |H_u(k)|^2 \quad (9.6)$$

The average capacity gain with a certain allocation can be thus derived as

$$\frac{1}{N_r} \sum \Delta C = \frac{1}{N_r} \sum_u \sum_{\mathcal{A}(k)=u} \log_2 |H_u(k)|^2 \quad (9.7)$$

and will be used as the ruler for evaluation of various allocation algorithms.

### 9.1.2 ARR Algorithms

In this section, three algorithms will be discussed, provided the same conditions as described in last section. They are respectively rotational allocation, maximum value allocation, and Hungarian algorithm based allocation.

#### 9.1.2.1 Rotational Rearrangement

The rotational allocation algorithm selects every time one random user, and allocates the best resource to the user. A user quits when it gets already the same number of allocated resources before rearrangement. The recursion ends until all users are allocated. The procedure is illustrated in figure 9.1.

The resource selection is accomplished with following steps:

1. A matrix is constructed with  $N_{\text{user}} \times N_r$  elements  $||H_u(k)||$ . Each row  $u$  represents one user and each column  $k$  denotes one resource. Prepare an  $N_r$ -element allocation array  $\mathcal{A}(k) = 0, \forall k$ , where the default value 0 denotes the resource is not allocated to any user.
2. Select randomly a user  $u_0$ . Find  $k_{\text{max}}$  with the maximum transfer function value in row  $u_0$ , i.e.  $k_{\text{max}} = \arg \max_k |H_{u_0}(k)|$ . Allocate resource  $k_{\text{max}}$  to user  $u_0$  (set  $\mathcal{A}(k_{\text{max}}) = u_0$ ) and remove column  $k_{\text{max}}$  from the matrix  $||H_u(k)||$ .

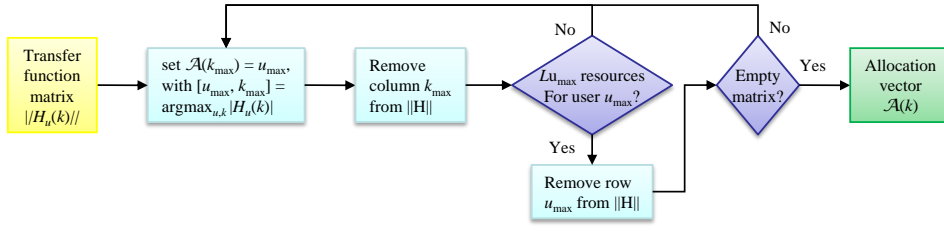


**Figure 9.2:** Maximum value algorithm

3. If  $L_{u_0}$  resources have been allocated to user  $u_0$ , remove row  $u_0$  from the matrix  $||H_u(k)||$ . Otherwise, jump to step (2).
4. If the matrix is empty, i. e. all users are served, output the allocation vector  $\mathcal{A}(k)$ . Otherwise, jump to step (2).

#### 9.1.2.2 Maximum Value Rearrangement

The core idea of maximum value rearrangement is to allocate in each turn one best possible resources to one user, considering all users and all available resources together. The procedure is illustrated in figure 9.2.

The resource rearrangement in this algorithm is accomplished with following steps:

1. A matrix is constructed with  $N_{\text{user}} \times N_r$  elements  $||H_u(k)||$ . Each row  $u$  represents one user and each column  $k$  denotes one resource. Prepare an  $N_r$ -element allocation array  $\mathcal{A}(k) = 0, \forall k$ , where the default value 0 denotes the resource is not allocated to any user.
2. Find the user  $u_{\text{max}}$  and the resource  $k_{\text{max}}$  with maximum value in the matrix, i. e.  $[u_{\text{max}}, k_{\text{max}}] = \arg \max_{u,k} |H_u(k)|$ . Allocate resource  $k_{\text{max}}$  to user  $u_{\text{max}}$  (set  $\mathcal{A}(k_{\text{max}}) = u_{\text{max}}$ ).
3. Remove resource (column)  $k_{\text{max}}$  from the matrix.
4. Once the user  $u_{\text{max}}$  already has sufficient resources, remove row  $u_{\text{max}}$  from the matrix. Otherwise, jump back to step (2).
5. If all users are satisfied, output the allocation vector  $\mathcal{A}(k)$ ; otherwise jump to step (2).

#### 9.1.2.3 Hungarian Algorithm Based Rearrangement

The Hungarian method is firstly introduced in [Kuh55] by H.W. Kuhn in 1955, giving an optimized solution to the assignment problem which tries to

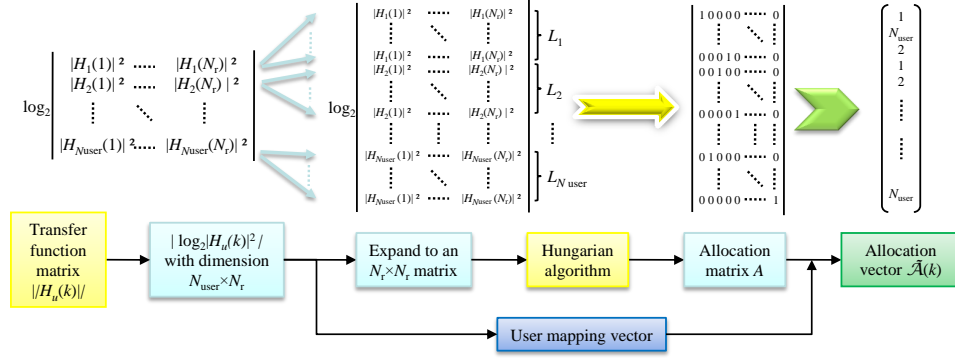


**Figure 9.3:** Hungarian algorithm based resource rearrangement

assign jobs to workers so as to minimize the total cost. A modified 6-step implementation of this algorithm in [Mun] is adopted as the reference for the resource allocation algorithm considered here. The target is relevantly altered to the maximization of the average capacity gain in equation (9.7). The allocation vector  $\tilde{\mathcal{A}}$  as a solution can be mathematically expressed by

$$\tilde{\mathcal{A}}(k) = \arg \max_{\mathcal{A}} \sum_u \sum_{\mathcal{A}(k)=u} \log_2 |H_u(k)|^2 \quad (9.8)$$

To comply with equation (9.8), the input matrix of channel transfer factor has to be converted to  $|\log_2 |H_u(k)|^2|$  at first.

The original Hungarian algorithm is dedicated to the matrix with an identical number of users and resources, and each user is allocated only one resources. When this algorithm is applied in the considered situation, the  $N_{\text{user}} \times N_r$  matrix shall be expanded to an  $N_r \times N_r$  square matrix. The  $u$ -th user is represented by  $L_u$  virtual users in the new matrix. The number  $L_u$  is identical to the number of resources allocated to user  $u$  before ARR.

An example process is described in figure 9.3, containing following steps.

1. An  $N_{\text{user}} \times N_r$  matrix  $|\log_2 |H_u(k)|^2|$  is derived from the original channel transfer factor matrix  $||H_u(k)||$ . Each row  $u$  represents one user and each column  $k$  denotes one resource.
2. Expand to an  $N_r \times N_r$  matrix. The  $u$ -th row in the original matrix maps to  $L_u$  rows with same elements in the newly generated matrix, where  $L_u$  is identical to the number of previously allocated resources to the  $u$ -th user. Those mappings between real users  $u$  and virtual users  $u'$  are stored in an  $N_r$ -element mapping vector and will be used again in the last step.

**Table 9.1:** Comparison of ARR algorithms

	Rotational	Maximum value	Hungarian based
Capacity gain	Low	Medium	High
Complexity	$O(N_r^2)$	$O(N_r^2 \cdot N_{\text{user}})$	$O(N_r^3)$

3. Apply Hungarian method to the new matrix and output an  $N_r \times N_r$  allocation matrix. When resource  $k$  is allocated to the virtual user  $u'$ , the element  $A(u', k)$  is set 1. All other elements have same value of "0". Only one "1" can exists in each row or column. That means an exclusive allocation of resources to each virtual user, and each virtual user gets only one resource.
4. Convert the output matrix to allocation vector  $\tilde{\mathcal{A}}$  in accordance with the mapping vector obtained from step (2).

The above algorithm can reach an optimized allocation, when the total capacity gain is adopted as the criterion.

Table 9.1 lists the comparison between those three proposed algorithms.

Obviously, the Hungarian algorithm based allocation requires much more calculation power than the other two algorithms, although it brings the highest capacity gain. The quantitative performances of those algorithms will be simulated and compared in the following section.

## 9.2 ARR in a Cellular Network with SO-RRM

This section investigates the performance of those algorithms described in the previous section, in a cellular network with self-organized radio resource management. The simulation is divided into two parts. The performance of ARR in a single cell will be firstly investigated, followed with the behavior in a cellular network.

### 9.2.1 Performance in a Single Cell

In this simulation part, an OFDM-FDMA single cell system is considered with 10 users. Each of them is allocated three resources. The amplitude of channel transfer factor is assumed uncorrelated between resources and Rayleigh distributed. Including path loss and shadowing, an average SNR of 10 dB is assumed in the downlink at each MT.

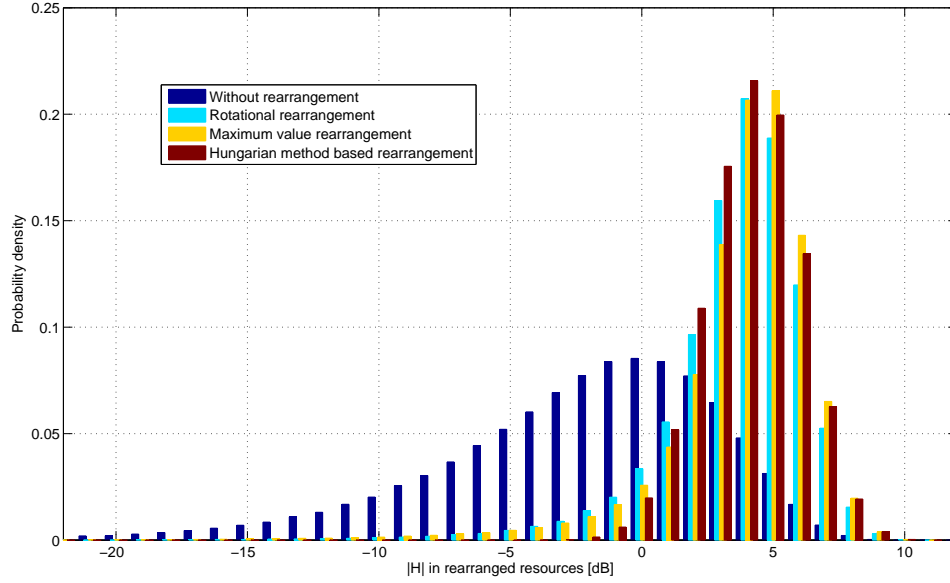


**Figure 9.4:** Channel transfer factors in rearranged resources, single cell

The performances of three ARR algorithms are compared with the original allocation. In the allocations after rearrangement, the modulation and coding in an individual resource is selected based on its instantaneous SNR value, as shown in section 5.2.2.

#### Channel transfer factor and capacity gain

A direct output of an ARR algorithm is the new channel transfer factor  $|H(u, k)|$ , which reflects how good the resource is to a user. The criterion used to evaluate an algorithm, average capacity gain, is also calculated from those values. Figure 9.4 compares the histograms of  $|H|$  outputted from three algorithms.

Without rearrangement, the magnitude of factors  $|H|$  in allocated resources to a user complies with the Rayleigh fading. When the absolute values are converted into dB, the mean of those values is -2.4 dB. That is, the Rayleigh fading causes performance degradation, comparing with the AWGN channel. This can be however overcome by resource rearrangement.

All three algorithms brings almost 4 dB gain comparing with the AWGN channel and about 6 dB gain with the Rayleigh channel. Looking in detail, the maximum value algorithm has more chances to choose very high  $|H|$  values, whereas the deviation of those values are also the greatest and results in more deep fading. The Hungarian method based algorithm has the greatest mean value and the least standard deviation. Nearly every selected resource has a channel transfer factor  $|H| > 1$ . The mean values and standard deviations of those algorithms are listed in table 9.2.



**Table 9.2:** Capacity gain of adaptive resource rearrangement, single cell

	Mean of $\lg( H ^2)$ [dB]	Deviation of $\lg( H ^2)$ [dB]	Capacity gain [bits/s/Hz]
AWGN	0	0	0
Rayleigh	-2.44	5.52	-0.81
Rotational	3.49	2.79	1.16
Max. value	3.71	2.98	1.24
Hungarian based	4.08	1.80	1.37

Their total capacity gains are calculated by equation (9.7). The Hungarian method based rearrangement has the highest gain of 1.37 bits/s/Hz, while the rotational algorithm and maximum values bring respectively 20% and 10% less gains.

#### Selected PHY mode and spectrum efficiency

For each rearranged resource, a suitable modulation and coding scheme will be decided in accordance with the QoS requirement. Figure 9.5 plots the histograms of selected modulations without and with different ARR algorithms. The coding rate is selected 1/2 with each modulation. The instantaneous SNR value is calculated as the product of the average SNR of 10 dB and the instantaneous  $|H|$  in each resource.

Without rearrangement, nearly 10% of the resource is left idle due to instant deep fading in some frames. The most frequently used modulations are QPSK and 16-QAM, which cover about 60% out of all. BPSK and 64-QAM occupies each about 10%, and the highest mode 256-QAM is rarely used.

The adaptive rearrangement reduces remarkably the probability of using a low rate modulation and the probability of unused resources. The majority of adopted modulation shifts to 16-QAM and 64-QAM, covering respectively about 30% and more than 60%. The algorithms enable also a regular usage of 256-QAM. By the Hungarian method based algorithm, even the BPSK is not used because of the good channel quality in new resources.

The spectrum efficiency  $\mu$  can thus derived by

$$\mu = \frac{1}{N_r} \sum_{k=1}^{N_r} 0.5 \cdot x_k \quad (9.9)$$

In resource  $k$  a  $2^{x_k}$ -modulation is adopted, and  $x_k$  is set 0 when the resource is not used. The results are listed in table 9.3.

By comparison with those theoretical values in table 9.2, it can be found that the possible gain is not fully achieved. The reason is that the possible

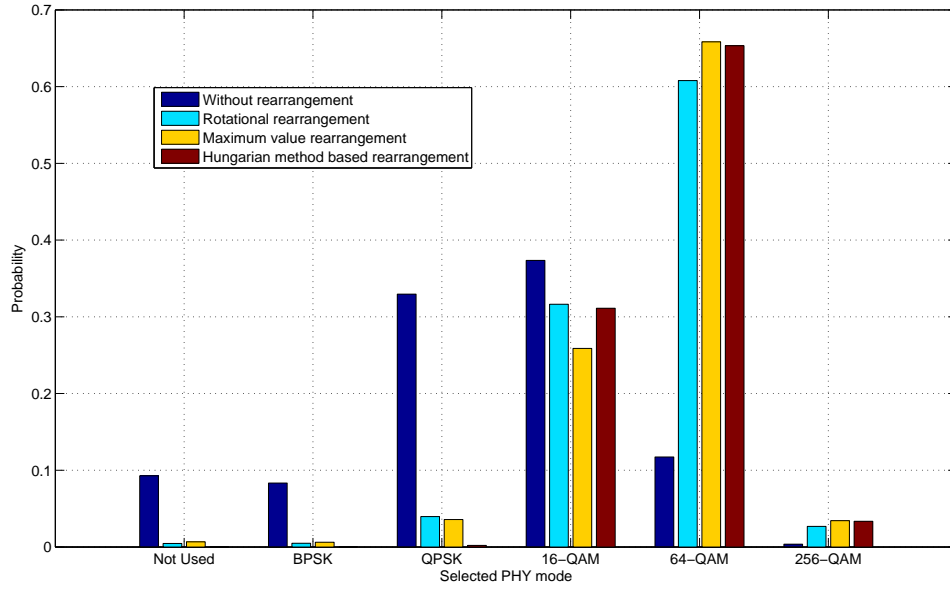


**Figure 9.5:** Selected PHY modes in rearranged resources, single cell

PHY mode is discrete, and the selection procedure implies a quantization operation. For example in the simulation, only 60% of the maximum capacity gain is converted to a real increase. Introducing more PHY modes will bring more benefit in the efficiency.

### 9.2.2 Performance in a Cellular Network

The simulation in the previous section shows the performance enhancement by different algorithms in a single cell. This section will apply ARR in a cellular network with self-organized radio resource management. A time invariant channel and a uniform user distribution are assumed.

Different from in the time-variant environment, the instantaneous SINR

**Table 9.3:** Spectrum efficiency in ARR, single cell

ARR algorithm	Spectrum efficiency [bits/s/Hz]	Increase [bits/s/Hz]	Increase (%)
Not rearranged	1.49	0	0
Rotational	2.61	1.12	75%
Maximum value	2.67	1.18	79%
Hungarian based	2.72	1.23	83%

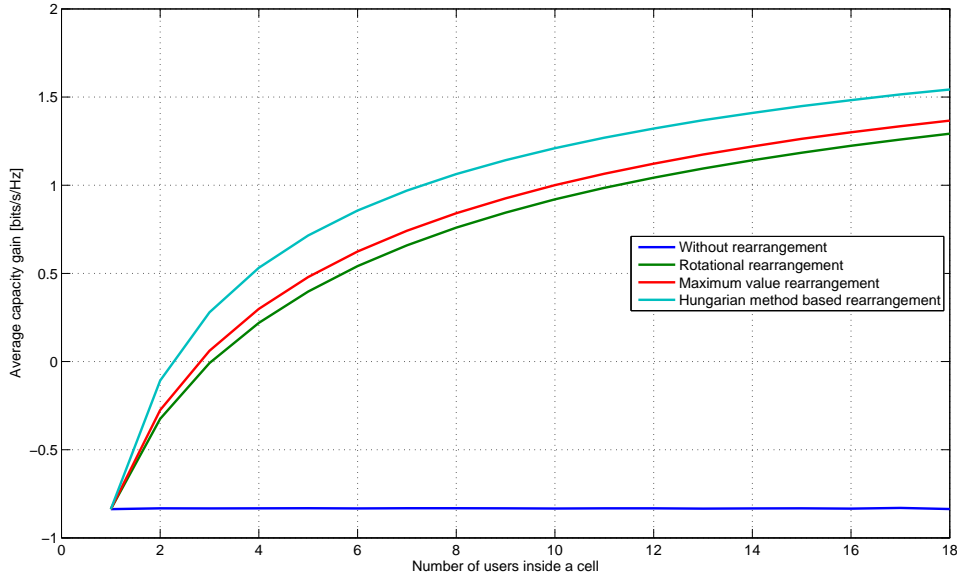


**Figure 9.6:** Average capacity gain of ARR with different number of users in a cellular system

in each resource replaces the average value, working as the input to the resource allocation algorithm. The ARR is performed when new resources are allocated to a new user. It shall be noted that the resource rearrangement can be only used in the downlink, in order to keep the whole interference situation unchanged in the network.

The same cellular structure and parameters are imported from previous simulations. Adaptive resource rearrangement is then applied to all cells. The performances are shown as follows.

### Capacity gain

As the mathematical criterion, the average capacity gains in the cases of different number of users are firstly compared in figure 9.6. All gains are calculated using an AWGN channel as the reference.

Without rearrangement, the capacity gain is constant when the number of users changes. However, it is much lower than the one with an AWGN channel. By resource rearrangement, a significant gain can be observed. In the case of 3 users, the results of those proposed ARR algorithms are better than an AWGN channel.

The more users included in the rearrangement, the higher gain can be achieved. The Hungarian method based algorithm shows the best performance. It brings even a gain of 1.5 bits/s/Hz comparing to AWGN channel when it is applied to a group of 17 users. Considering an average number

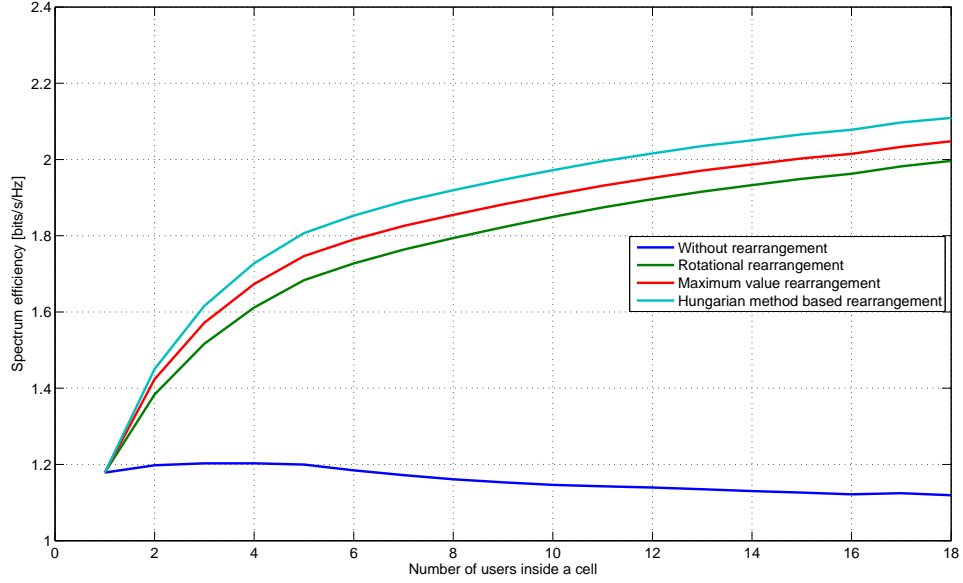


**Figure 9.7:** Comparison of spectrum efficiency in adaptive resource rearrangement

of 11 users in the cellular network with a global satisfaction rate of 95% as discussed in chapter 7, the rotational rearrangement, the maximum value algorithm, and the Hungarian method based algorithm can provide respectively a gain of 1, 1.1, and 1.3 bits/s/Hz.

### Spectrum efficiency

As explained the capacity gain is only a theoretical improvement of performance. The conversion of those gains into transmission is through an adaptive PHY mode selection. Figure 9.7 compares the consequent spectrum efficiencies in the considered cases.

Considering firstly the reference system, its average spectrum efficiency decreases with more users in a cell. The reason is that more interferers appear with high traffic load, and thus the SINR is globally decreased. More resources shall be allocated to users for a same data rate.

After rearrangement, almost all users get better resources than before and new PHY modes with higher data rates can be applied. Although more users means more diversity and higher ARR gain, the interference brought with them limits the use of highest PHY mode like 256-QAM. The average spectrum efficiency at the point with 18 users is about 2 bits/s/Hz, which is equivalent to 16-QAM with a coding rate 0.5.

Nevertheless, the usage of high rate PHY modes after rearrangement implies that less resources than before are needed to support the same data rate.

---

The temporarily unused resources can be left idle to mitigate the generated interference to communications in the nearby area.



## Chapter 10

# Conclusions

WIRELESS application has more and more rich contents such as video telephony or mobile internet surfing. Those require high transmission rates in communication and thus calls for wideband data transmission. However the multi-path propagation causes a fluctuation of radio channel in frequency, which needs a complicated equalizer in a single carrier transmission system.

The OFDM technique solves this problem with a multi-carrier transmission. The whole bandwidth is subdivided into a large number of narrow bands, each of which can be treated as a flat subchannel. With a specially designed signal spectrum, those subcarriers are orthogonal to each other. The traditional guard bands between adjacent subcarriers can be removed. The corresponding spectrum efficiency is increased. By using a large number of low rate subcarriers, the symbol duration becomes longer than the delay and the ISI can be easily and completely removed by adding a cyclic prefix. With those advantages, the OFDM technique has been adopted as a fundamental component in the next generation mobile communication systems like LTE.

The investigation in this thesis is done in an OFDM-FDMA based cellular system. A TDD-FDMA structure is adopted, as the TDD can benefit from the reciprocity of downlink and uplink channel between the transmitter and the receiver and is suitable for a small cell size in a typical urban environment. With FDMA, adaptive modulation and coding can be applied to choose the most suitable transmission parameters for each subcarrier based on the QoS requirements. A channel with a high SNR value can transmit more data packets, while another one suffering from strong interference can be assigned only a low-rate data stream to ensure the quality of service. Link adaption is also applied in the time direction against the channel fluctuation, which is the consequence of the Doppler frequency shift.

The OFDM technique facilitates the implementation of a single frequency network, where each BS transmits signals in the same carrier frequency simultaneously. Radio resources can be reused in cells at a sufficient long distance. A scheme of self-organized radio resource management with more efficiency and flexibility is proposed for an OFDM based single frequency cellular system. Resources are not segmented and pre-allocated to cells, but are concentrated in a common pool, which is accessible to all BS's. A single resource is defined as several adjacent subcarriers, which have similar channel attenuations. All resources are used according to the current traffic demand and the instant channel condition. Nevertheless, the exchange of allocation information between BSs or the coordination of allocations by a CC is not required any more. All BSs allocate independently radio resources to their MTs. To avoid the potential conflict, BSs collect information about resource allocation and channel condition in nearby area through network sensing.

For each new call request, radio resources are selected according to the estimated SINR values. The uplink interference is measured at the BS continuously, while the downlink interference is measured at the MT during the connection setup phase. To provide an interference-free measurement of signal power, a dedicated "signal measurement" slot is introduced at the end of each uplink frame. Test signals are exclusively transmitted from the terminal to the station, carrying the information about downlink candidate resources and the measured CCI values on them. The collision of test signal transmissions in several cells due to independence has been verified to have only a negligible impact to the measurement results. According to the property of a WSSUS channel, the power fluctuation of the received test signal in different subcarriers is statistically similar to the fluctuation of the signal in the time direction in any resource. This can be used in the estimation of the long-term channel behavior in one resource. The measured average SINR values are firstly converted to the supplied data rate with a predefined resource quality mapping function. The resources with highest possible transmission rates are allocated.

A dropping occurs when an existing transmission is not able to keep sufficient quality due to new interferers appearing after the resource allocation. It has become the main restriction factor in a system with a self-organized structure. To reduce the dropping probability, two schemes have been proposed in this thesis. The interference margin works as an active solution. Its principle is to reserve some space in the measured SINR value of any resource during selection. That margin increases in advance the tolerance of a transmission against the potential new interference. When several resources are allocated with margins, more robustness can be achieved. A compromise is necessary in the selection of margin size. A small margin improves only a bit in performance, whereas a big one may lead to more resources allocated



and thus a loss in efficiency.

Another passive solution is reallocation, which activates a new allocation process if the transmission quality degrades for a certain time. The system capacity improves significantly with this method at a very low cost. The simulation result has already shown that the reallocation scheme is a very useful enhancement to the basic SO-RRM scheme. Moreover, an additional margin does not bring any benefit to a system already with reallocation enabled.

Another typical advantage of such a self-organized structure has been presented in a cellular network with non-uniform user distribution. A full access of radio resources implies that the resource can be freely shifted to any cell if necessary. Comparing with the fixed resource allocation, the SO-RRM scheme shows its high flexibility in adapting to the frequent change of user distribution or traffic load in cellular systems.

In a multi-user system, different users observe different channel attenuation in frequency. Such multi-user diversity gives a chance to improve the system performance by rearrangement of resources, trying to serve each user with best possible ones. This is applicable with static or quasi-stationary communications, where a time-invariant channel can be assumed for long time duration. In the proposed system with self-organized resource management, the adaptive resource rearrangement can be only performed in downlink, where the exchange of resources does not change the total interference situation to the other cells. Out of three considered algorithm, the Hungarian method based algorithm brings the greatest gain, at the cost of the highest complexity.

In conclusion, the self-organized network structure and resource allocation, benefiting from its flexibility and adaptivity to any traffic distribution, can be a good candidate for OFDM based next generation mobile communication systems. Reallocation is an efficient and necessary anti-dropping scheme to the basic SO-RRM scheme.



# Glossary

Abbreviation	Full expression
AMC	Adaptive Modulation and Coding
ARR	Adaptive Resource Rearrangement
AWGN	Additive White Gaussian Noise
BCCH	Broadcast Control CHannel
BPSK	Binary Phase Shift Keying
BS	Base Station
CC	Central Controller
CCCH	Common Control CHannel
CCI	Co-Channel Interference
CDMA	Code Division Multiple Access
CP	Cyclic Prefix
DAB	Digital Audio Broadcasting
DCA	Dynamic Channel Allocation
DECT	Digital Enhanced Cordless Telecommunications
DFT	Discrete Fourier Transformation
DL	DownLink
DRA	Dynamic Resource Allocation
DRM	Digital Radio Mondiale
DSP	Digital Signal Processing
DVB	Digital Video Broadcasting
EDGE	Enhanced Data rates for GSM Evolution
FCA	Fixed Channel Allocation
FDD	Frequency Division Duplex
FDMA	Frequency Division Multiple Access
FRA	Fixed Resource Allocation
GPRS	General Packet Radio Service
GSM	Global System for Mobile communication

Abbreviation	Full expression
HSDPA	High Speed Downlink Packet Access
ICI	Inter-Carrier Interference
ID	IDentifier
IDFT	Inverse Discrete Fourier Transformation
IEEE	Institute of Electrical and Electronics Engineers
ISI	Inter-Symbol Interference
LLC	Logic Link Control
LOS	Line Of Sight
LTE	Long Term Evolution
LTI	Linear Time Invariant
MAC	Medium Access Control
MIMO	Multi-Input Multi-Output
MT	Mobile Terminal
OFDM	Orthogonal Frequency Division Multiplexing
PDF	Probability Density Function
PER	Packet Error Rate
PHY	PHYsical (layer)
QAM	Quadrature Amplitude Modulation
QoS	Quality of Service
QPSK	Quadrature Phase Shift Keying
RMSD	Root Mean Square Deviation
Rx	Receiver
SDMA	Space-Division Multiple Access
SFN	Single Frequency Network
SINR	Signal-to-Interference-and-Noise Ratio
SIR	Signal-to-Interference Ratio
SM	Signal Measurement
SNR	Signal-to-Noise Ratio
SO-DCA	Self-Organized Dynamic Channel Allocation
SO-RRM	Self-Organized Radio Resource Management
TDD	Time Division Duplex
TDMA	Time Division Multiple Access
TD-SCDMA	Time Division Synchronous CDMA
Tx	Transmitter
UL	UpLink
UMTS	Universal Mobile Telecommunications System
WiMAX	Worldwide interoperability for Microwave Access

---

Abbreviation	Full expression
WLAN	Wireless Local Access Network
WSSUS	Wide-Sense Stationary Uncorrelated Scattering
2G	Second Generation
3G	Third Generation



# Symbol

Variable	Physical meaning
$\mathcal{A}$	Resource allocation vector
$a_l$	Attenuation factor of the $l$ -th propagation path
$B$	System bandwidth
$B_c$	Coherence bandwidth of a frequency selective channel
$c$	Speed of light
$\bar{C}_u$	Average spectrum efficiency of user $u$
$C_u(k)$	Spectrum efficiency of user $u$ in resource $k$
$d_0$	Reference distance in the path loss model
$\tilde{d}$	Distance between a receiver and the effective interferer
$f_{D,l}$	Doppler frequency shift on the $l$ -th propagation path
$f_{D,\max}$	Maximum Doppler frequency shift
$f_0$	Central carrier frequency
$g_k(t)$	Mask function for the $k$ -th subcarrier
$G_k(f)$	Spectrum mask for the $k$ -th subcarrier
$ H $	Channel transfer factor
$H(f, t)$	Channel transfer function
$h(\tau, t)$	Impulse response
$I_i$	Interference from the $i$ -th co-channel cell
$I_{k,DL/UL}$	DL/UL co-channel interference in resource $k$
$L_f$	Number of OFDM symbols per resource per UL/DL phase
$L_p$	Number of bits per packet
$M_c$	Resource Quality mapping function
$M_f$	AMC mapping function
$M_k(t)$	Number of co-channel interferers in resource $k$
$N_0$	Power of universal thermal noise
$N_{\text{can}}$	Number of candidate resources fed back to base station
$N_f$	Number of subcarriers per resource

Variable	Physical meaning
$N_g$	Number of samples in cyclic prefix in OFDM
$N_i$	Number of info bits carried in one test signal
$N_{isi}$	Number of adjacent symbols influenced by ISI
$N_r$	Number of payload resources
$N_s$	Number of OFDM symbols per UL/DL phase
$N_{sc}$	Number of OFDM subcarriers
$N_{sig}$	Number of signaling subcarriers
$N_{tp}$	Number of transmitted packets in a frame
$N_{ts}$	Number of subcarriers for one test signal
$N_{user}$	Number of simultaneously active mobile users in one cell
$P_{blk}$	Blocking probability
$P_{drp}$	Dropping probability
$P_{sat}$	User satisfaction rate
$p(\cdot)$	Probability density function
$q$	Number of bits for a quantized CCI value
$R_c$	Cell radius in a cellular network
$R_k$	Supplied transmission rate in resource $k$
$R_{min}$	Minimum required transmission rate for an allocated resource
$R_0$	Universal data rate requirement for all users
$rect(\cdot)$	Rectangular function
$S_n$	$n$ -th discrete signal in an OFDM block
$S_k$	$k$ -th modulated symbol
$s(t)$	Signal within an OFDM block
$SINR_{im}$	Interference margin
$T$	Duration of an OFDM block
$T_c$	Coherent time of a time-variant channel
$T_{call}$	Time duration of each call
$T_f$	Time duration of one MAC frame
$T_g$	Time duration of a guard interval
$T_s$	Time duration of a symbol
$v_l$	Equivalent velocity on the $l$ -th propagation path
$X_\sigma$	Gaussian distributed shadowing with a standard deviation $\sigma$
$\alpha$	Propagation coefficient
$\Delta C(u, k)$	Normalized capacity gain by using resource $k$ for user $u$
$\Delta f$	Frequency spacing between two adjacent subcarriers
$\Delta S$	Error in the power measurement of test signal
$\Delta S_{avg}$	Signal measurement error due to averaging operation



---

Variable	Physical meaning
$\Delta t$	Sampling period in OFDM transmission system
$\mu$	Spectrum efficiency
$\rho$	Hotspot factor in non-uniform user distribution
$\sigma$	Standard deviation of Gaussian distributed shadowing factor
$\tau_l$	Propagation delay of the $l$ -th propagation path
$\tau_{\max}$	Maximum delay spread
$\tau_0$	Mean delay in multi-path propagation
$\theta_l$	Phase shift on the $l$ -th propagation path
$\psi_l$	Arriving azimuthal angle on the $l$ -th propagation path



# Bibliography

- [3GPP03] 3GPP TR 25.996, *Spatial channel model for Multiple Input Multiple Output (MIMO) simulations*, <http://www.3gpp.org>, 2003.
- [802-05] IEEE 802.20: *Evaluation Criteria*, <http://www.ieee.org>, September 2005.
- [Alt02] Z. Altman, J. M. Picard, S. Ben Jamaa, B. Fourestié, A. Caminada, T. Dony J. F. Morlier, and S. Mourniac, *New Challenges in Automatic Cell Planning of UMTS Networks*, Proceedings of IEEE 56th Vehicular Technology Conference, Vol. 2, pp. 951-954, Vancouver, Canada, September 2002.
- [Bin02] B. Bing, *Wireless Local Area Networks: The New Wireless Revolution*, John Wiley & Sons, New York, 2002.
- [Cal88] G. Calhoun, *Digital Cellular Radio*, Artech House, Boston, 1988.
- [Cat02] S. Catreux, V. Erceg, D. Gesbert, and R. W. Heath Jr., *Adaptive modulation and MIMO coding for broadband wireless data networks*, IEEE Communications Magazine, vol. 2, pp. 108-115, June 2002.
- [Che98] P. J. Cherriman, F. Romiti, and L. Hanzo, *Channel Allocation for Third-generation Mobile Radio Systems*, Proceedings of ACTS'98, Vol. 1, pp. 255-260, Rhodes, Greece, June 1998.
- [Din02] E. Dinan, A. Kurochkin, and S. Kettani, *UMTS Radio Interface System Planning and Optimization*, Bechtel Telecommunications Technical Journal, Vol. 1, No. 1, pp. 1-10, December 2002.
- [ETSI03] ETSI EN 300 175-3 v2.1.1, *Digital Enhanced Cordless Telecommunications (DECT); Common Interface (CI); Part 3: Medium Access Control (MAC) layer*, <http://www.etsi.org>, August 2007.
- [Fal04] S. Falahati, A. Svensson, T. Ekman, and M. Sternad, *Adaptive modulation systems for predicted wireless channels*, IEEE Transactions on Communications, Vol. 52, No. 2, pp. 307-316, February 2004.

- [For02] A. Forenza and R. W. Heath Jr., *Link Adaptation and Channel Prediction in Wireless OFDM Systems*, Proceedings of The 45th Midwest Symposium on Circuits and Systems, Vol. 3, pp. 211-214, August 2002.
- [Gal06] D. Galda, *Ein Beitrag zum Vielfachzugriff, zur Synchronisation und Kanalschätzung in einem OFDM-basierten Mobilfunksystem*, doctor thesis, Technische Universität Hamburg-Harburg, 2006.
- [Gal03] D. Galda, N. Meier, H. Rohling, and M. Weckerle, *System Concept for a Self-Organized Cellular Single Frequency OFDM Network*, Proceedings of 8th International OFDM Workshop, pp. 98-102, Hamburg, September 2003.
- [Gib99] J. D. Gibson, *The Mobile Communications Handbook, 2nd Edition*, CRC Press LLC, Florida, 1999.
- [Gie06] T. Giebel, *Kanaladaption und adaptiver Vielfachzugriff in codierten OFDM-Datenübertragungssystemen*, doctor thesis, Technische Universität Hamburg-Harburg, 2006.
- [Grü03] R. Grünheid, B. Chen, and H. Rohling, *Joint Layer Design for an Adaptive OFDM Transmission System*, Proceedings of IEEE VTC 2003-Fall, Vol. 1, pp. 542-546, Orlando, USA, October 2003.
- [GSMA] The GSM Association, <http://www.gsmworld.com>.
- [Gud91] M. Gudmundson, *Correlation Model for Shadow Fading in Mobile Radio Systems*, Electronics Letters, Vol. 27, No. 23, pp. 2145-2146, November 1991.
- [Hal04] M. A. Haleem and R. Chandramouli, *Adaptive Stochastic Iterative Rate Selection for Wireless Channels*, IEEE Communications Letters, Vol. 8, No. 5, pp. 292-294, May 2004.
- [Ham97] K. Hamidian and J. Payne, *Performance Analysis of a CDMA/FDMA Cellular Communication System with Cell Splitting*, Proceeding of 2nd IEEE Symposium on Computers and Communications, pp. 545-550, July 1997.
- [Hil04] A. Hills and B. Friday, *Radio Resource Management in Wireless LANs*, IEEE Communications Magazine, Vol. 42, No. 12, pp. S9-14, December 2004.
- [Hol02] H. Holma, Z. C. Honkasalo, S. Hämäläinen, J. Laiho, K. Sipilä, and A. Wacker, *WCDMA for UMTS: Radio Access for Third Generation Mobile Communications, 2nd Edition*, Chapter 8, John Wiley & Sons, Chichester, 2002.

- 
- [Ibr02] J. Ibrahim, *4G Features*, Bechtel Telecommunications Technical Journal, Vol. 1, No. 1, pp. 11-14, December 2002.
  - [InS09] <http://www.in-stat.com/>.
  - [ITUR03] ITU-R Recommendation M. 1645, *Framework and Overall Objectives of the Future Development of IMT-2000 and Systems Beyond IMT-2000*, ITU-R Radio Assembly, Geneva, June 2003.
  - [Jac94] J. M. Jacobsmeyer, *Improving Throughput and Availability of Cellular Digital Packet Data (CDPD)*, Proceedings of Virginia Tech. 4th Symposium on Wireless Personal Communications, June 1994.
  - [Jak93] W. C. Jakes, *Microwave Mobile Communications*, IEEE Press, New York, 1993.
  - [Kat96] I. Katzela and M. Naghshineh, *Channel Assignment Schemes for Cellular Mobile Telecommunication Systems: A Comprehensive Survey*, IEEE Personal Communications, Vol. 3, No. 3, pp. 10-31, June 1996.
  - [Kuh55] H. W. Kuhn, *The Hungarian Method for the Assignment Problem*, Naval Research Logistic, pp. 83-97, Q. 2, 1955.
  - [Lam04] M. Lampe, *Adaptive Techniques for Modulation and Channel Coding in OFDM Communication Systems*, Doctor thesis, Technische Universität Hamburg-Harburg, 2004.
  - [Lam02] M. Lampe, H. Rohling, and J. Eichinger, *PER-Prediction for Link Adaptation in OFDM Systems*, Proceedings of 7th International OFDM Workshop, pp. 163-167, Hamburg, Germany, August 2002.
  - [Law99] E. Lawrey and C. J. Kikkert, *Adaptive Frequency Hopping for Multiuser OFDM*, Proceedings of 2nd International Conference on Information, Communications & Signal Processing, Singapore, December 1999.
  - [Lee95] W. C. Y. Lee, *Mobile cellular telecommunications: analog and digital systems, 2nd Edition*, McGraw-Hill, New York, 1995.
  - [Loz02] A. Lozano and D. C. Cox, *Distributed Dynamic Channel Assignment in TDMA Mobile Communication Systems*, IEEE Transactions on Vehicular Technology, Vol. 51, No. 6, pp. 1397-1406, November 2002.
  - [May00] T. May, *Differentielle Modulation und Kanalcodierung in breitbandigen OFDM Funkübertragungssystemen*, doctor thesis, Technische Universität Hamburg-Harburg, 2000.

- [Mei09] N. Meier, *Zur Ressourcenvergabe in einem selbstorganisierenden zellularen OFDM Mobilfunksystem*, doctor thesis, Technische Universität Hamburg-Harburg, 2009.
- [Moo94] P. H. Moose, *A Technique for Orthogonal Frequency Division Multiplexing Frequency Offset Correction*, IEEE Transactions on Communications. Vol. 42, No. 10, pp. 2908-2914, October 1994.
- [Mun] <http://216.249.163.93/bob.pilgrim/445/munkres.html>.
- [Nie99] J. H. Nie and S. Haykin, *A Q-Learning-Based Dynamic Channel Assignment Technique for Mobile Communication Systems*, IEEE Transactions on Vehicular Technology, Vol. 48, No. 5, pp. 1676-1687, September 1999.
- [Olo06] S. Olonbayar, *Multiple Access Techniques and Channel Estimation in OFDM Communication Systems*, doctor thesis, Technische Universität Hamburg-Harburg, 2006.
- [Par01] J. D. Parsons, *The mobile radio propagation channel, 2nd Edition*, John Wiley & Sons, Chichester, 2001.
- [Pro01] J. G. Proakis, *Digital Communications, 4th Edition*, McGraw-Hill, Boston, 2001.
- [Pro94] J. G. Proakis and M. Salehi, *Communication Systems Engineering*, Prentice Hall, New Jersey, 1994.
- [Pro91] J. G. Proakis, *Adaptive Equalization for TDMA Digital Mobile Radio*, IEEE Transactions on Vehicular Technology, Vol. 40, No. 2, pp. 333-341, May 1991.
- [Rap02] T. S. Rappaport, *Wireless Communications: Principles and Practice, 2nd Edition*, Prentice Hall, New Jersey, 2002.
- [Rod99] C. Rodríguez, F. Schoute, and R. Prasad, *A Novel Concept for Fourth Generation Mobile Multimedia Communication*, Proceedings of IEEE Vehicular Technology Conference '99, Amsterdam, The Netherlands, September 1999.
- [Roh04] H. Rohling and D. Galda, *An OFDM based Cellular Single Frequency Communication Network*, Proceedings of Wireless World Research Forum (WWRF), Beijing, China, February 2004.
- [Roh99] H. Rohling, T. May, K. Brüninghaus, and R. Grünheid, *Broad-Band OFDM Radio Transmission for Multimedia Applications*, Proceedings of the IEEE, Vol. 87, No. 10, pp. 1778-1789, October 1999.

- 
- [Ste99] M. Stege, J. Jelitto, M. Bronzel, and G. Fettweis, *A Space-Time Channel Model with Stochastic Fading Simulation*, Proceedings of ITG-Fachtagung Intelligente Antennae, Stuttgart, April 1999.
  - [Ste03] M. Sternad and D. Aronsson, *Channel Estimation and Prediction for Adaptive OFDM Downlinks*, Proceedings of IEEE 58th Vehicular Technology Conference, Vol. 2, pp. 1283-1287, Orlando, USA, October 2003.
  - [Sti09] C. Stimming, *Multiple Antenna Concepts in OFDM Transmission Systems*, doctor thesis, Technische Universität Hamburg-Harburg, 2009.
  - [Stü01] G.L. Stüber, *Principles of Mobile Communication*, Kluwer Academic Publishers, Boston, 2001.
  - [Tab00] S. Tabbane, *Handbook of Mobile Radio Networks*, Artech House, Boston, 2000.
  - [WIND210] IST WINNER D2.10, *Identified RI key technologies, system concept, and their assessment*, <https://www.ist-winner.org>, December 2005.
  - [WIND28] IST WINNER D2.8, *Assessment of Key Enhanced Radio Protocols*, <https://www.ist-winner.org>, February 2005.
  - [WIND51] IST WINNER D5.1, *A set of channel and propagation models for early link and system level simulations*, <https://www.ist-winner.org>, August 2004.
  - [Won02] S.H. Wong and I.J. Wassell, *Dynamic Channel Allocation Using a Genetic Algorithm for a TDD Broadband Fixed Wireless Access Network*, Proceedings of International Conference in Wireless and Optical Communications, pp. 521-526, Banff, Canada, July 2002.
  - [Ye02] S. Ye, R.S. Blum, and L.J. Cimini Jr., *Adaptive Modulation for Variable-Rate OFDM Systems with Imperfect Channel Information*, Proceedings of IEEE 55th Vehicular Technology Conference, Vol. 2, pp. 767-771, Birmingham, UK, May 2002.
  - [Zha91] M. Zhang and T.S. Yum, *The Non-Uniform Compact Pattern Allocation Algorithm for Cellular Mobile Systems*, IEEE Transactions on Vehicular Technology, Vol. 40, pp. 387-391, 1991.
  - [Zha89] M. Zhang, *Comparisons of Channel-Assignment Strategies in Cellular Mobile Telephone Systems*, IEEE Transactions on Vehicular Technology, Vol. 38, pp. 211-215, 1989.

- [Zir01] W. Zirwas, T. Giebel, N. Esseling, E. Schulz, J. Eichinger, and H. Rohing, *Synchronization of Single Frequency Networks*, 6th International OFDM Workshop, Hamburg, Germany, September 2001.



# Lebenslauf

Name	Chen
Vorname	Ting
Geburtsdatum	11.05.1979
Geburtsort	Fuzhou, China
09.1984 - 07.1990	Grundschule in Fuzhou, China
09.1990 - 07.1996	Mittelschule in Fuzhou, China
09.1996 - 07.2000	Studium der Electronic Techniques and Information Systems Tsinghua Universität, Beijing, China Abschluss: Bachelor of Engineering
10.2000 - 03.2003	Studium der Information and Communication Systems Technische Universität Hamburg-Harburg Abschluss: Master of Science
04.2003 - 04.2007	Wissenschaftlicher Mitarbeiter im Institut für Nachrichtentechnik (Prof. Rohling) Technische Universität Hamburg-Harburg
07.2007 - 08.2009	Systemingenieur bei der Bishop GmbH